Week 10: Project 1 - FULL HYDRO case set up (PFI)

Engine Geometric Parameters

1. Bore = 0.086 m
2. Stroke = 0.09 m
3. Connecting rod length = 0.18 m
4. RPM = 3000

Run parameters

1. Simulation mode: Full Hydro

Simulation time parameters

1. Start time: -520 deg
2. End time: 120 deg

Boundary conditions

1. Piston temperature - 450K
2. Liner temperature - 450K
3. Head temperature - 450K
4. Spark Plug temperature - 550K
5. Spark Plug electrode temperature - 600K
6. Exhaust ports temperature - 500K
7. Exhaut outflow - 1 bar
8. Exhaust outlflow temperature - 800k
9. Exhaust species concentration - Calculate the stoichiometric condition
10. Exhaust valve top temperature - 525K
11. Exhaust valve angle temperature - 525K
12. Exhaust valve bottom temperature - 525K
13. Intake port - 1 temperature 425K
14. Intake port - 2 temperature 425K
15. Inflow pressure - 1 bar total pressure

16. Inflow temperature - 363K
17. Inflow species - Air
18. Intake valve top temperature - 480K
19. Intake valve angle temperature - 480K
20. Intake valve bottom temperature - 480K

Initial conditions

- Intake port - 1 (closer to combustion chamber)
  - IC_8H_{18} - 0.025508
  - O_2 - 0.20157
  - N_2 - 0.77292
  - Temperature – 390 K
  - pressure - 1 bar
- Intake port - 2 (away from combustion chamber)
  - Air
  - Temperature – 370 K
  - Pressure - 1 bar
- Cylinder
  - Pressure - 1.85731 bar
  - Temperature – 1360 K
  - Stoichiometric composition

Injection Parameters

1. Fuel flow rate = $7.5e^{-4}$ kg/second
2. Injection start time = -480.0 deg
3. Injection duration = 191.2 deg
4. Fuel temperature = 330 K

Nozzle positions

Nozzle diameter = 250 micro-meters

Circular injection radius = Nozzle radius

Spray cone angle = 10 deg

- Nozzle 0
  - Center: 0.0823357 0.00100001 0.07019
  - Align Vector: -0.732501 0.210489 -0.647408
- Nozzle 1
  - Center: 0.0823357 -0.00099999 0.07019
  - Align Vector: -0.732501 -0.210489 -0.647408
- Nozzle 2
  - Center: 0.0823357 -0.0004 0.07019
  - Align Vector: -0.5 -0.2 -0.647408
- Nozzle 3
  - Center: 0.0823357 0.0003 0.07019
  - Align Vector: -0.5 0.2 -0.647408

Spark Ignition Parameters

- Start of spark = -15 deg
- Spark duration = 10 deg
- Spark location = -0.003 0 0.0091
- Spark radius = 0.0005m

With the inputs provided in the challenge description, find out the following:

1. What is the compression ratio of this engine?

2. Why do we need a wall heat transfer model? Why cannot we predict the wall temperature from the CFD simulation?

3. Calculate the combustion efficiency of this engine

4. Use the engine performance calculator to determine the power and torque for this engine.

NOTE: Since Work and Torque have the same unit (N·m), it does not mean value for Torque and Work will be the same.

Both are different quantities and have totally different meanings.

So, the value for work that you will be getting from the engine performance calculator is not the value for the torque.

Calculate the value for the torque using the formula as shown below,

Power (P) = $(2\pi NT)/60$

5. What is the significance of CA10, CA50 and CA90?

NOTE:

Also create an animation and upload it on YouTube and provide the YouTube link for an animation in your report.

Solution

The goal of this project is to conduct a comprehensive hydro simulation for a port fuel injection (PFI) engine using the provided geometry, operational parameters, and boundary conditions to evaluate engine performance metrics such as compression ratio, combustion efficiency, power output, and torque. The study also aims to understand the significance of critical combustion angles (CA10, CA50, and CA90) and the necessity of incorporating a wall heat transfer model in the simulation.

Objectives

- Set up the simulation case in CONVERGE CFD, including importing the CAD model, defining grid size, material properties, and boundary conditions.
- Solve the case using the appropriate solver and convert the results for visualization in ParaView.
- Analyze engine performance by calculating compression ratio, combustion efficiency, power, and torque, and interpreting CA10, CA50, and CA90.
- Create visualizations and animations of the results and share them via YouTube for further analysis.

Description

In the PFI engine, fuel is injected into the intake port, just before the intake valves and cylinder [1]. The fuel injection system sprays fuel into the incoming air, creating a mixture that is drawn into the cylinder during the intake stroke. As the piston moves upward during the compression stroke, this air-fuel mixture is compressed. The spark plug then ignites the compressed mixture, causing a rapid combustion that drives the piston downward during the power stroke, thereby rotating the crankshaft. This process converts chemical energy into mechanical work, powering the engine.

The PFI system offers several advantages, such as improved fuel atomization, better control over the air-fuel ratio, and reduced emissions. However, the placement of the injector before the intake valve also means that fuel can accumulate on the valve and intake walls, which can affect engine performance and efficiency [2]. Figure 1 provides a visual comparison between Port Injection and Direct Injection systems, highlighting the differences in fuel delivery methods.

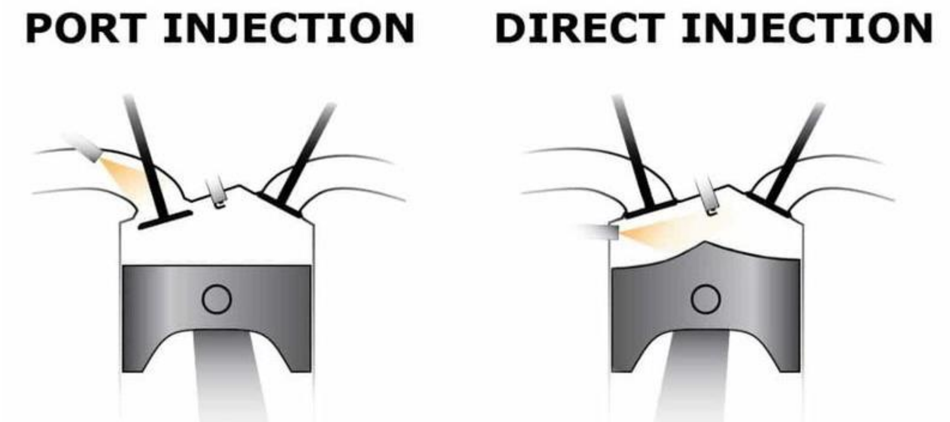

Figure 1: Comparative Illustration of Port Injection and Direct Injection Systems in an Internal Combustion Engine. [Source]

In Figure 1, the left side illustrates the Port Injection system, where fuel is injected into the intake port before the intake valve. This allows the fuel to mix with the air as it enters the cylinder. The advantage of this method is that it promotes better fuel atomization and mixing before combustion, which can improve combustion efficiency and reduce emissions. However, because the fuel is injected upstream of the intake valve, there can be issues with fuel pooling and wall wetting, potentially leading to deposits on the intake valves over time.

The right side of Figure 1 shows a Direct Injection system, where fuel is injected directly into the combustion chamber. This method allows for greater control over the air-fuel mixture, enabling higher compression ratios and more efficient combustion [3]. Direct Injection engines are known for their improved performance and fuel efficiency, as well as reduced emissions. However, they are generally more complex and expensive to manufacture than Port Injection systems.

The choice between Port Injection and Direct Injection depends on engine goals, performance needs, and costs. Direct Injection improves efficiency and emissions, while Port Injection offers simplicity and reliability.

Solution Procedures

To carry out this simulation, these procedures are followed:

1. Geometry Cleanup
2. Case Setup
3. Solution Execution
4. Post-Processing

Successfully completing these procedures ensures that all requirements are fully addressed.

1. Geometry Cleanup

Import the provided .stl file into CONVERGE CFD and perform a diagnosis on it.

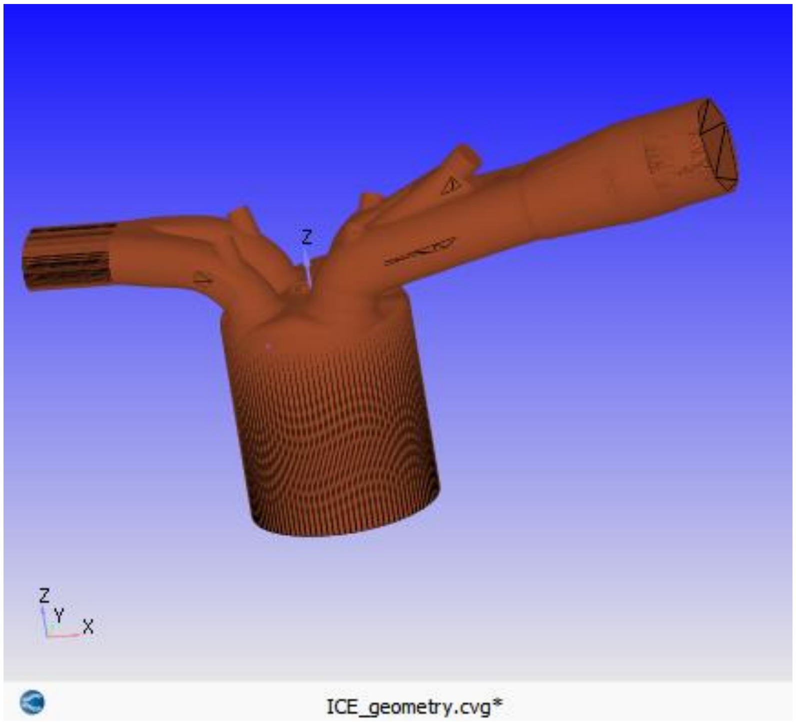

The diagnosis reveals a list of multiple errors that need to be addressed. However, before cleaning up the geometry, flag all the necessary boundaries, as this will assist in the geometry cleanup process.

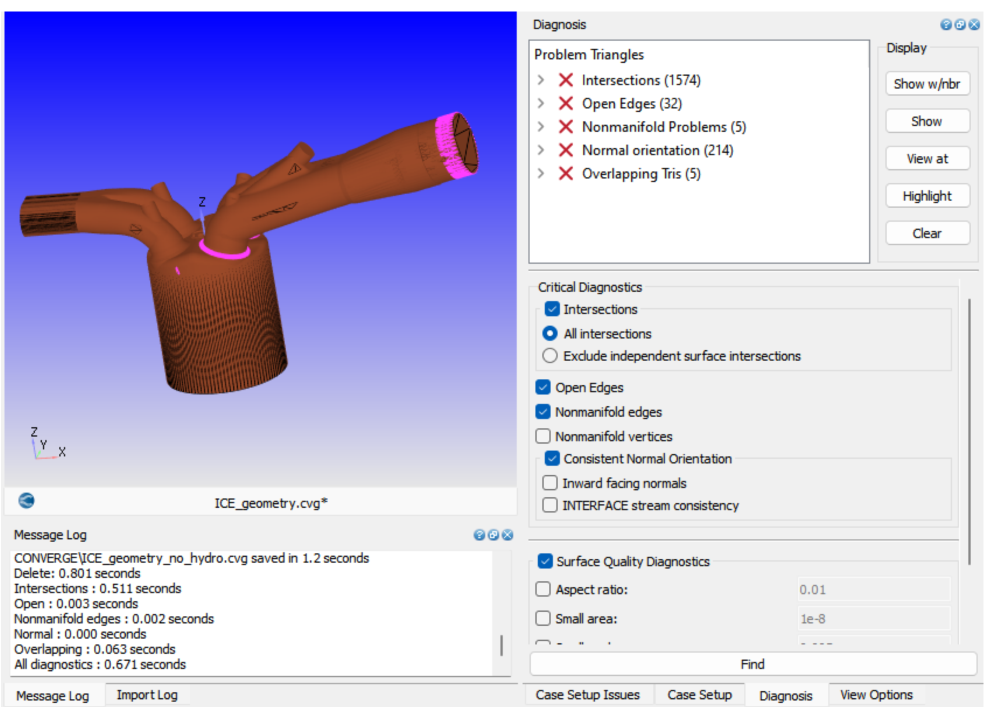

- **Boundary Flagging**

To flag boundaries, go to Geometry → Boundary →Flag.

Piston

Go to Boundary → Fence →By selected edges → using by arc, select the edge as shown in the image → Mark fence.

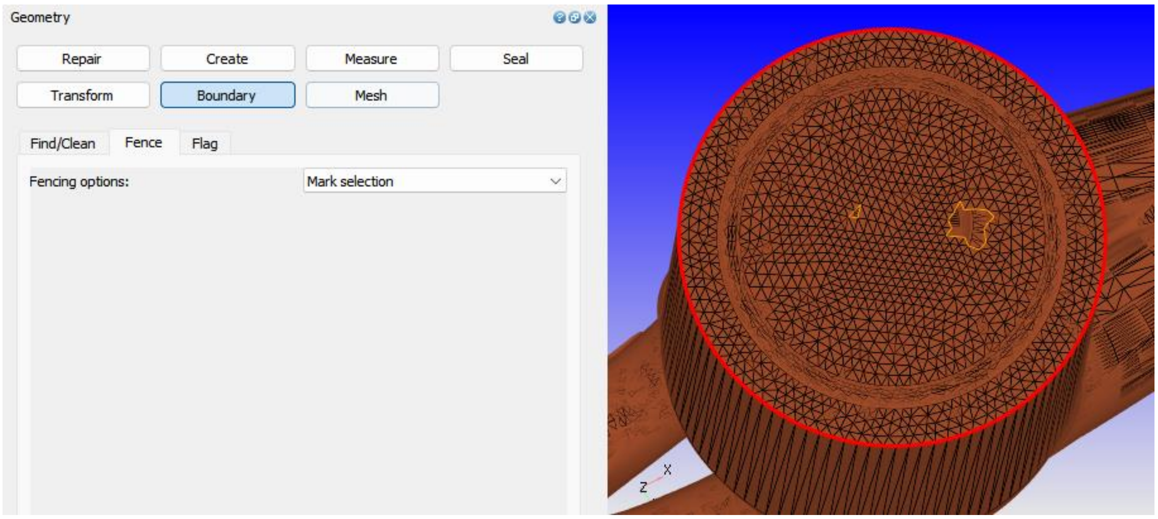

Go to Geometry → Boundary →Flag → using by boundary fence, select piston → name boundary as piston → Apply.

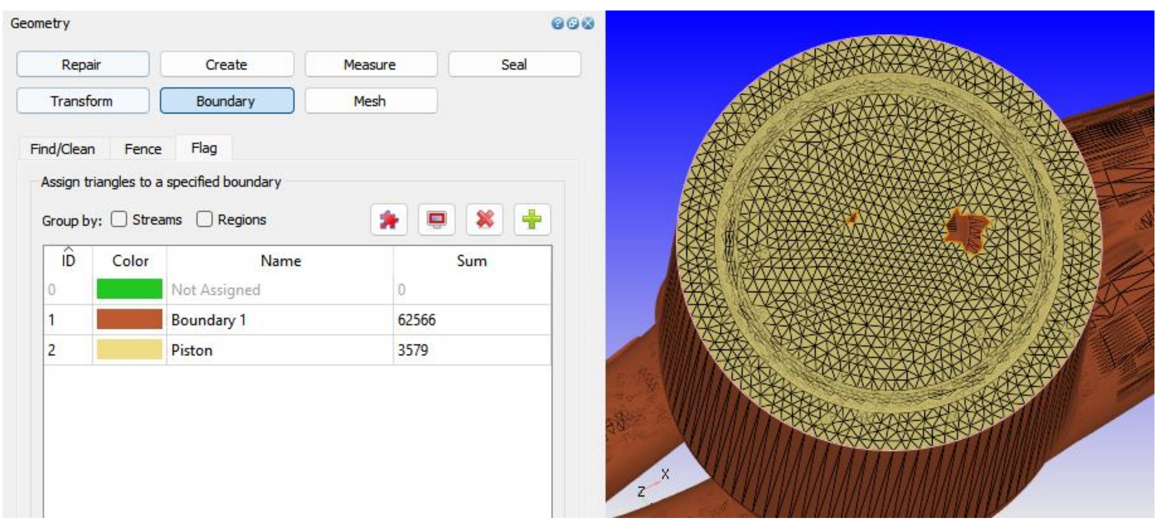

Liner

Go to Boundary → Fence →By selected edges → using by arc, select the edge as shown in the image → Mark fence.

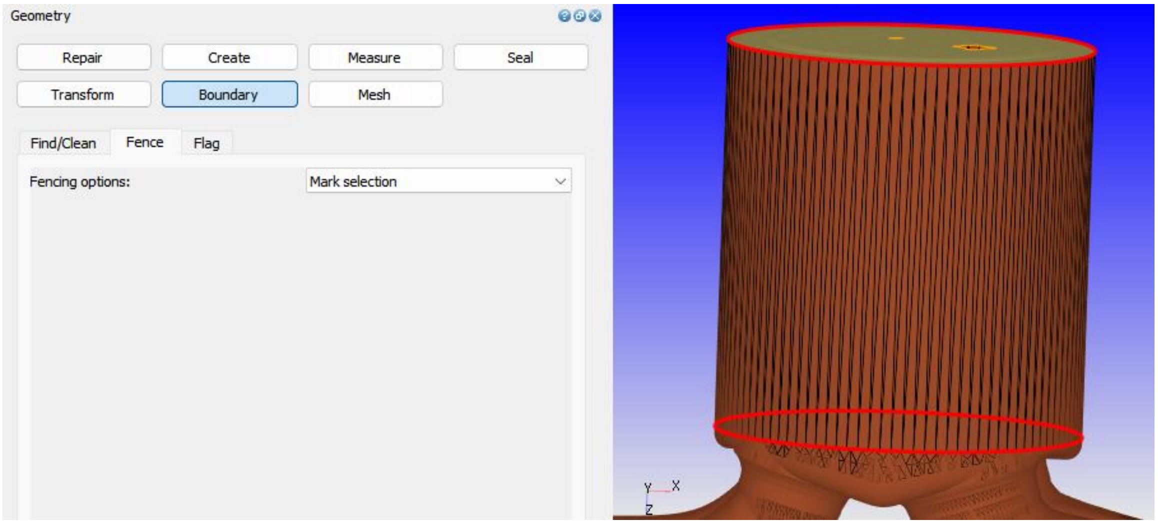

Go to Geometry → Boundary →Flag → using by boundary fence, select cylinder → name boundary as liner → Apply.

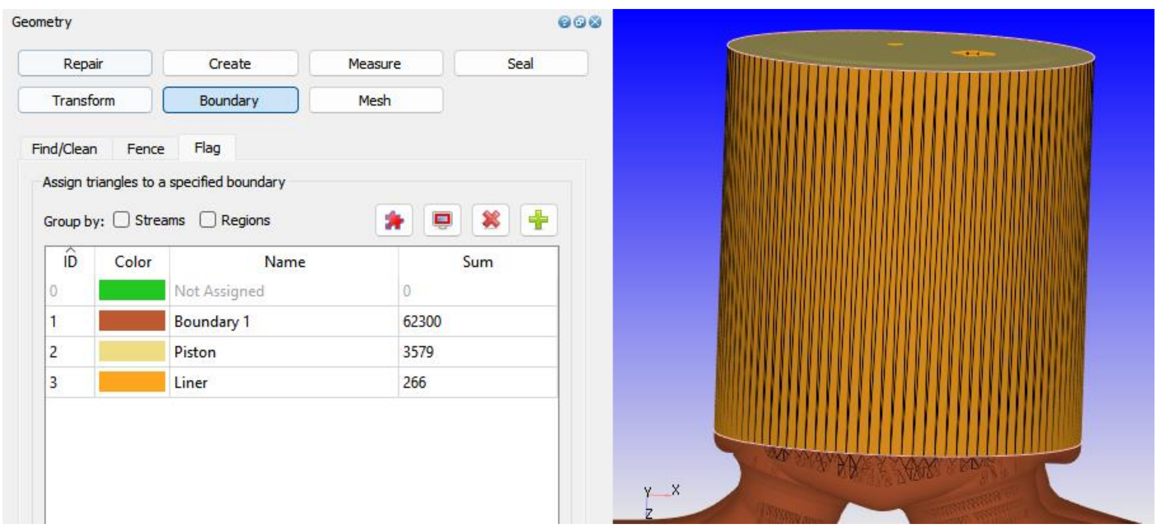

Inflow

Go to Geometry → Boundary →Flag → using by angle triangle, select inlet → name boundary as inflow → Apply.

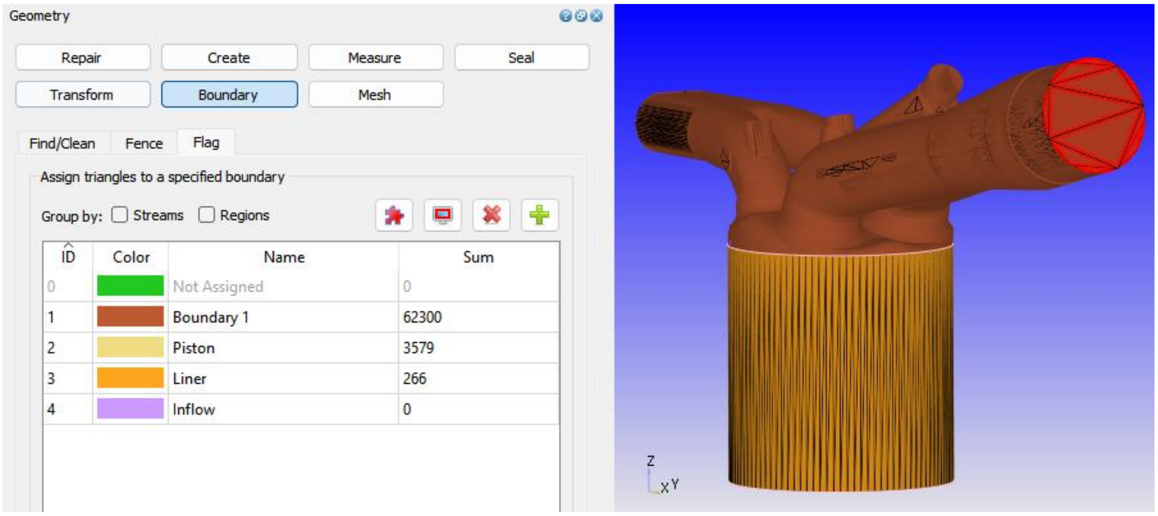

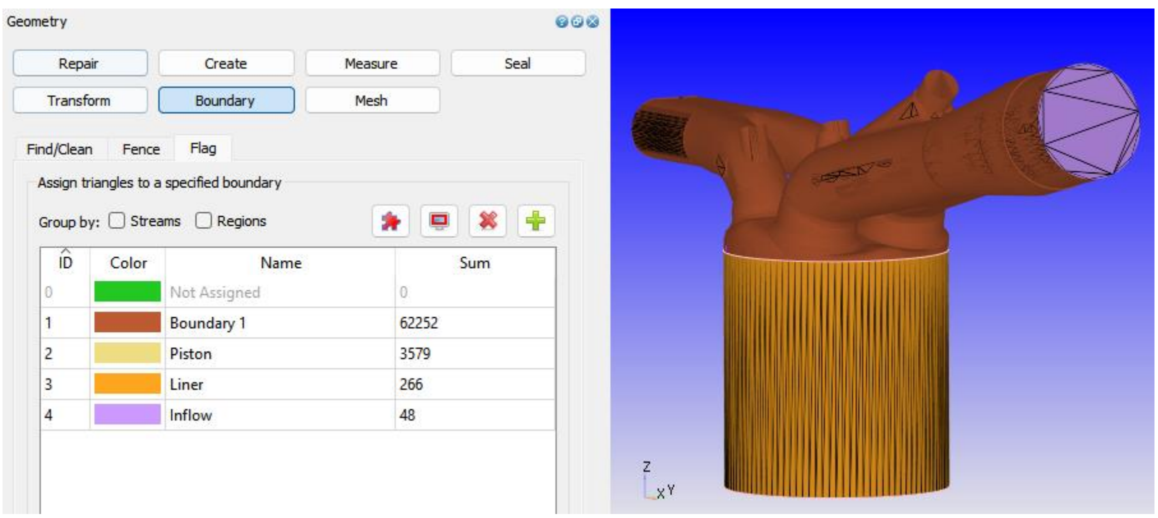

Cylinder Head

Go to Boundary → Fence →By selected edges → using by arc, select the edge as shown in the image → Mark fence.

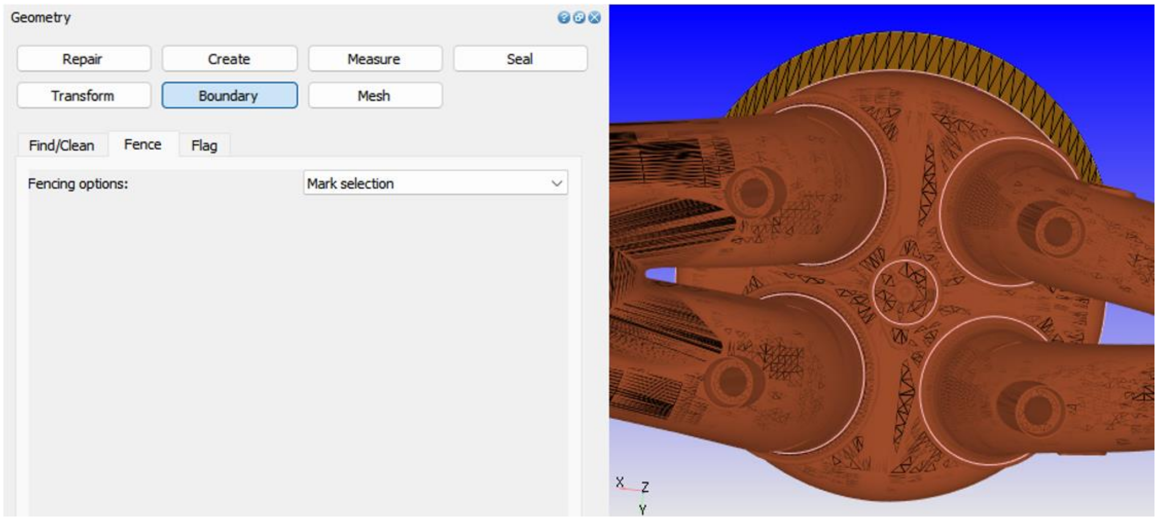

Go to Geometry → Boundary →Flag → using by boundary fence, select cylinder head → name boundary as cylinder head → Apply.

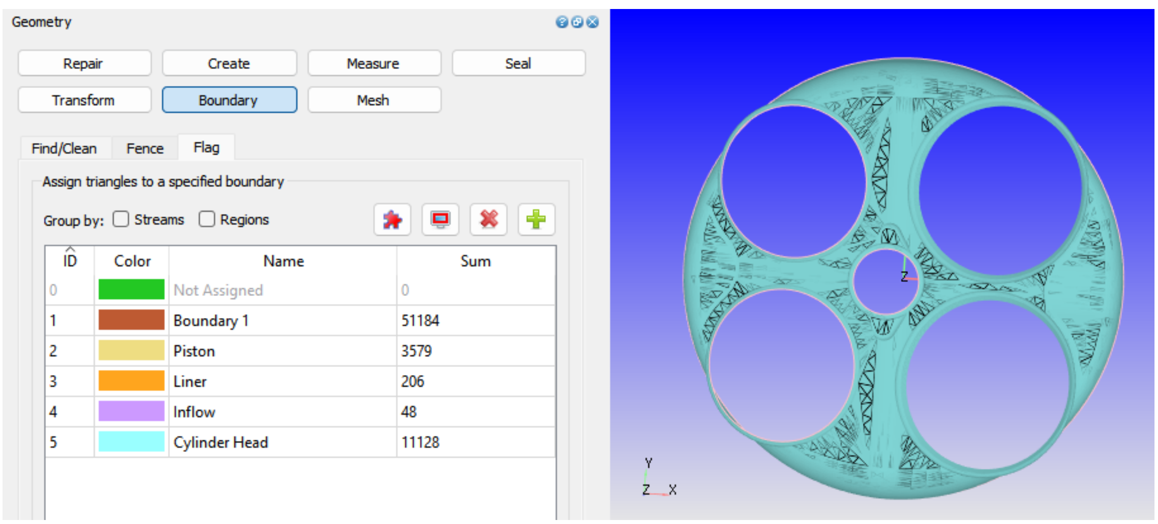

Exhaust Port

Go to Geometry → Boundary →Flag → using by angle triangle, select port → name boundary as exhaust port → Apply.

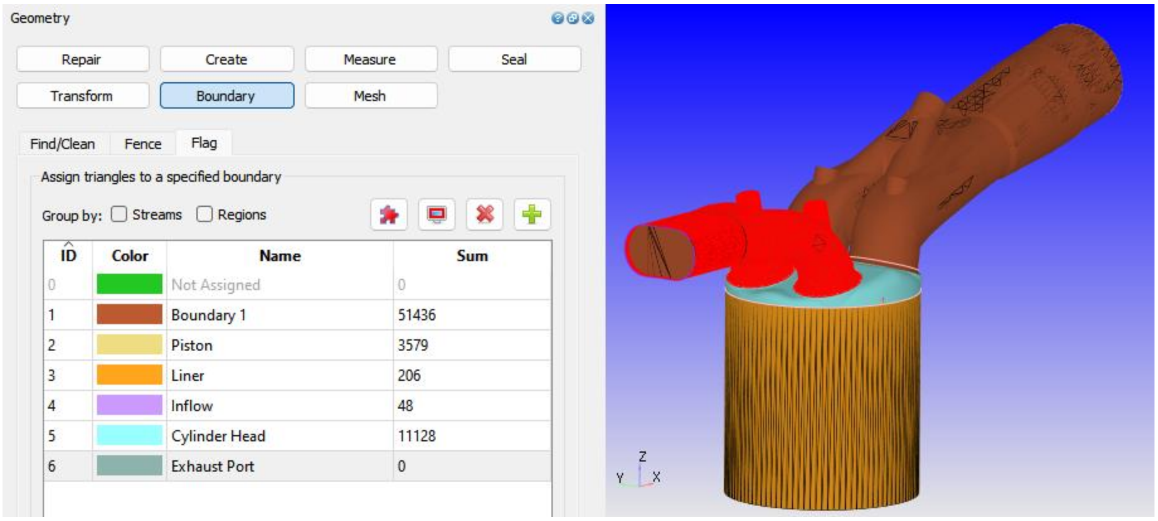

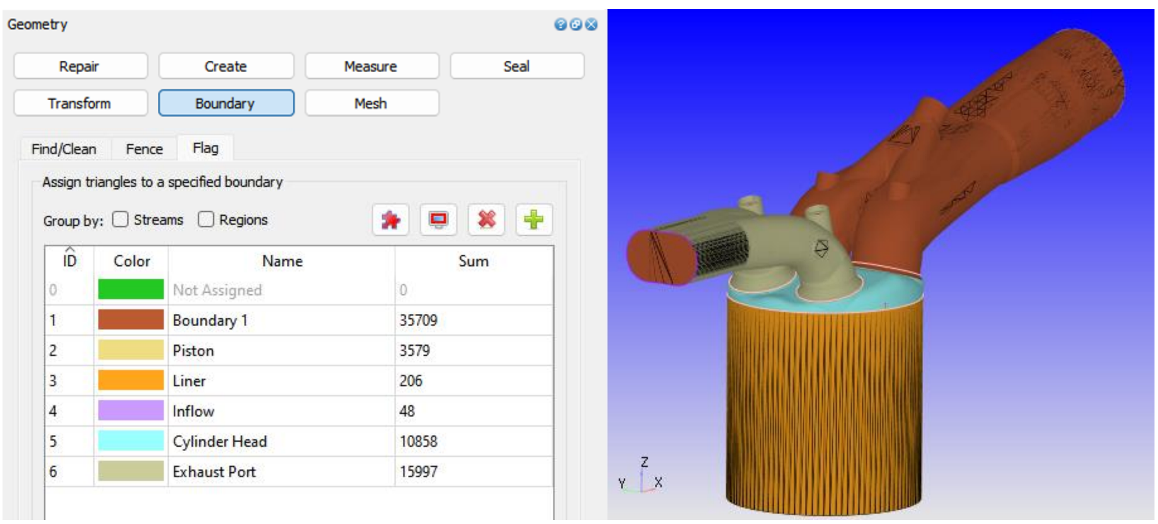

Hide all boundaries except for boundary 1. This will reveal any remaining triangles that were not previously selected and added to the exhaust port boundary, allowing them to be selected and included now.

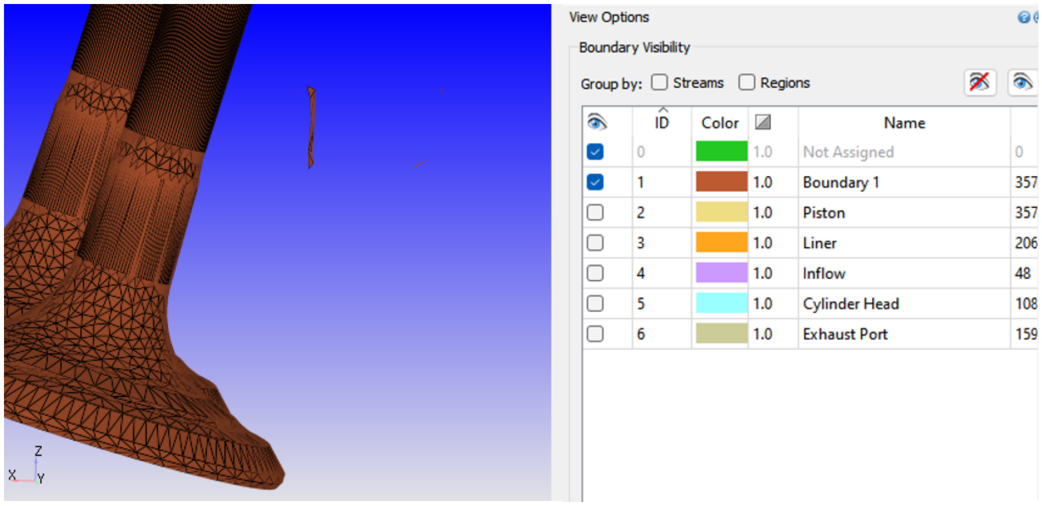

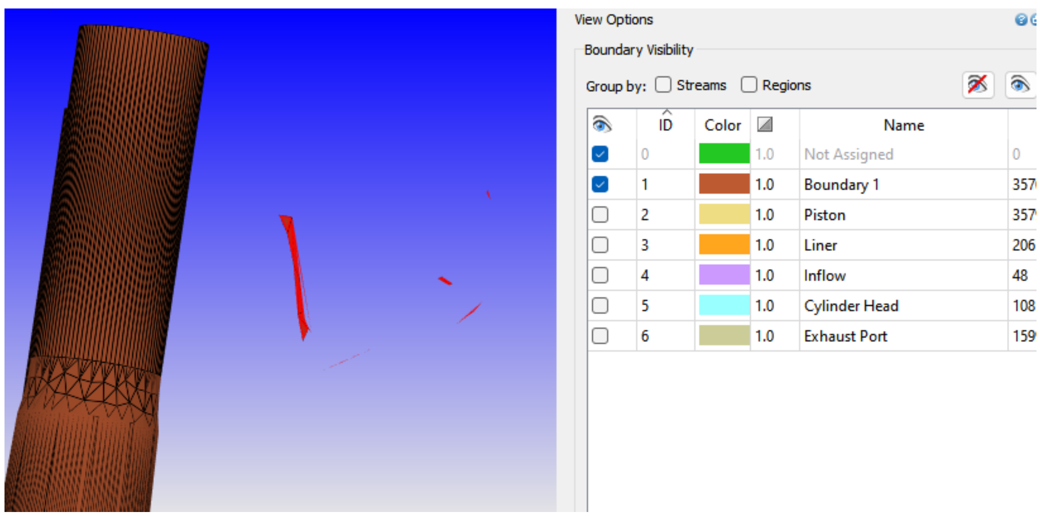

The selected triangles will be assigned to the exhaust port boundary.

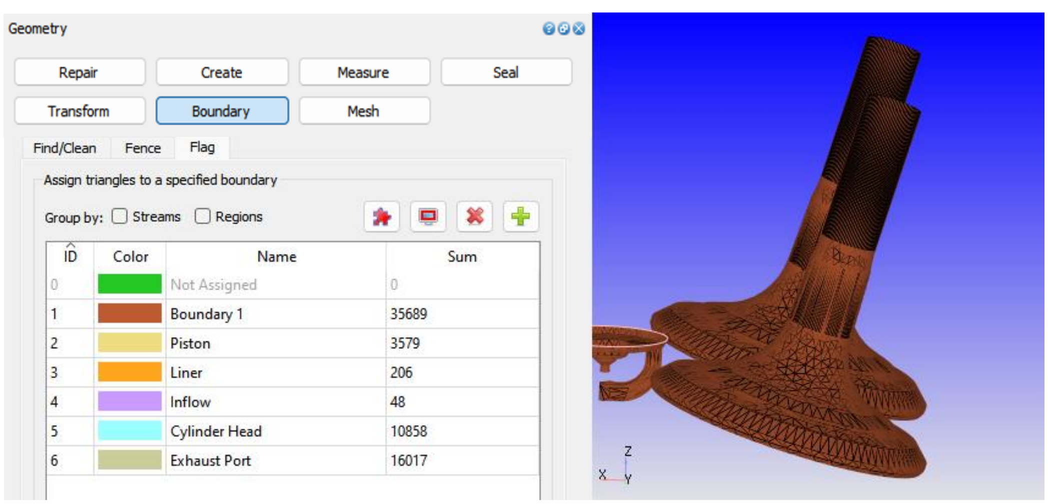

Outflow

Go to Geometry → Boundary →Flag → using by angle triangle, select outlet → name boundary as outflow → Apply.

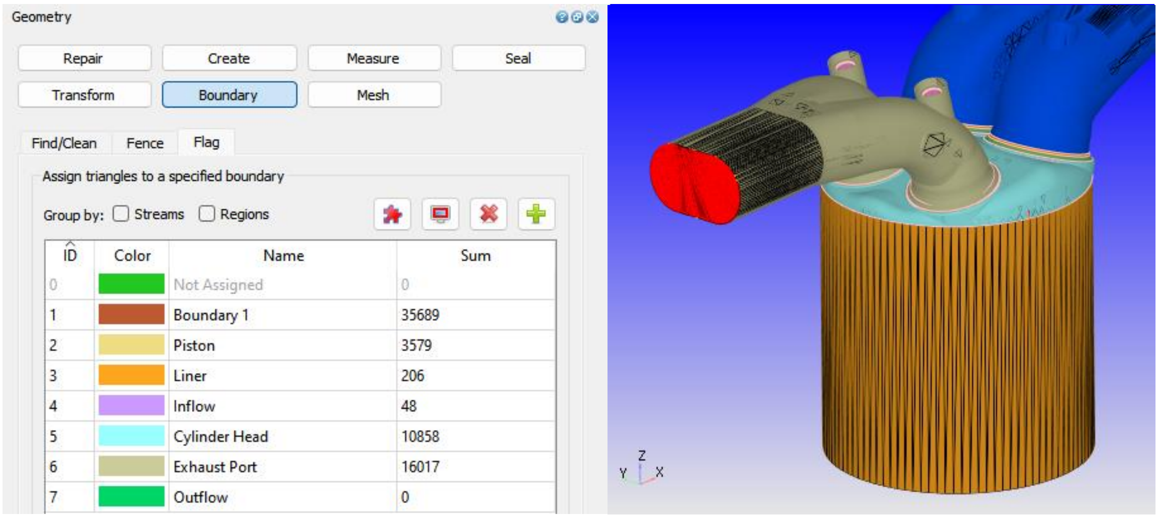

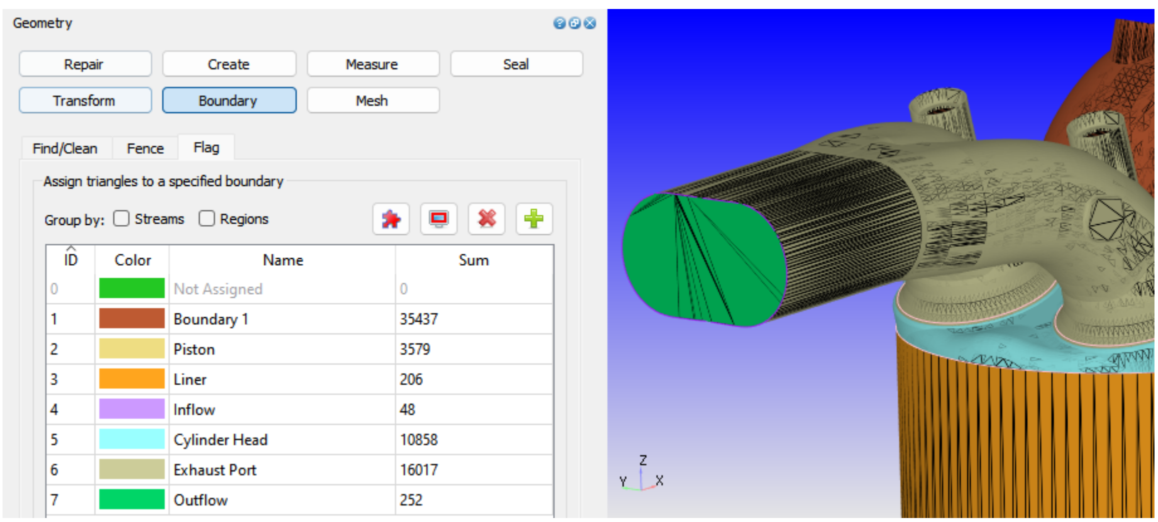

Exhaust Valve Top, Exhaust Valve Angle, and Exhaust Valve Bottom

Go to Geometry → Boundary →Flag → using by boundary fence, create three boundaries named as exhaust valve top, exhaust valve angle, and exhaust valve bottom.

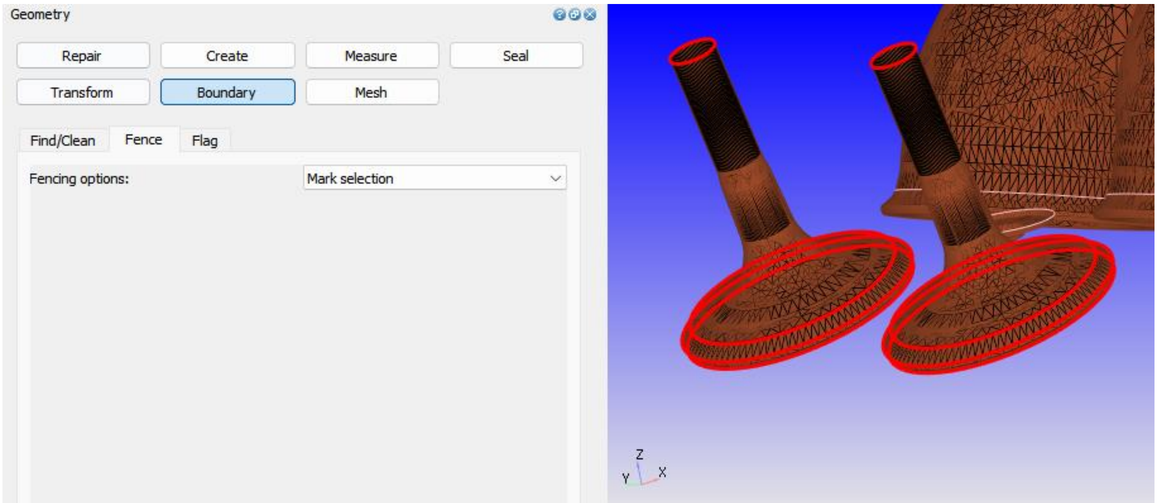

Exhaust Valve Top

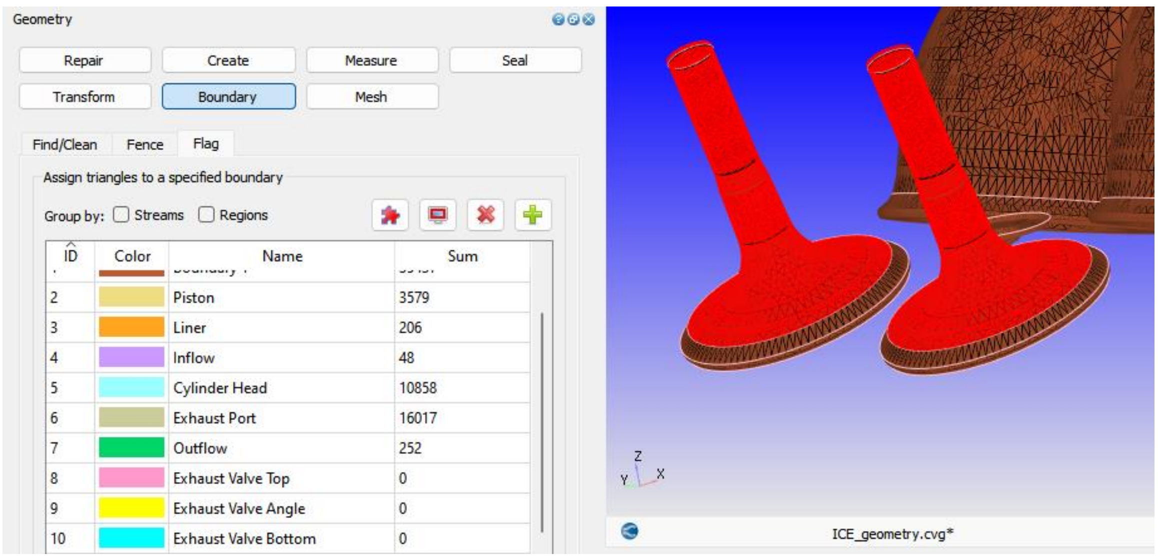

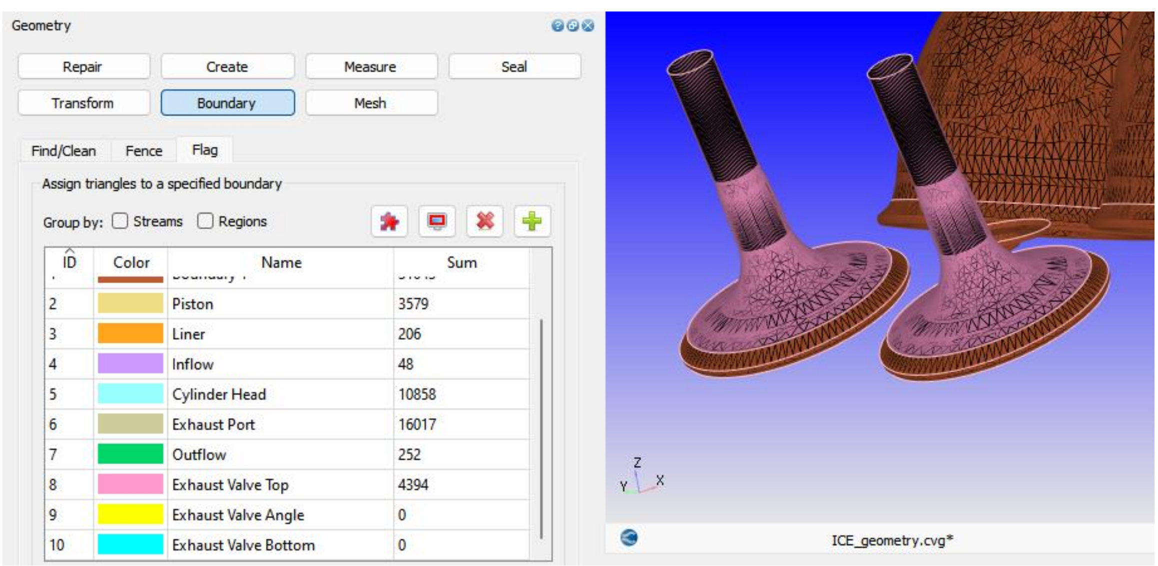

Exhaust Valve Angle

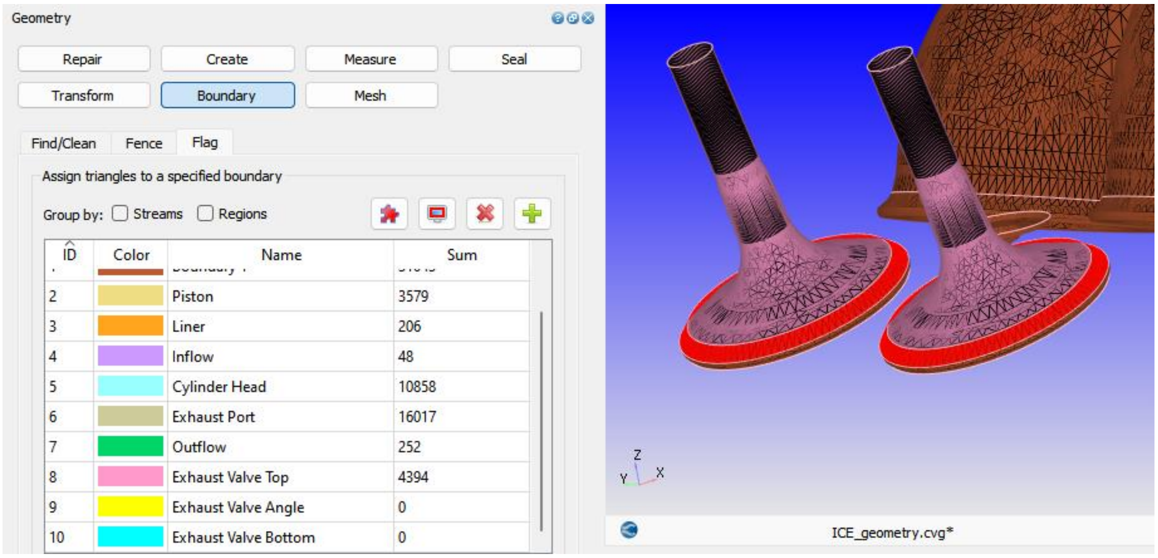

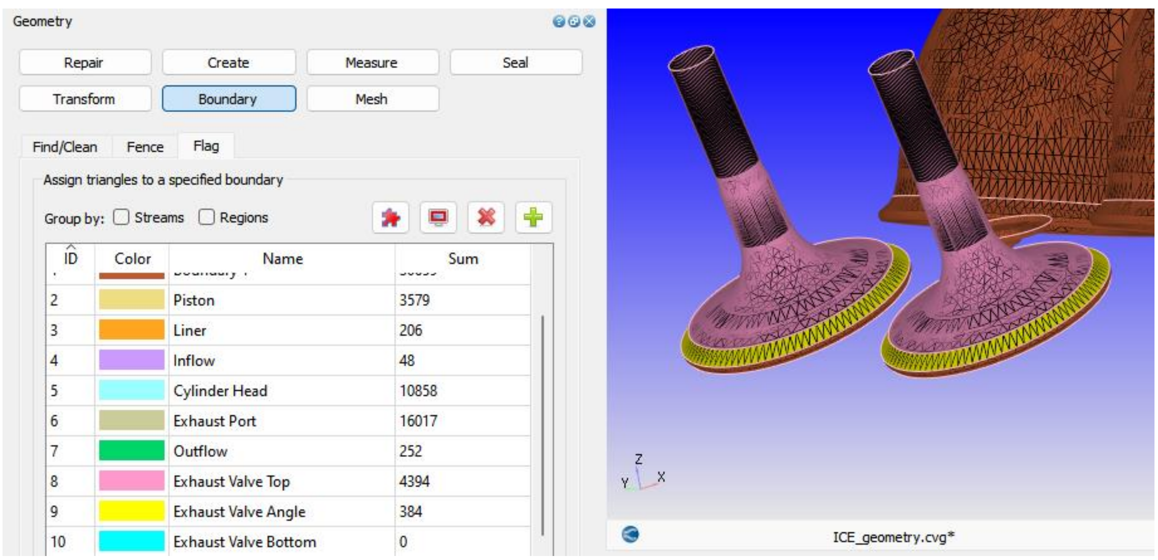

Exhaust Valve Bottom

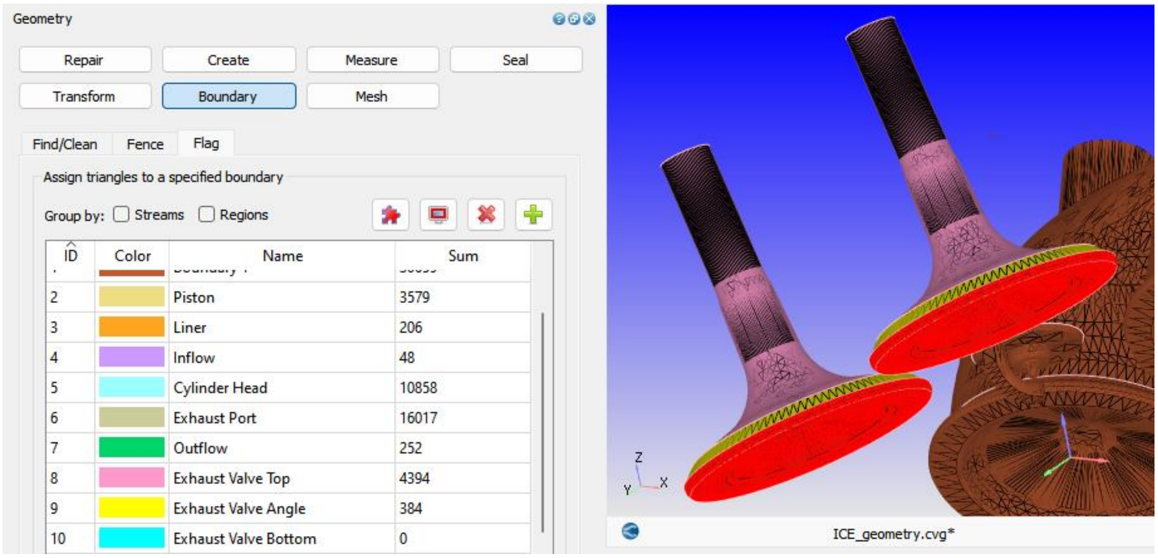

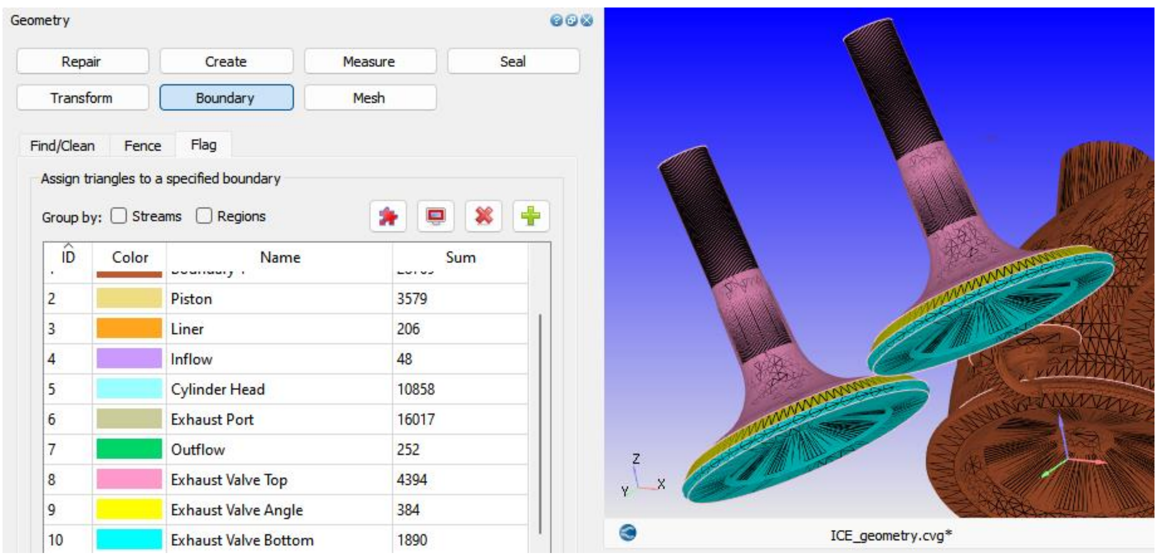

Intake Port 1 and Intake Port 2

Divide the intake port into two sections using fences. Label the section closest to the cylinder head as 'Intake Port 1' and the other as 'Intake Port 2'.

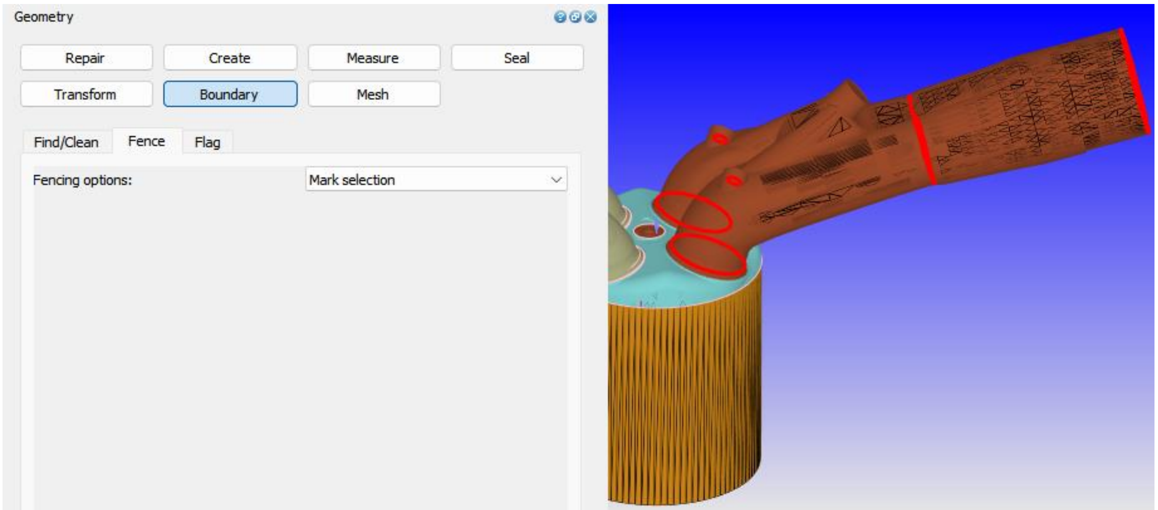

Intake Port 1

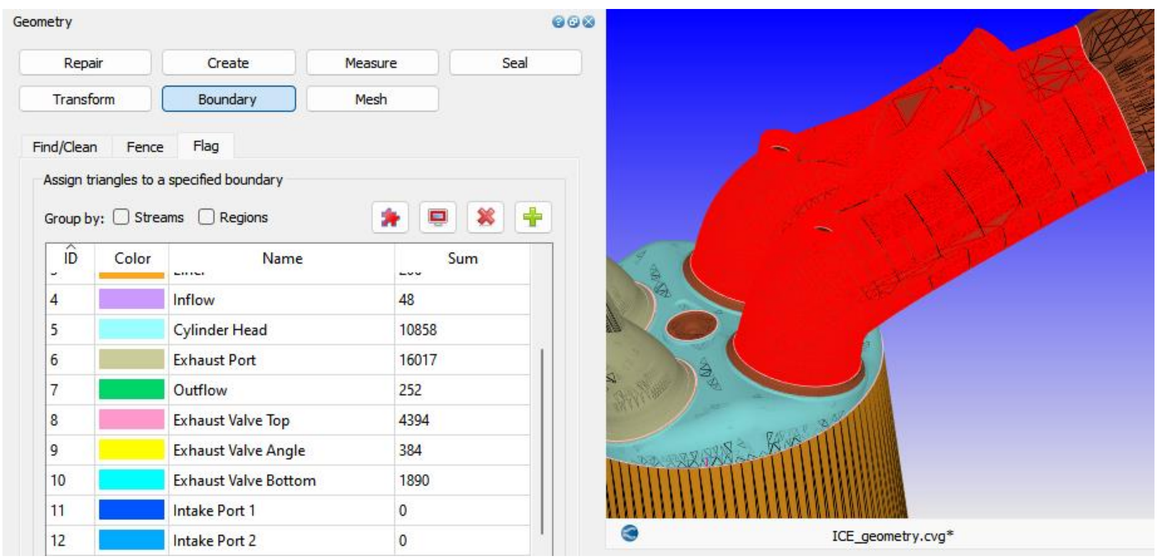

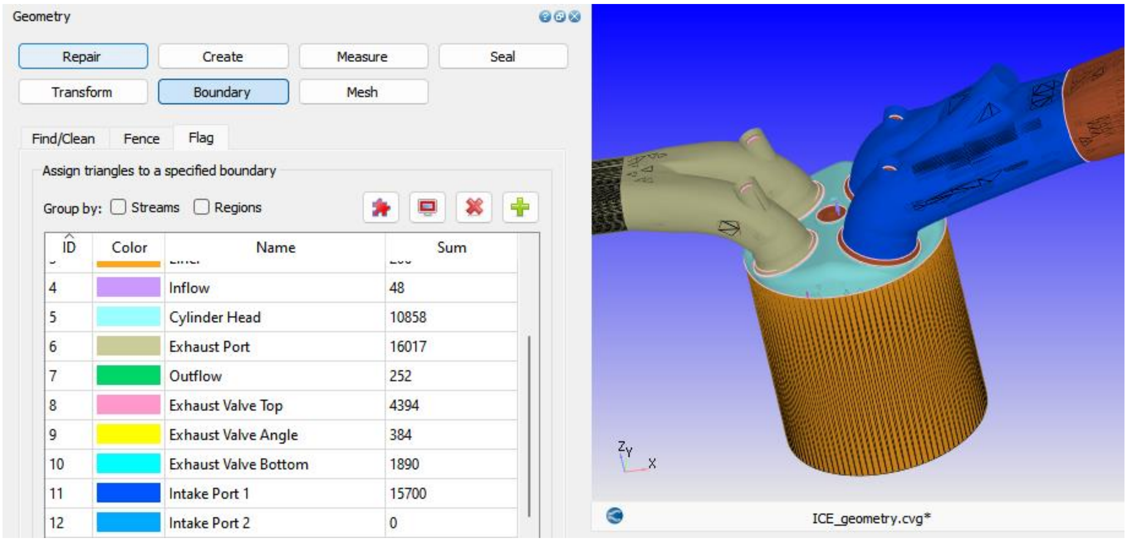

Intake Port 2

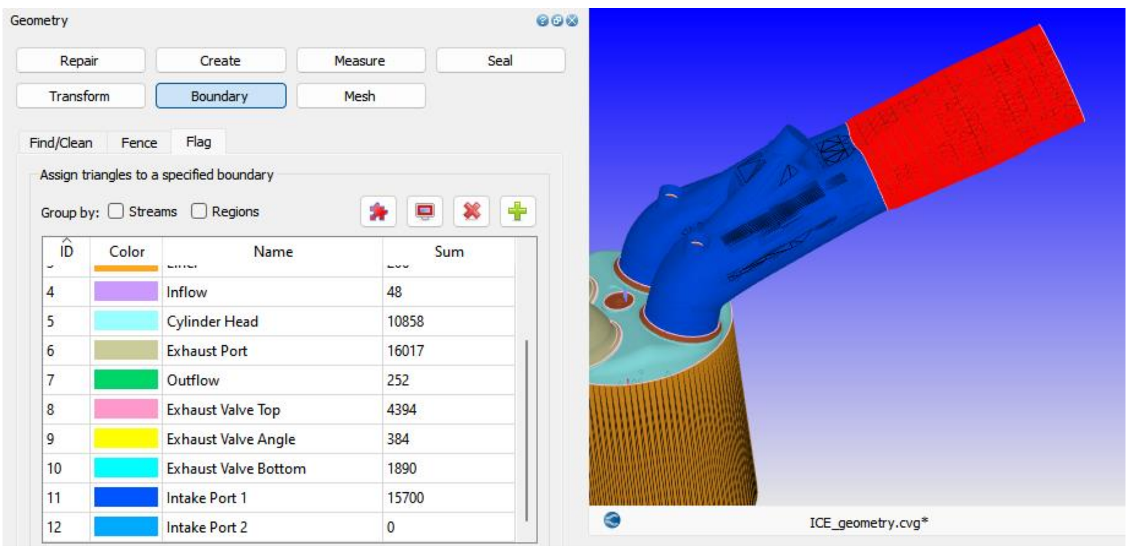

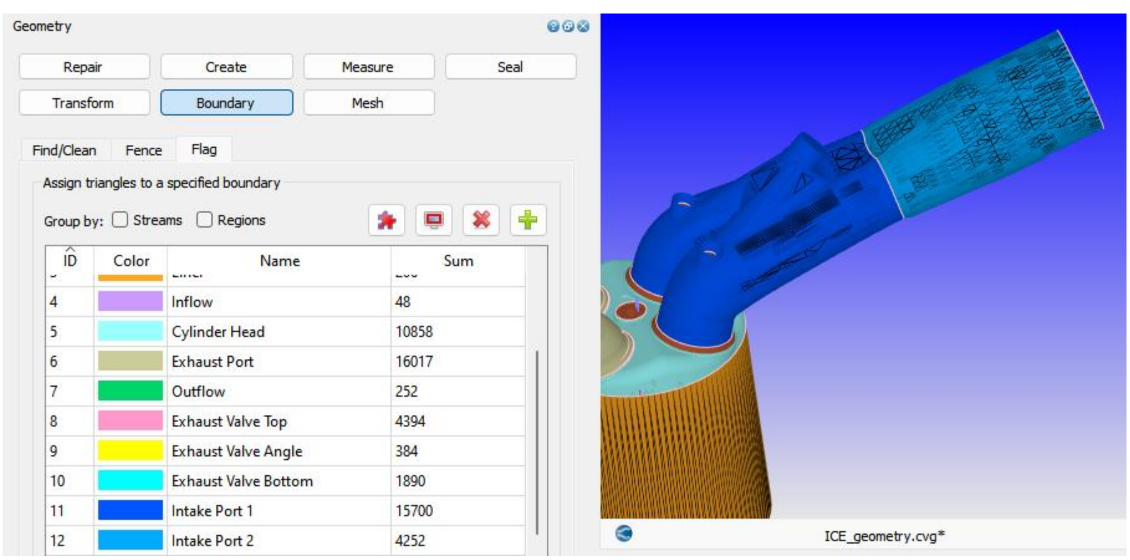

Assign ring triangles to the corresponding exhaust and intake ports.

For the exhaust port:

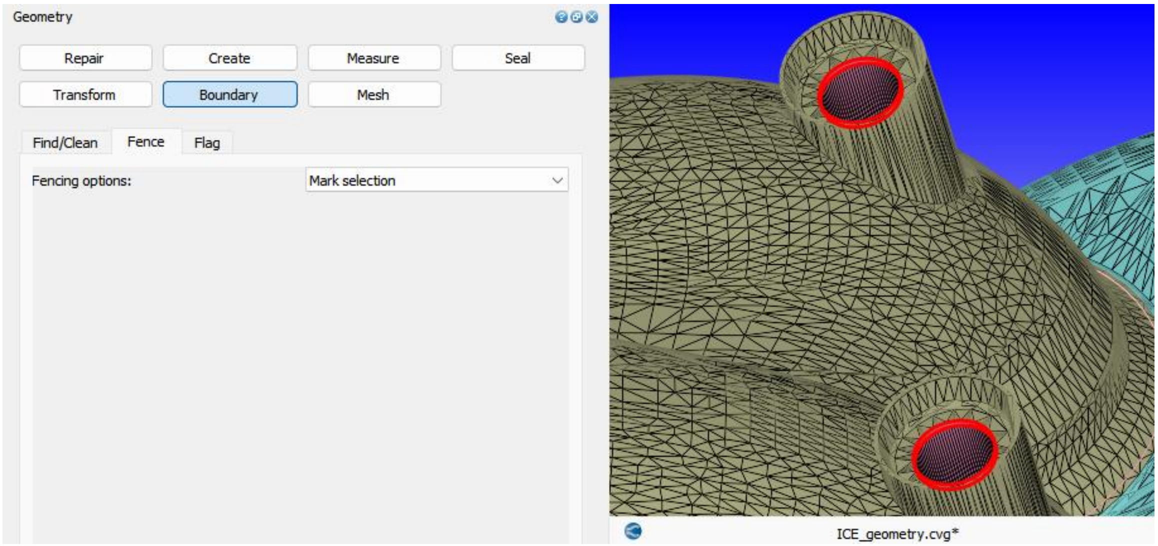

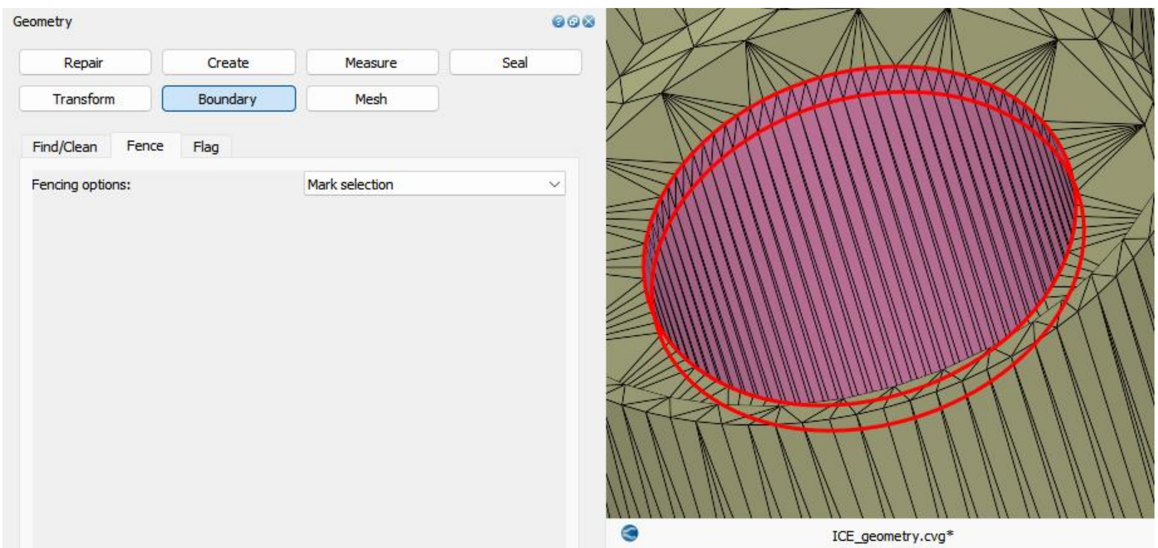

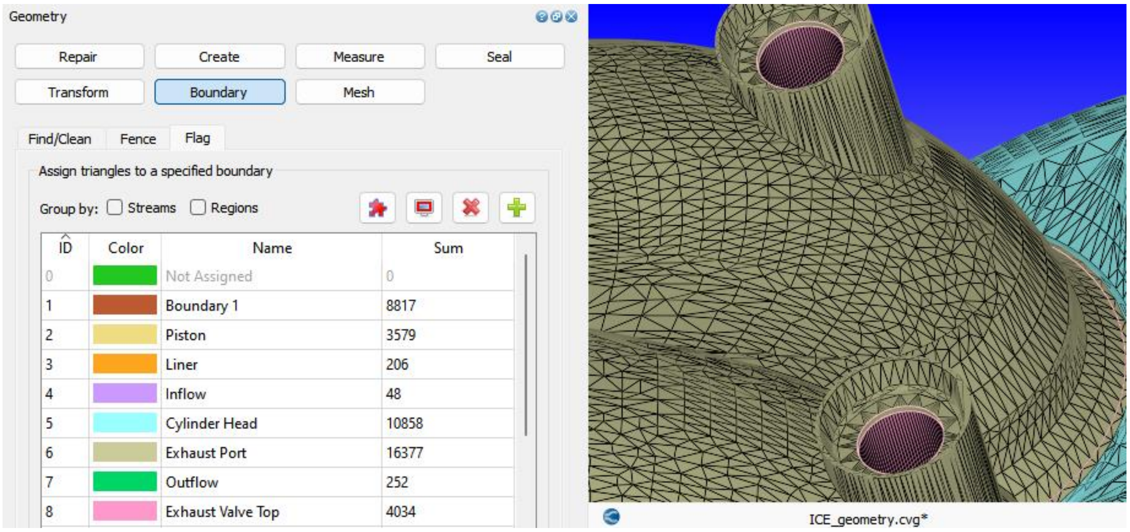

For the intake port:

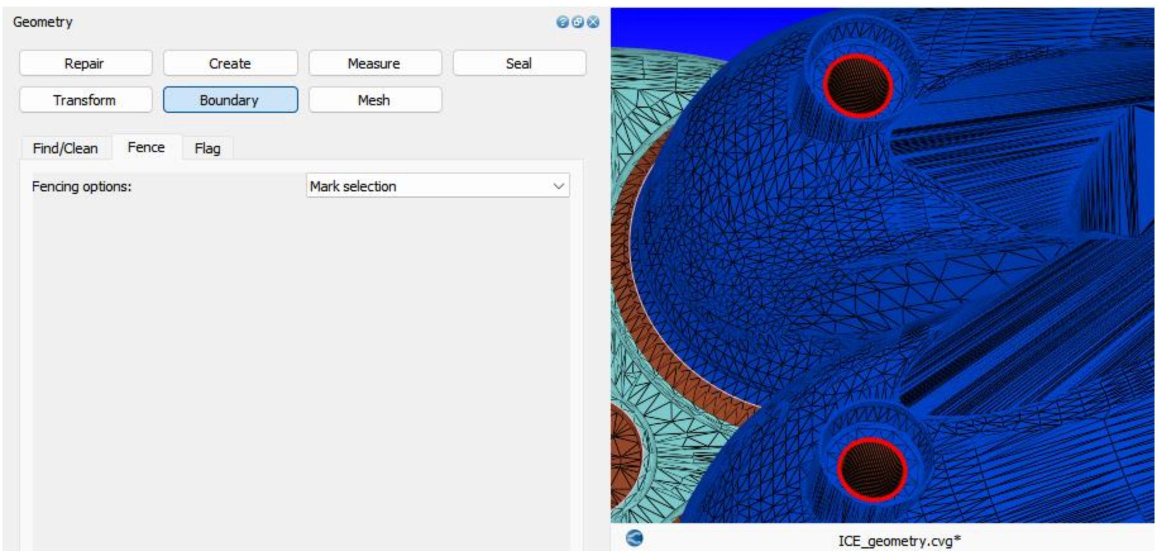

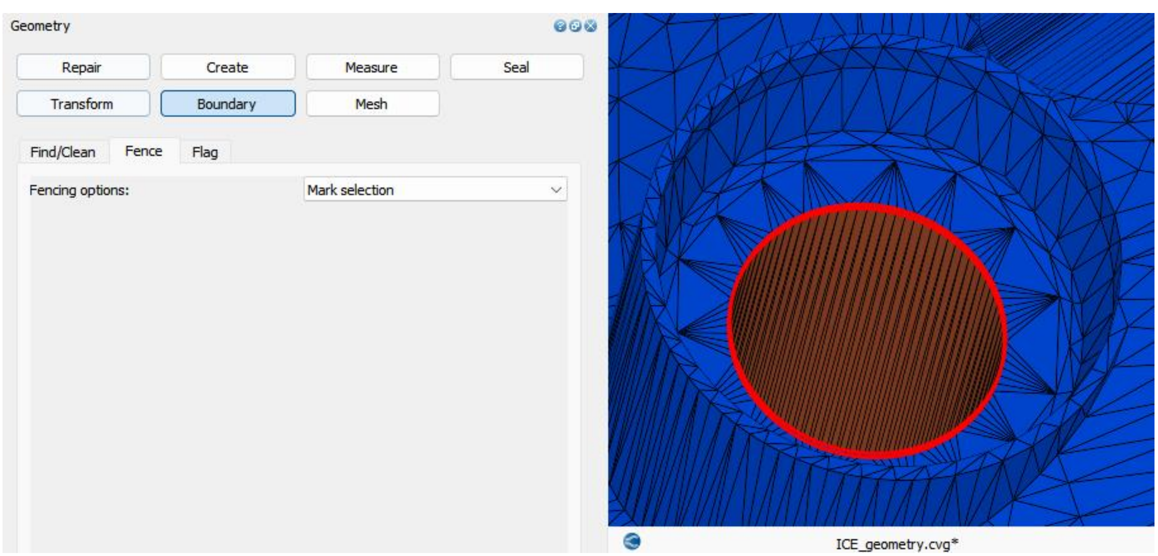

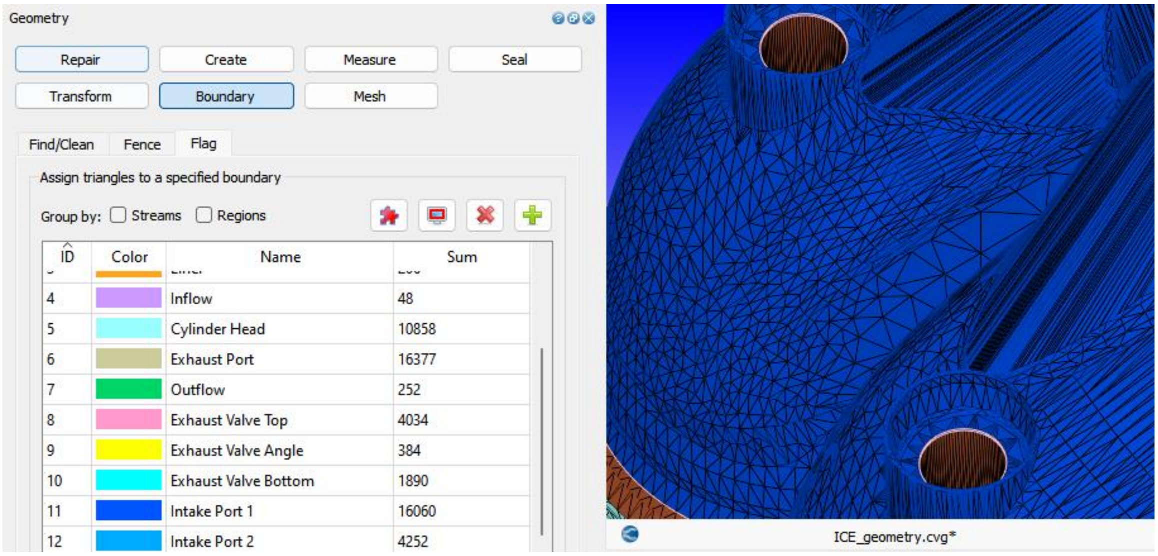

Intake Valve Top, Intake Valve Angle, and Intake Valve Bottom

Go to Geometry → Boundary →Flag → using by boundary fence, create three boundaries named as intake valve top, intake valve angle, and intake valve bottom.

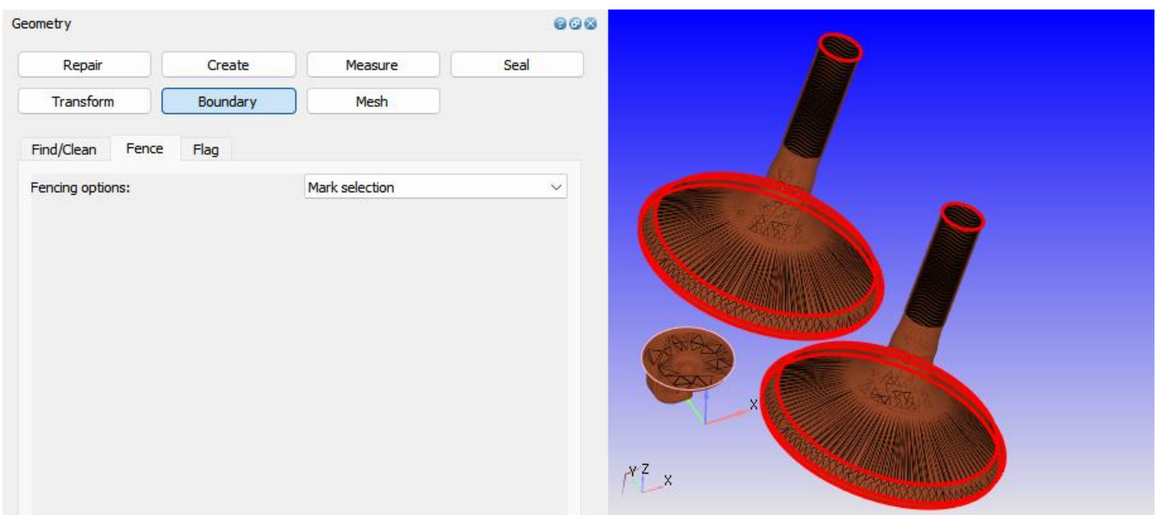

Intake Valve Top

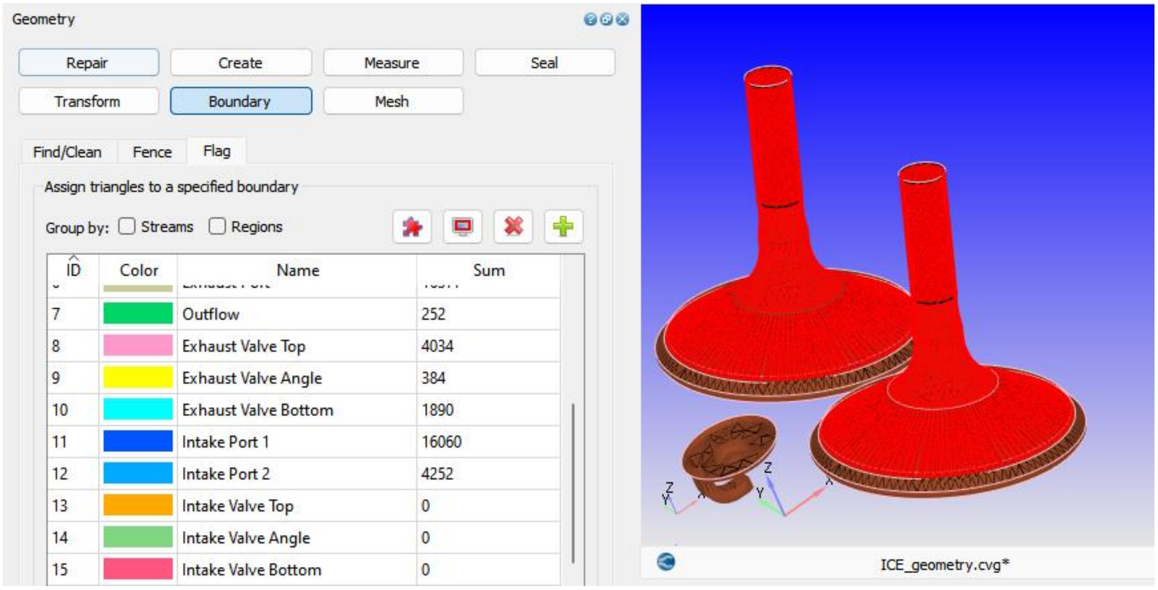

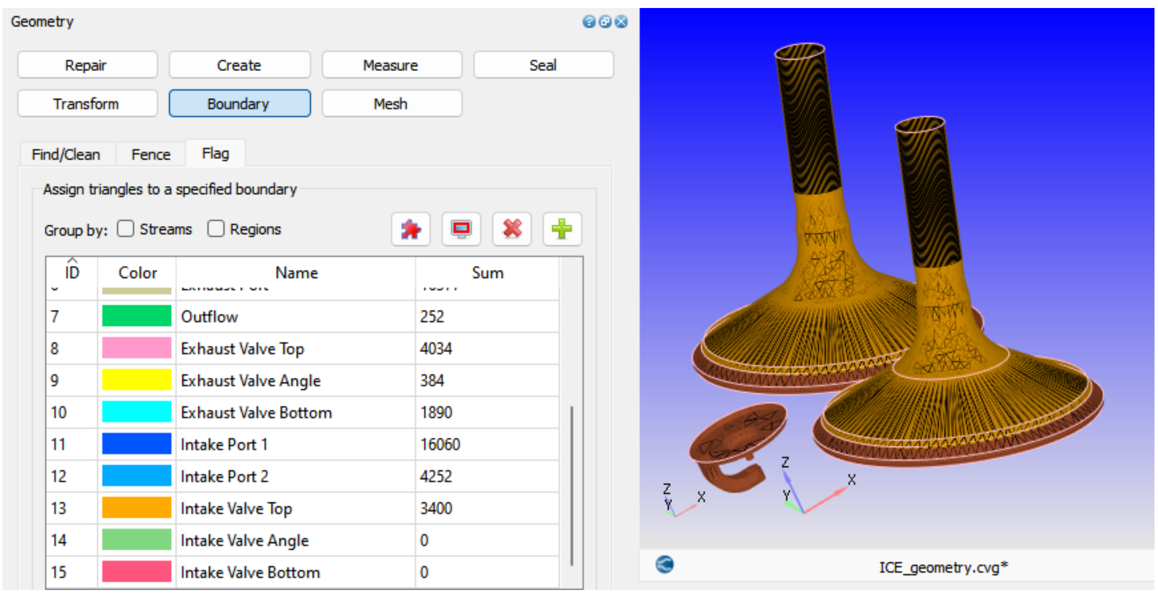

Intake Valve Angle

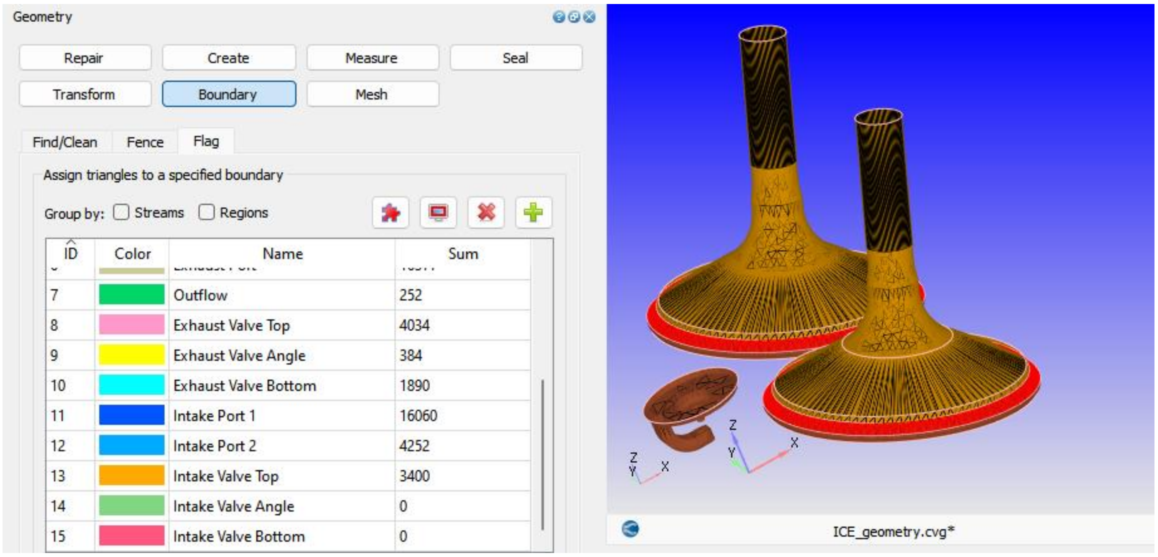

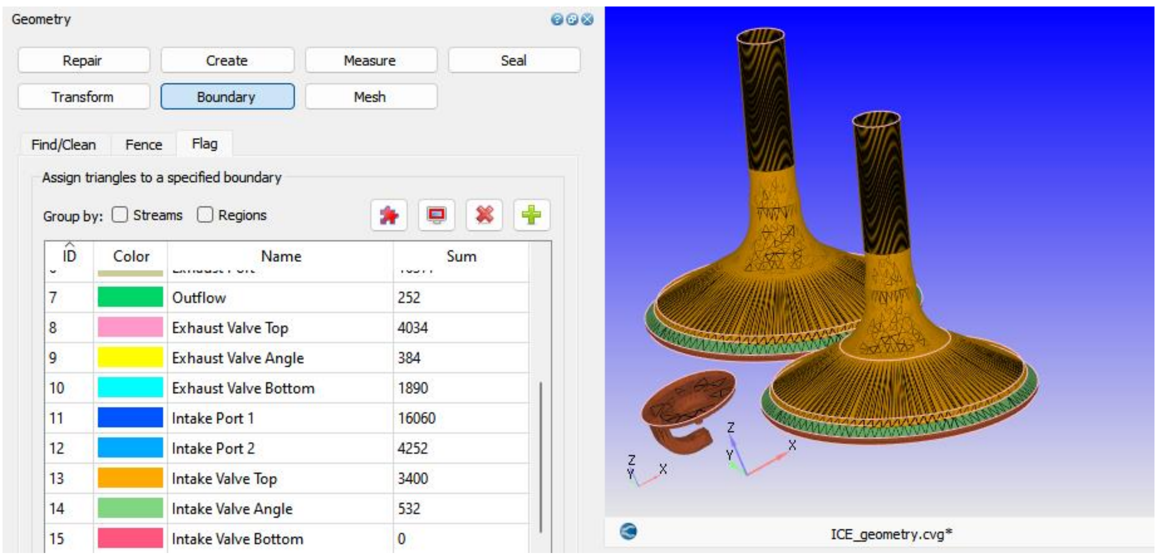

Intake Valve Bottom

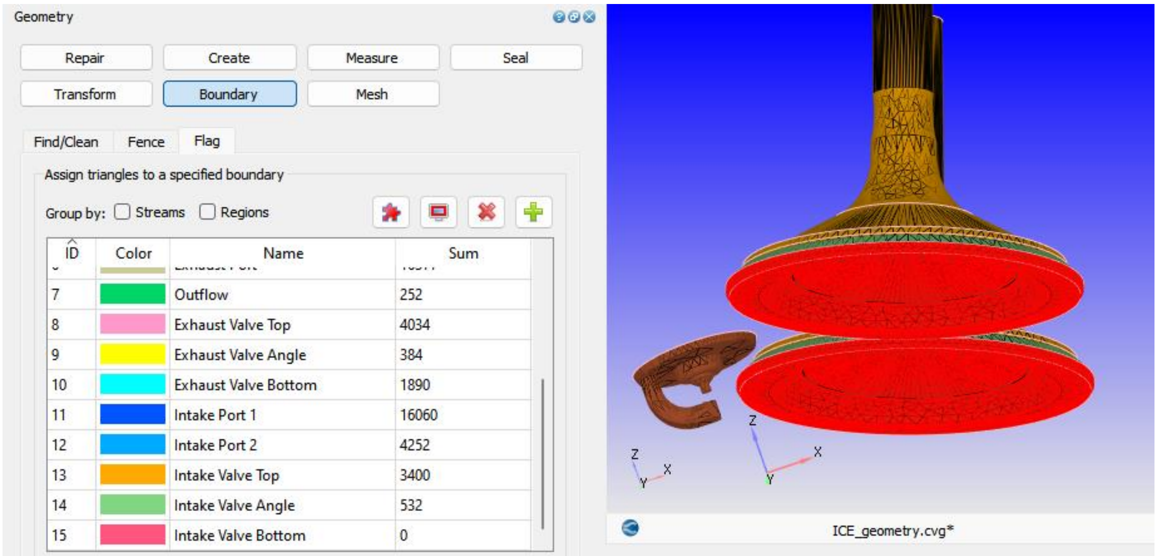

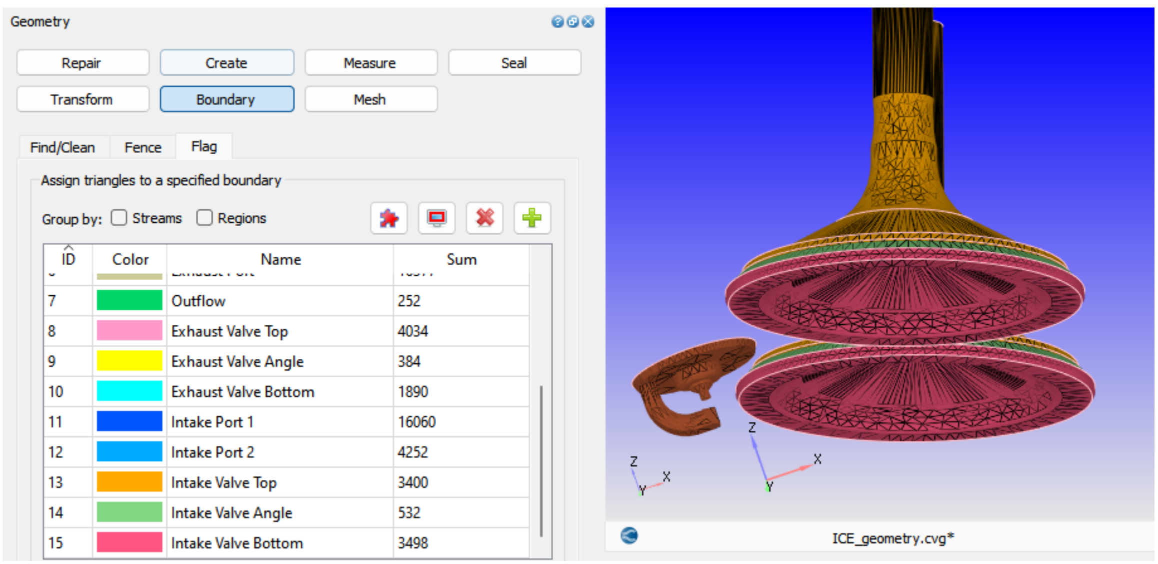

Spark Plug

Go to Geometry → Boundary →Flag → using by boundary fence, select spark plug → name boundary as spark plug → Apply.

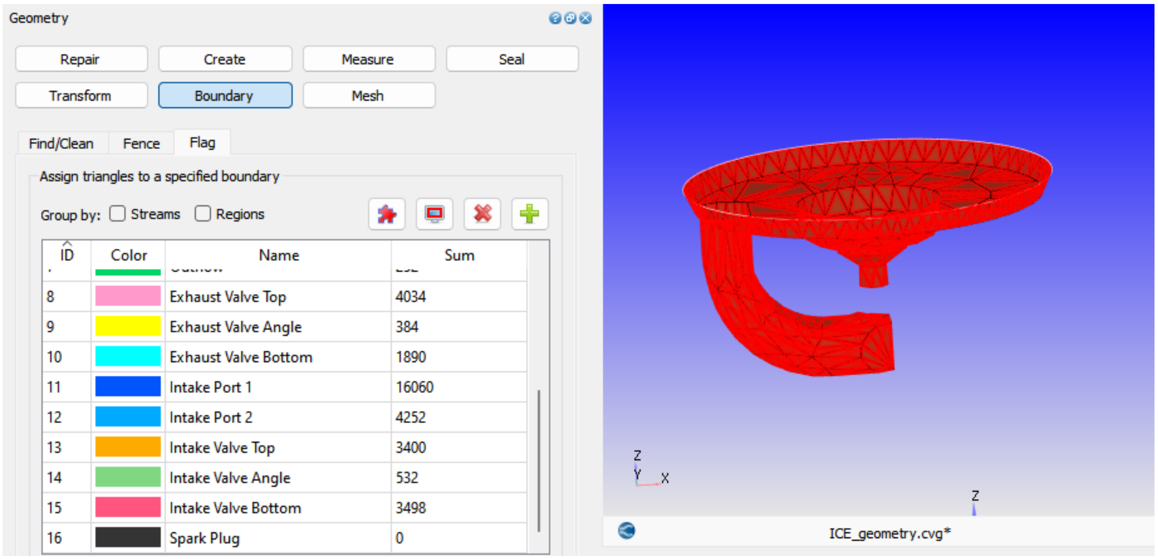

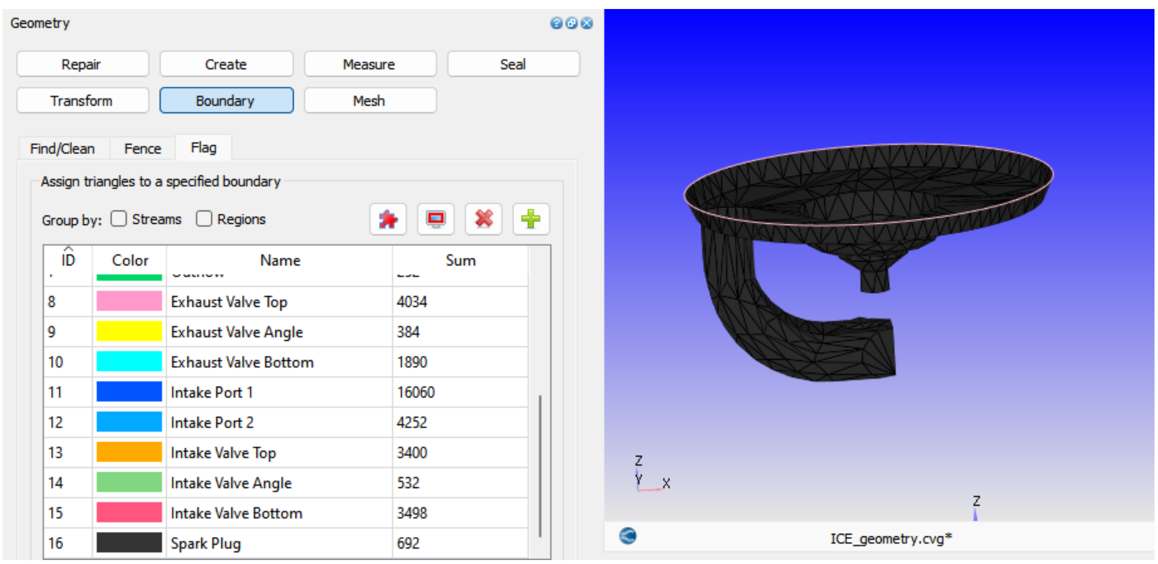

Spark Plug Terminal

Go to Geometry → Boundary →Flag → using by angle triangle, select spark plug terminal → name boundary as spark plug terminal → Apply.

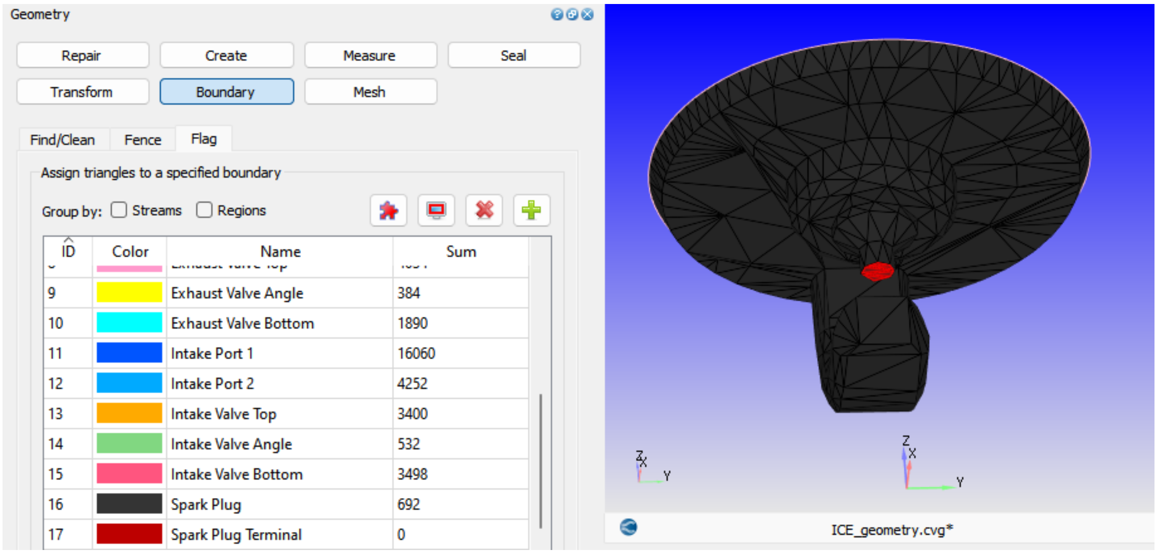

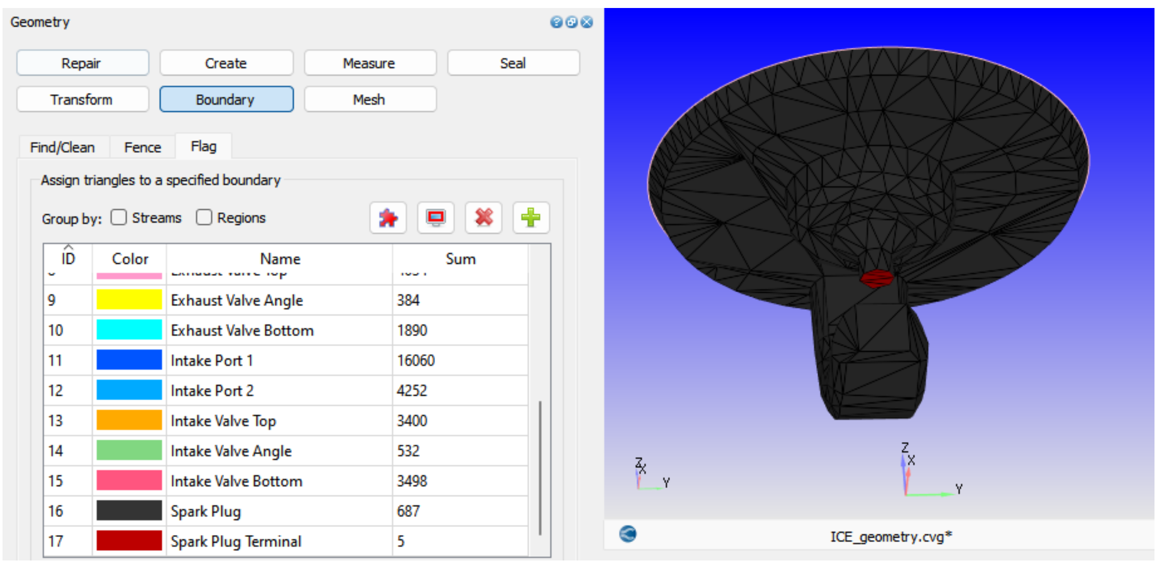

Boundary Flagging Checkup

After flagging all the boundaries, 71 triangles remain unassigned to their respective boundaries. These need to be identified and properly assigned to the appropriate boundaries.

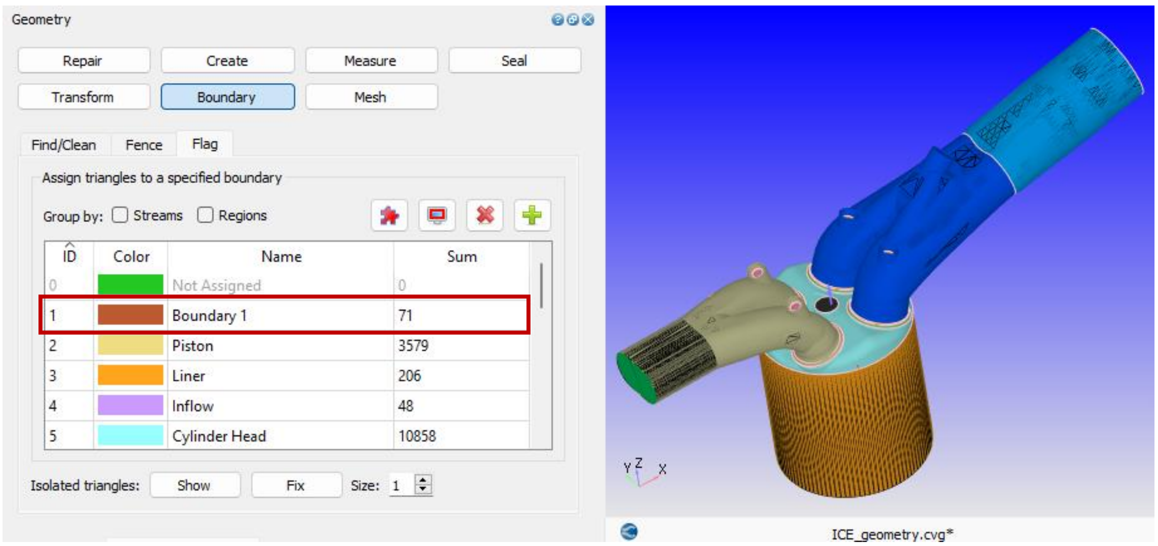

By hiding all the boundaries and showing boundary 1 only, it will be easier to identify these triangles.

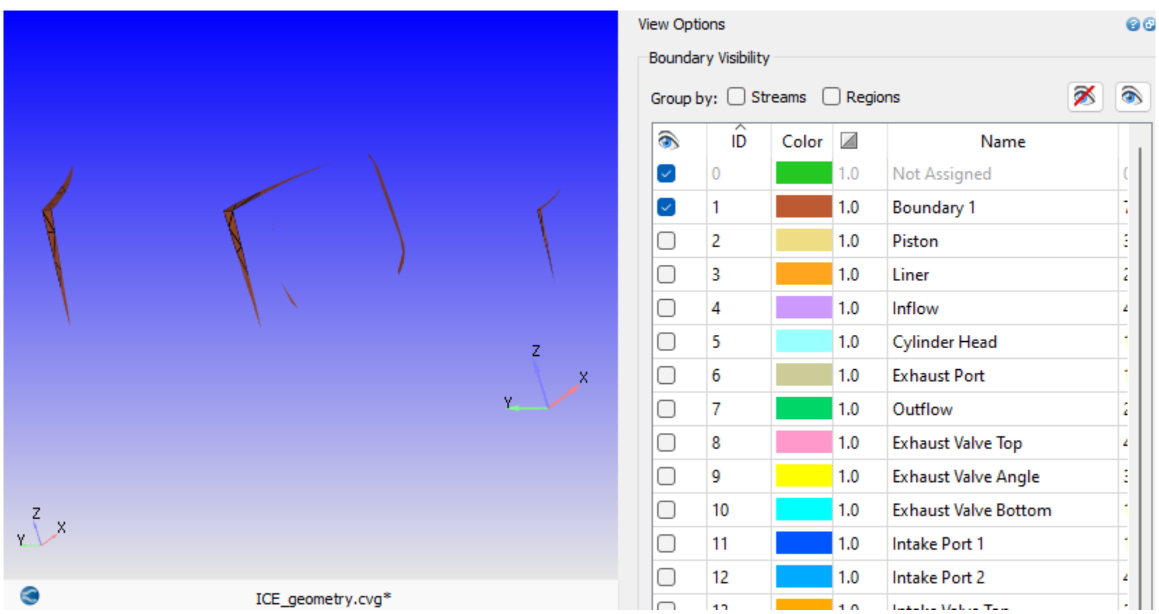

Once the triangles are assigned to their appropriate boundaries, the number of triangles assigned to boundary 1 should be reduced to zero.

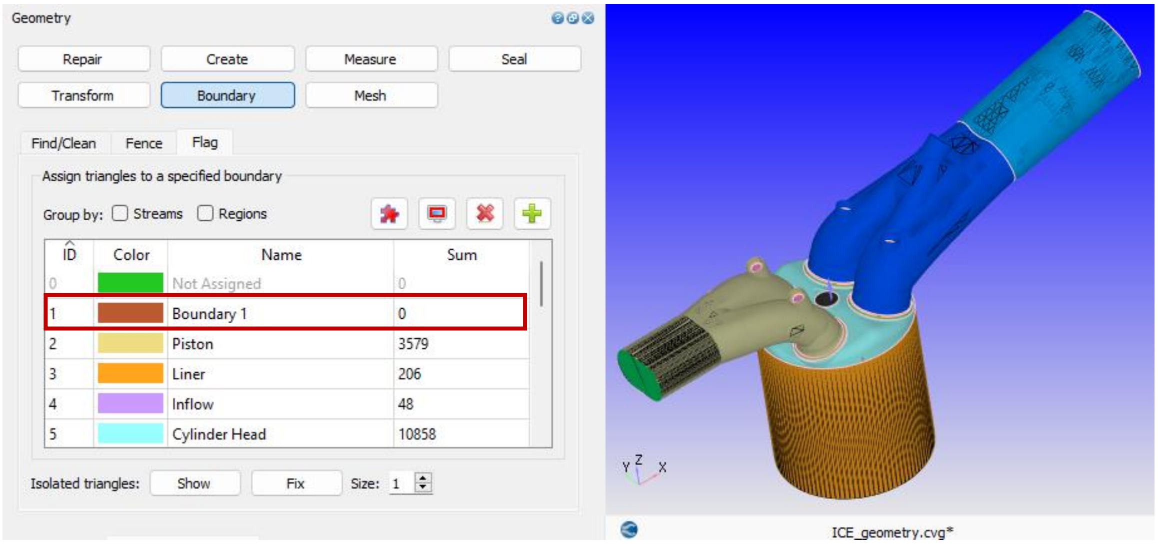

After confirming that, boundary 1 can be deleted.

Diagnosis Check-up

After setting up the geometry, a diagnostic check was conducted to identify the errors in geometry.

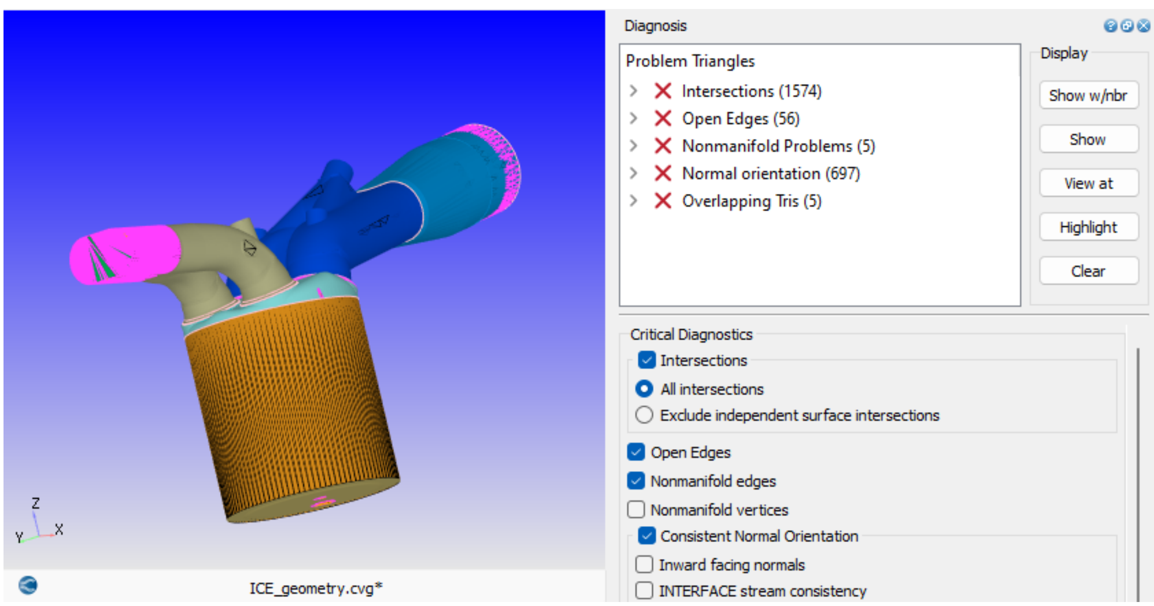

There are 1,574 intersection problems, 56 open edges, 5 non-manifold issues, 697 normal orientation problems, and 5 overlapping triangles that need to be addressed.

Intersection errors

Intersection errors occur when more than two triangles intersect with each other. In this case, the errors are happening because the intake valves are lifted too high. As shown in the image below, the intake valves are protruding into the intake port (hidden for better visibility).

To resolve this issue, it is required to move the valves down. To do this, go to Transform → Translate → Selected boundaries, select intake valve top, intake valve angle, and intake valve bottom → enter a translation value of 0.002 m → Apply.

Additionally, the intersecting triangles issue highlighted in the red circle can be resolved by re-arranging them (deleting and recreating new ones) to prevent intersection as shown in the image below.

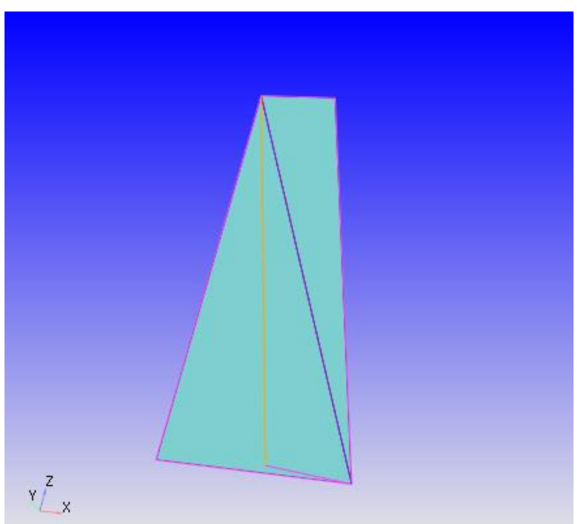

Open edges

These issues arise from incomplete triangle formation on the surface. To resolve them, go to the repair tool, select 'Patch,' choose the free edge loop, and use the open edge patch option to fix the affected surface.

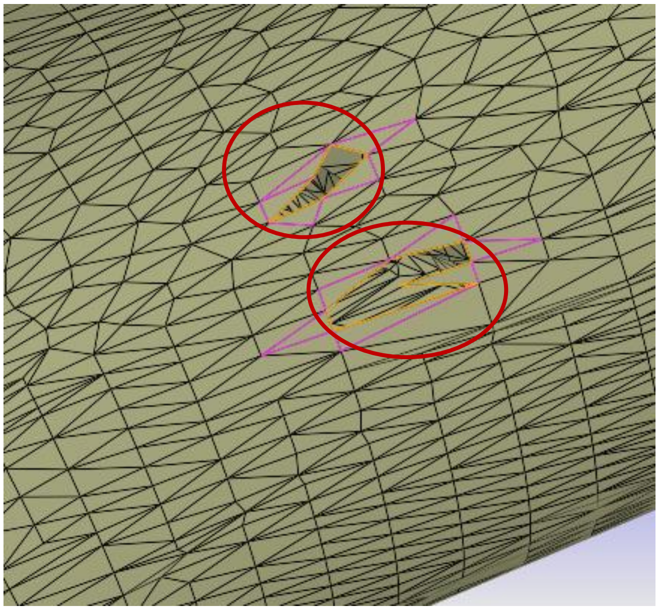

Nonmanifold problems

These occur when more than two triangles share the same edges. To resolve them, delete the overlapping triangles and create new ones.

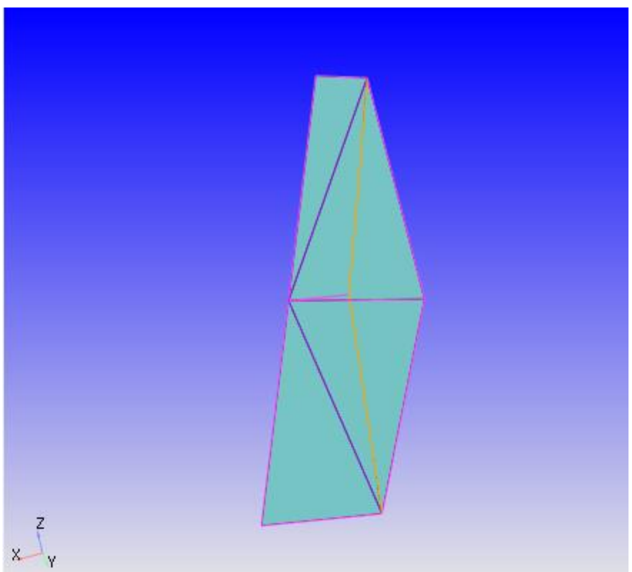

Normal Orientation

Normal orientation refers to the direction of a triangle's surface normal vector points. Correct orientation ensures accurate simulations, typically with normals pointing outward. If the normals are misaligned, they should be transformed inward to correct the issue.

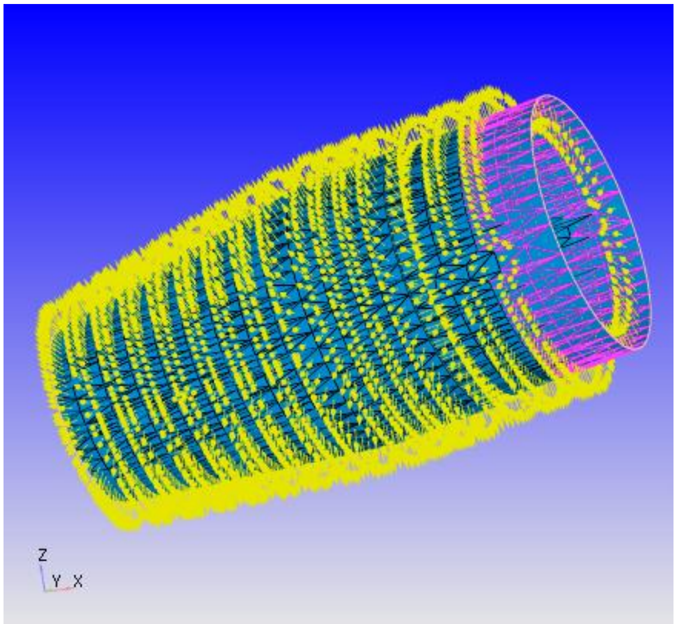

Overlapping triangles

Overlapping triangles are triangles that are stacked on top of each other. These can typically be fixed by deleting the overlapping triangles and then patching them back together.

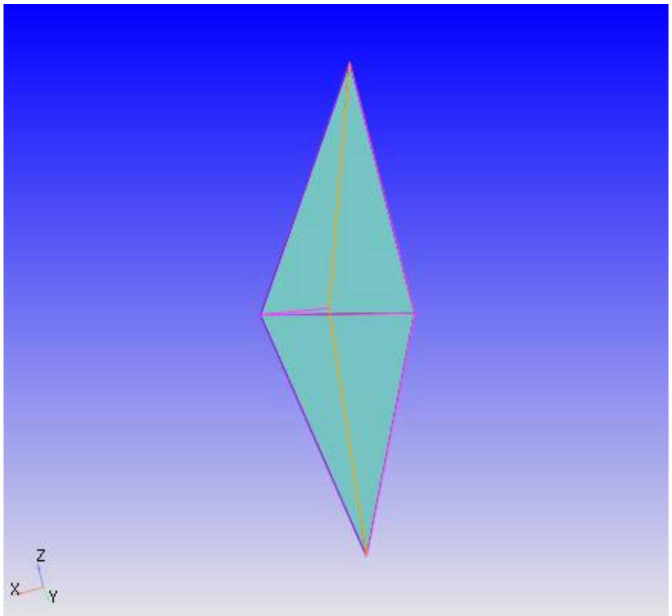

After resolving all the issues, a new diagnostic check was performed, confirming that no problems remain in the geometry.

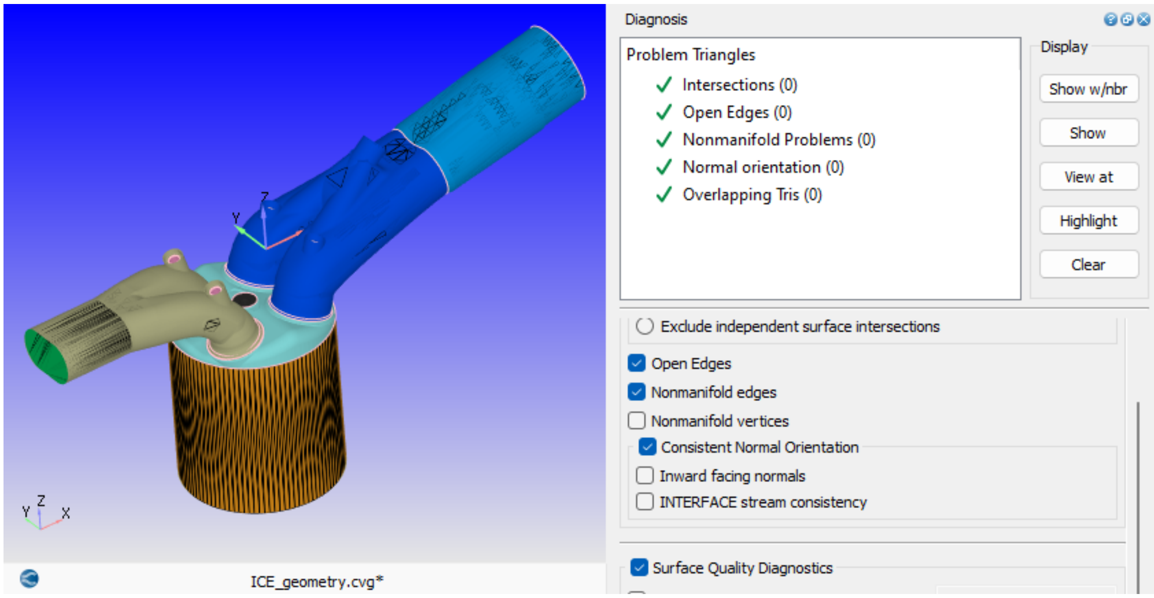

This concludes the geometry clean up procedure.

2. Case Setup

Application Type

A crank angle-based IC engine simulation was chosen for this analysis.

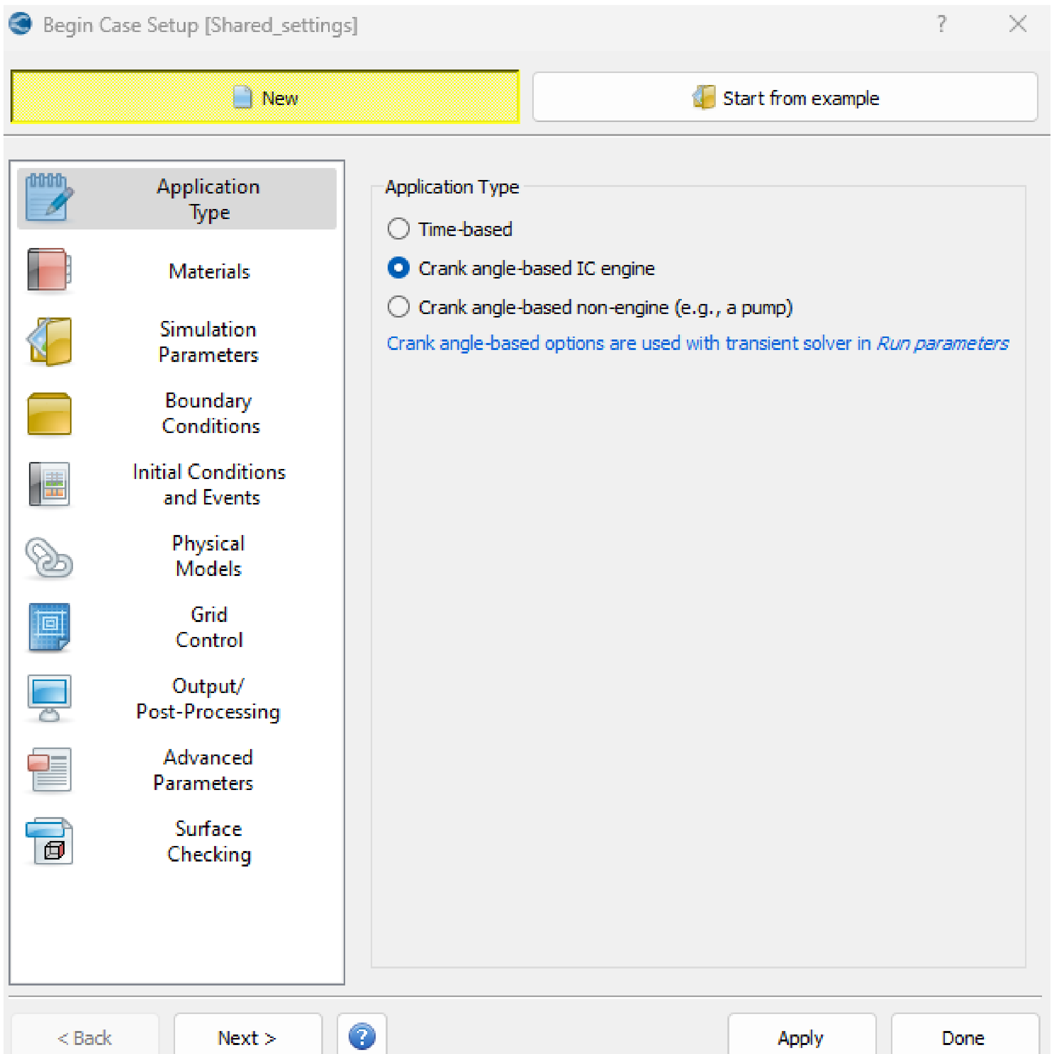

- Crank angle-based (e.g., IC engine)

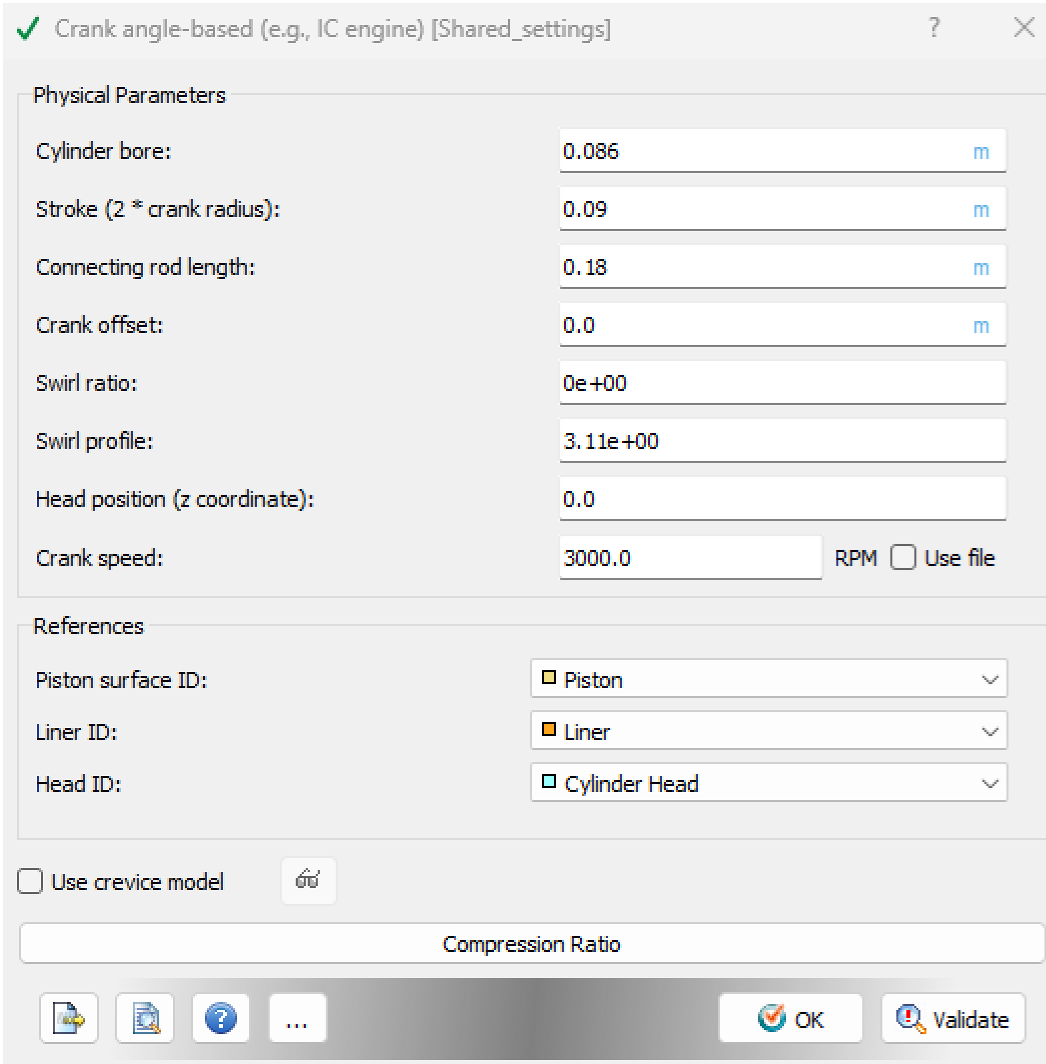

Materials

In materials, enable the liquid parcel simulation and the reaction mechanism (mech.dat).

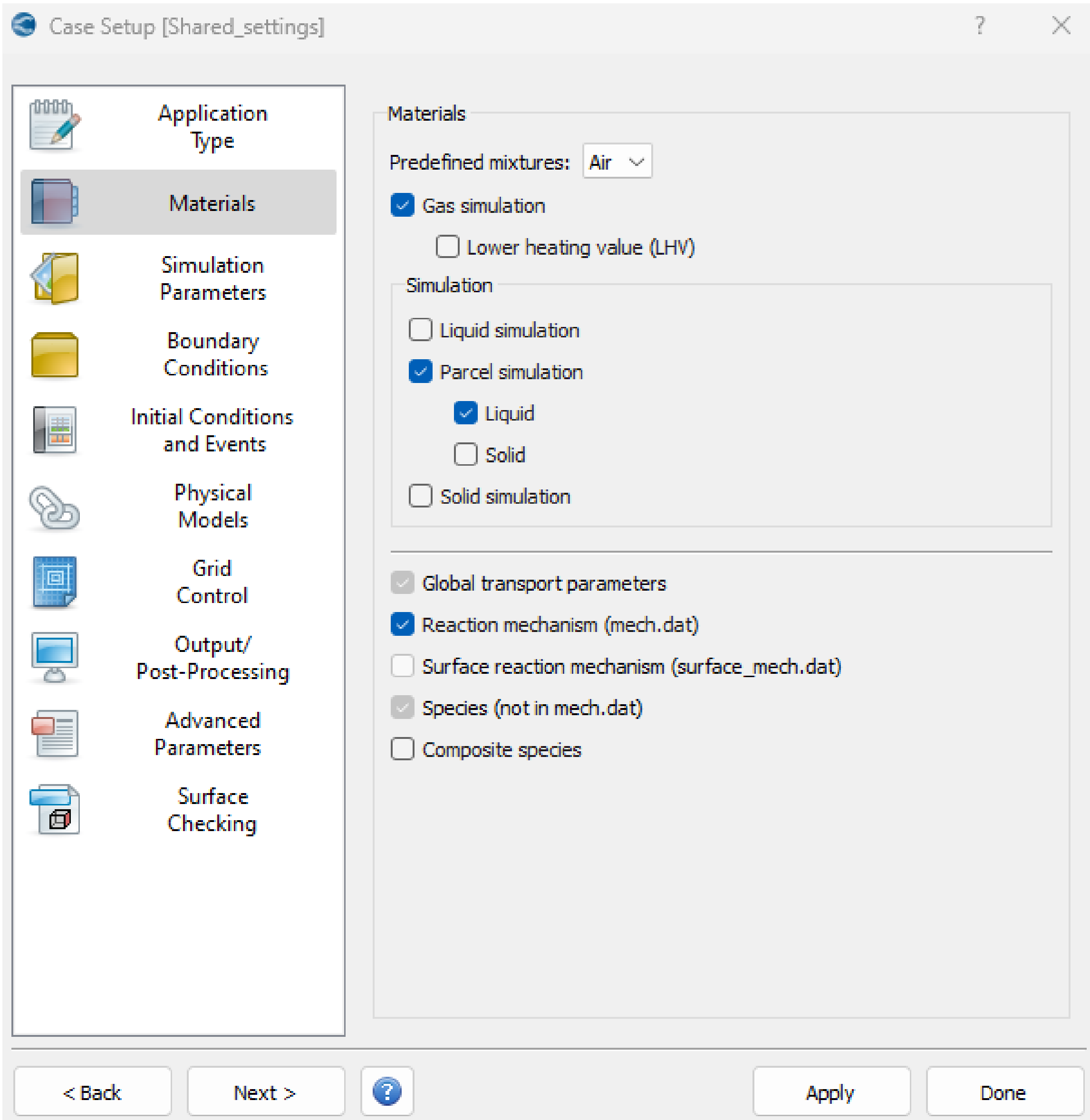

- Gas simulation

Add the provided `therm.dat` file to the gas simulation.

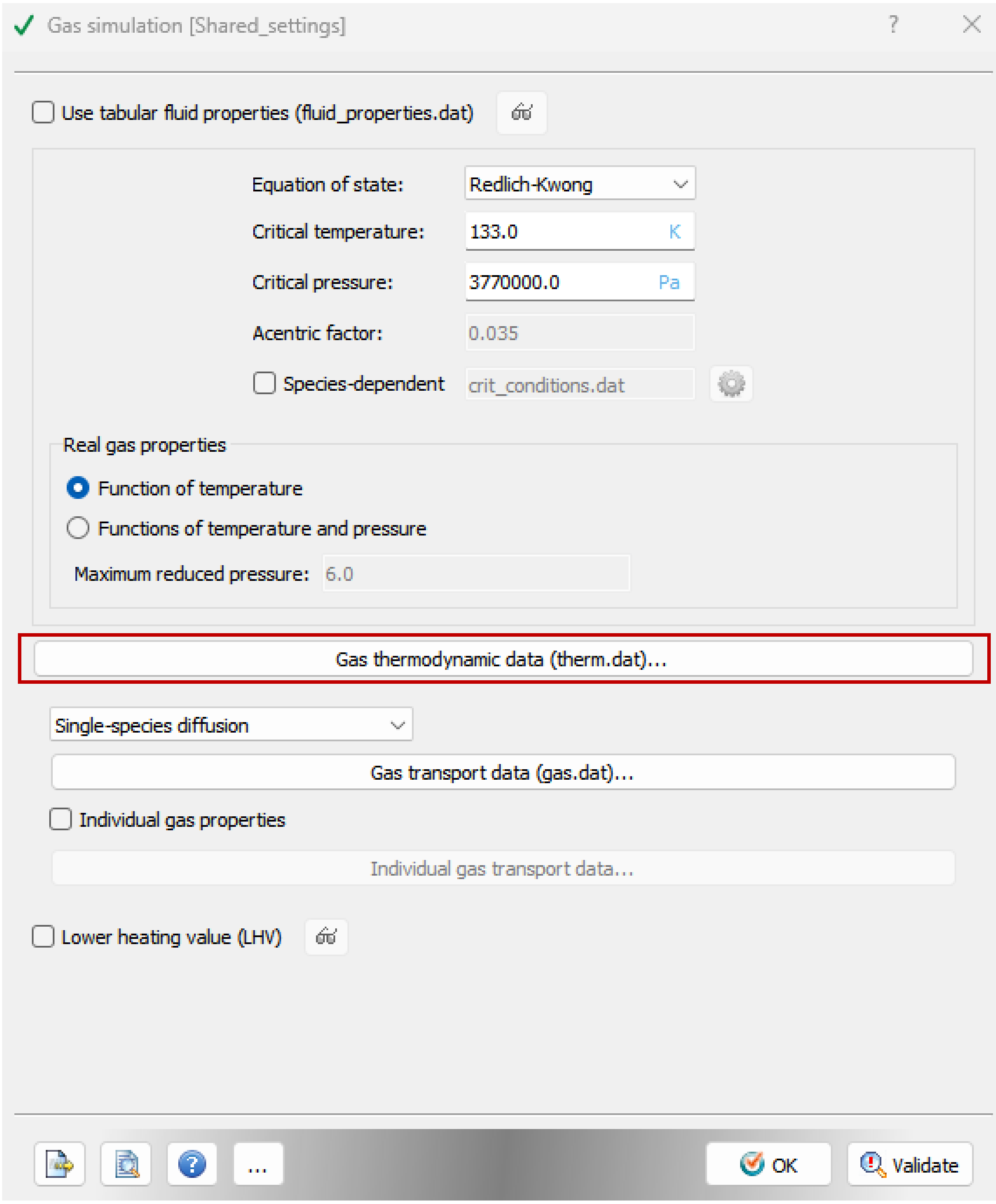

- Parcel simulation

In the parcel simulation, the "Predefined liquids" option is selected, and the fuel IC_8H_{18} is chosen from the list of available liquid options.

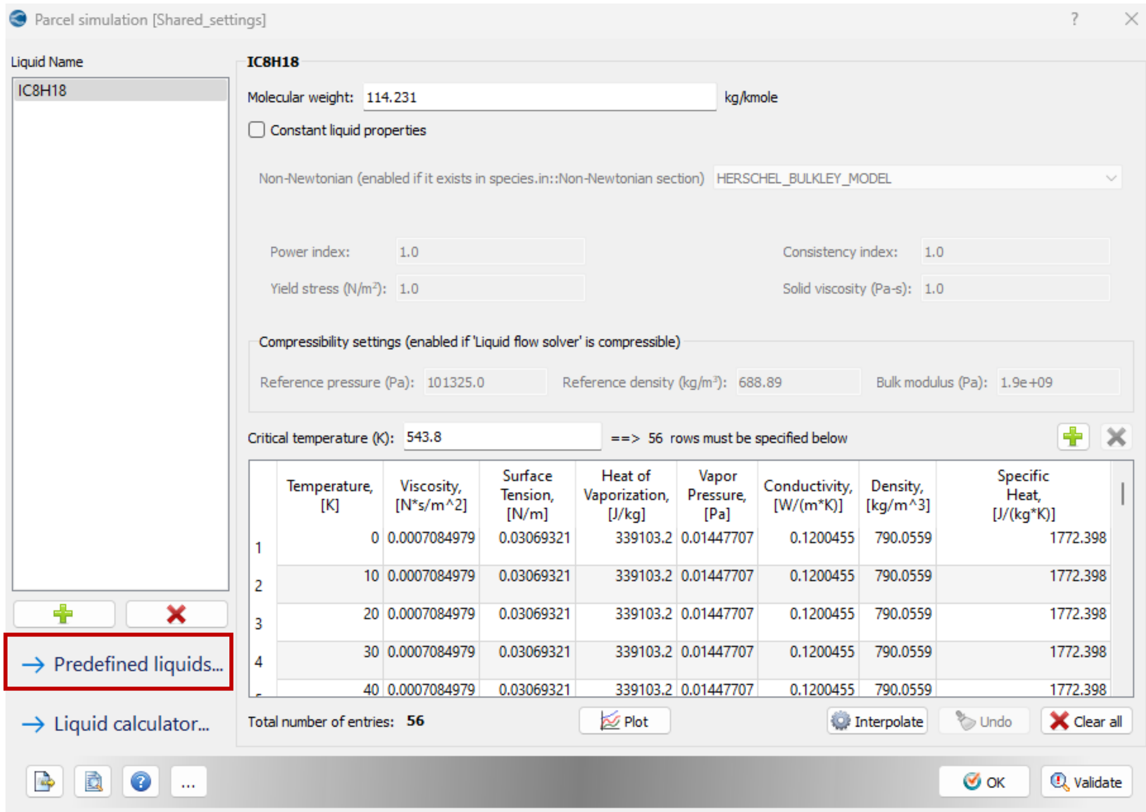

- Global transport parameters

Use default parameters.

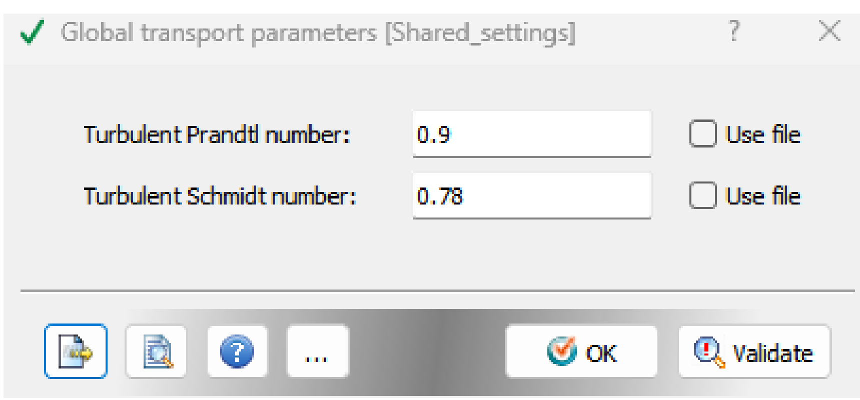

- Reaction mechanism

Add the provided `mech.dat` file to the reaction mechanism.

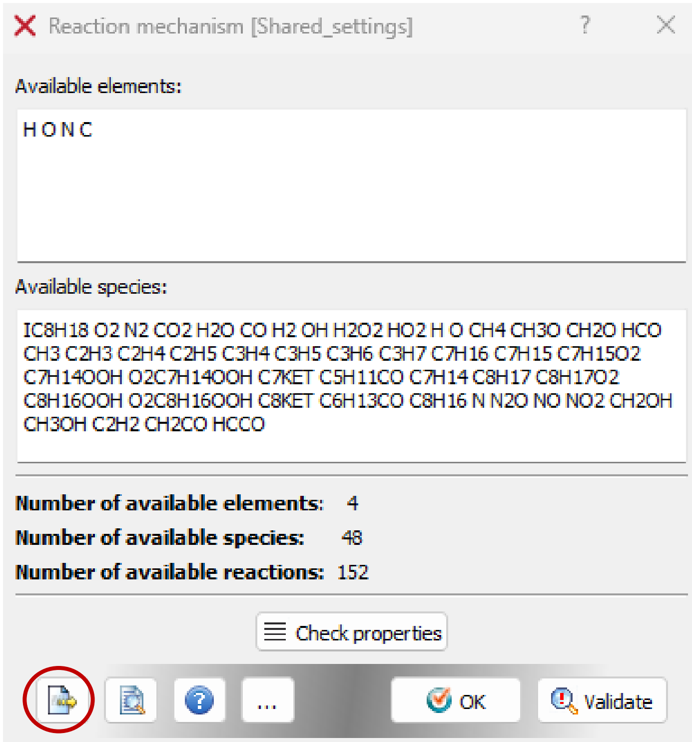

- Species

The gas species are automatically handled within the reaction mechanism, so for the liquid parcel species, select IC_8H_{18}.

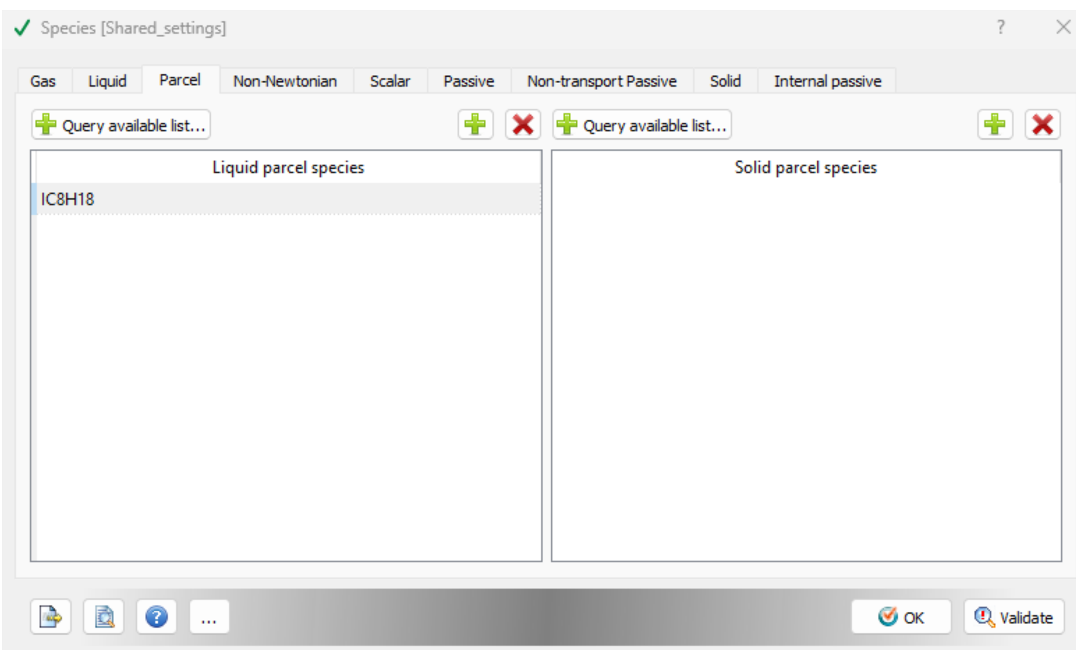

Simulation Parameters

- Run parameters

In the run parameters, the transient solver type is selected with the full hydrodynamic simulation mode to account for the interactions between liquids and gases. A crank angle-based engine simulation is chosen for the temporal type to specifically run the simulation based on varying crank angles.

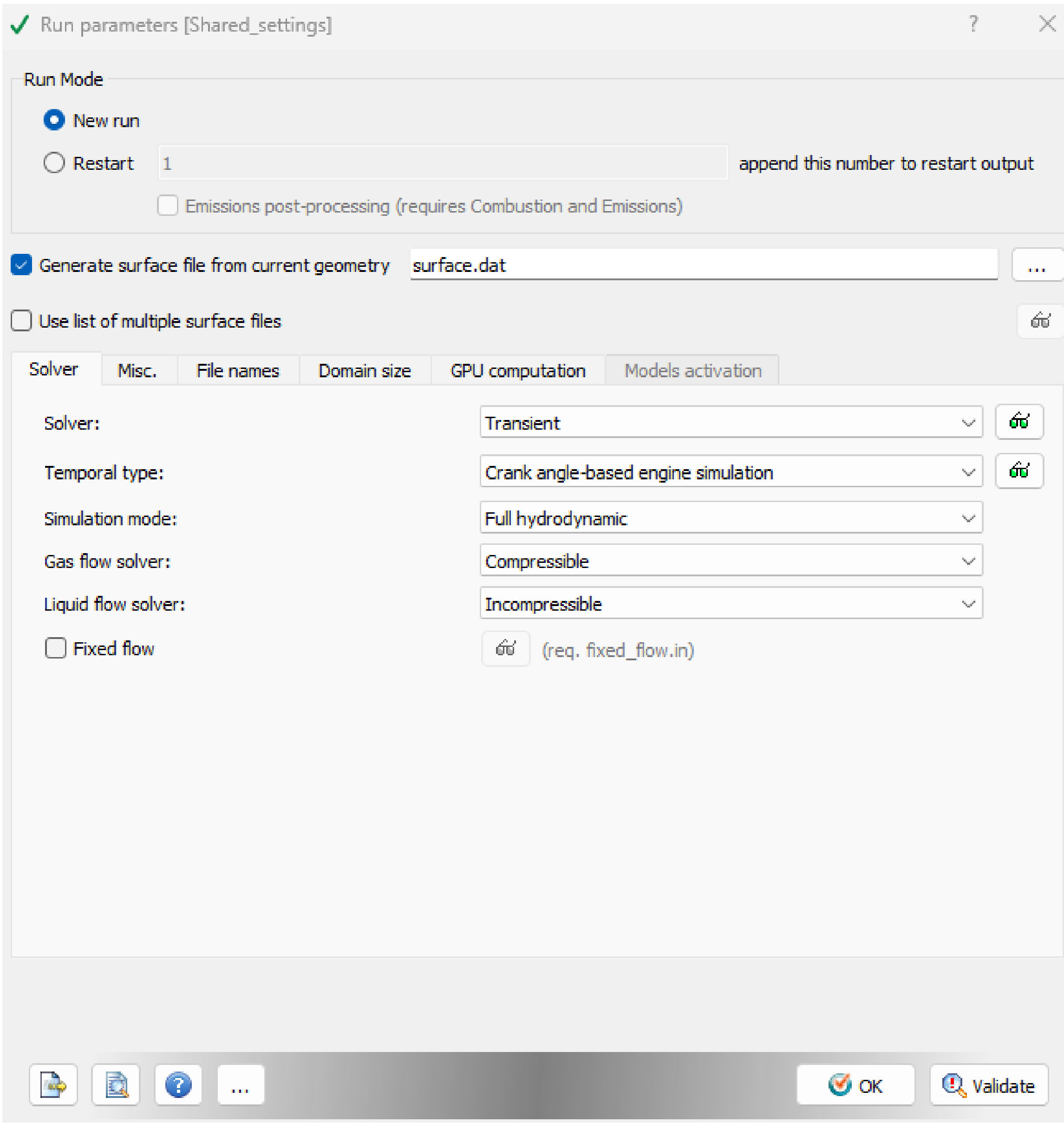

- Simulation time parameters

Set the appropriate simulation time parameters.

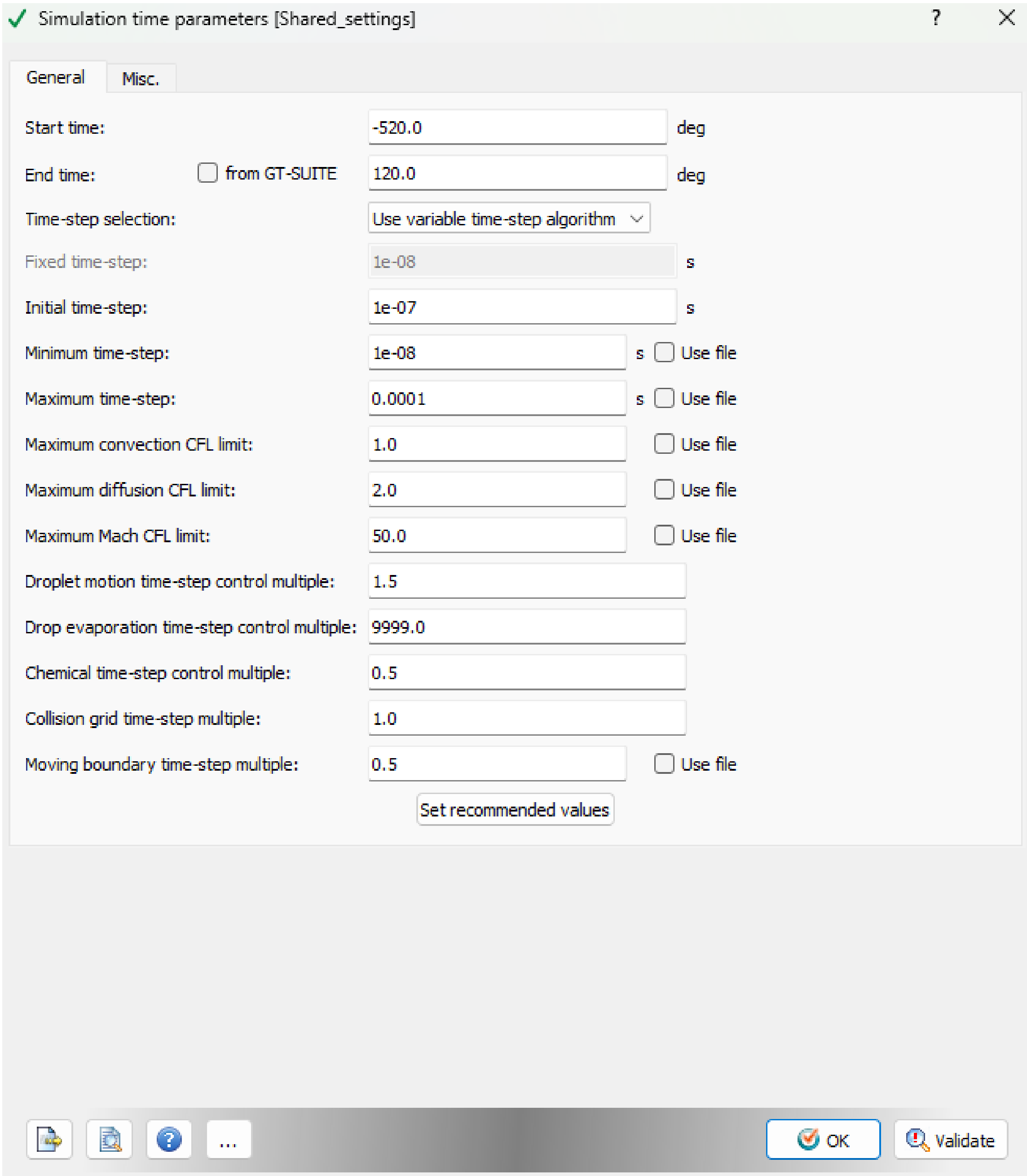

- Solver parameters [Transient]

Retain the default solver parameters.

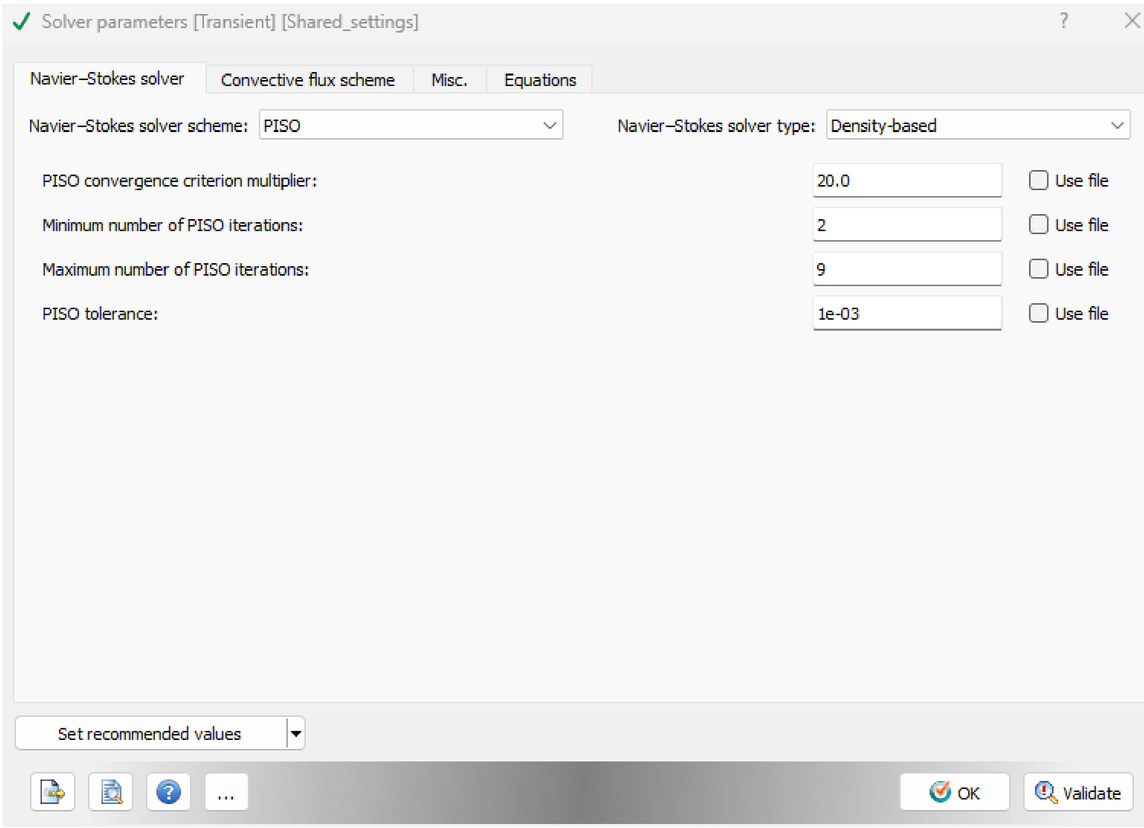

Initial Conditions and Events

In addition to 'Regions and initialization', the 'Events' box is checked.

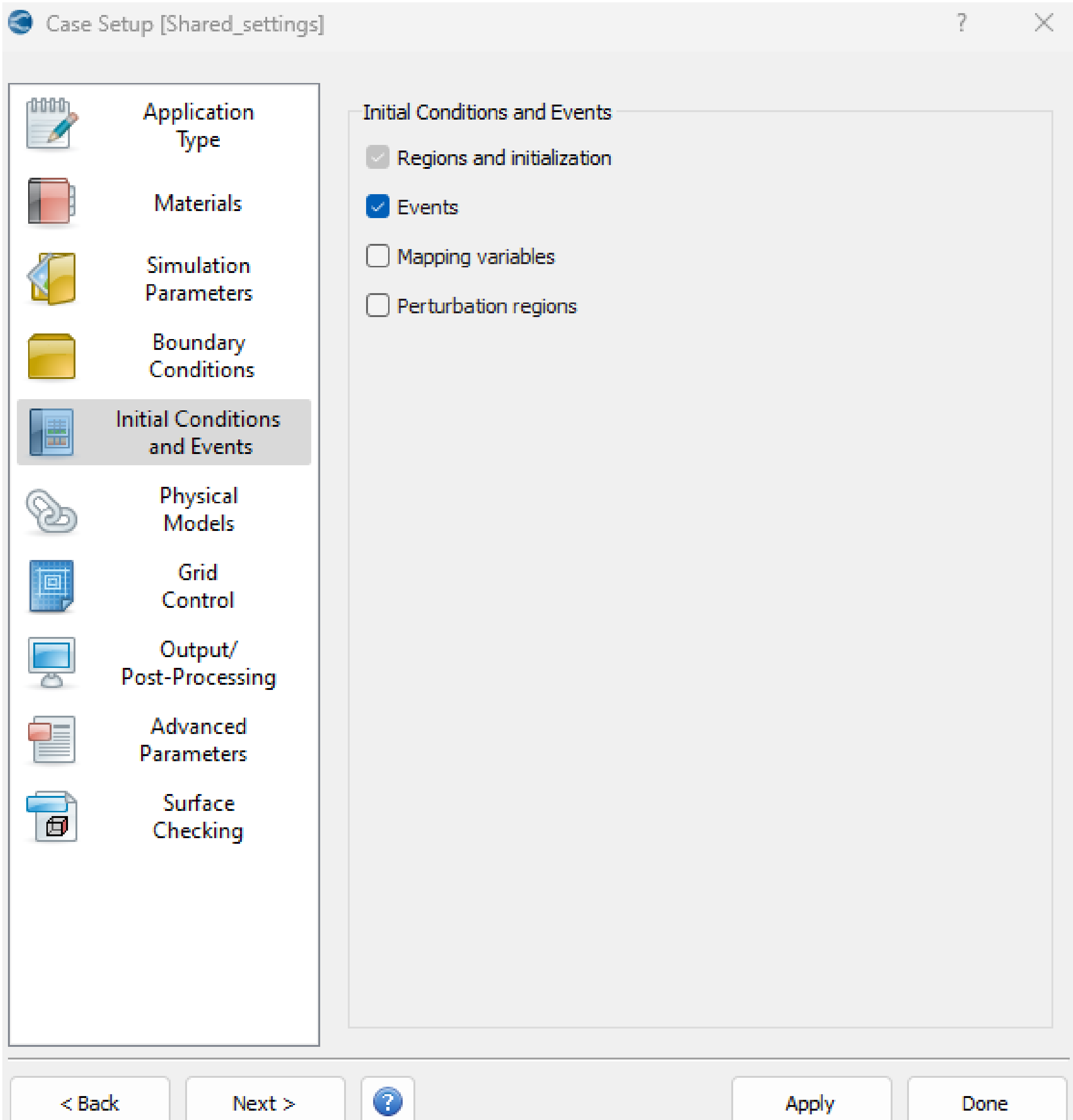

- Regions and initialization

The following four regions are added, with their parameters configured as follows:

- Cylinder region

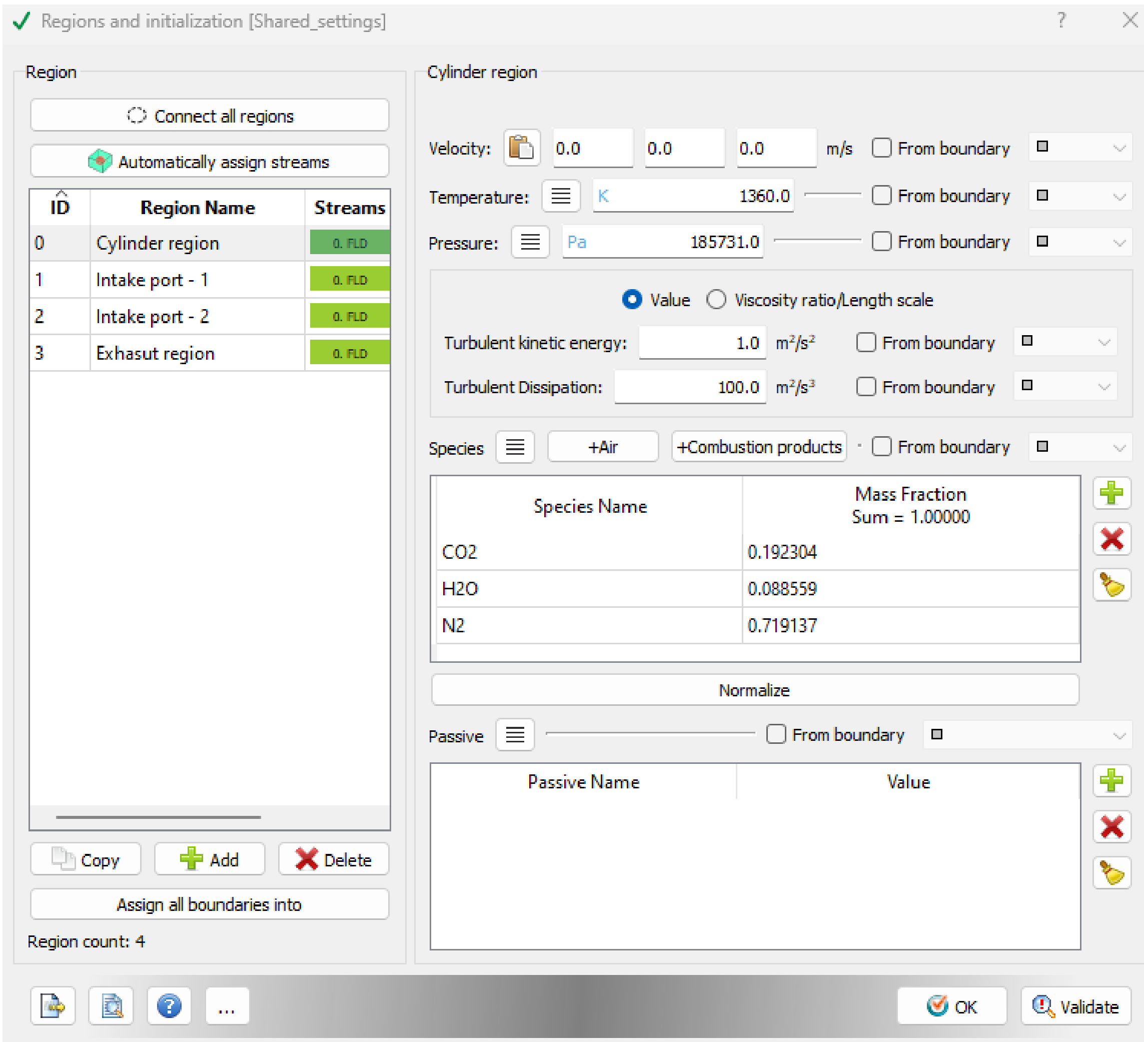

- Intake port - 1

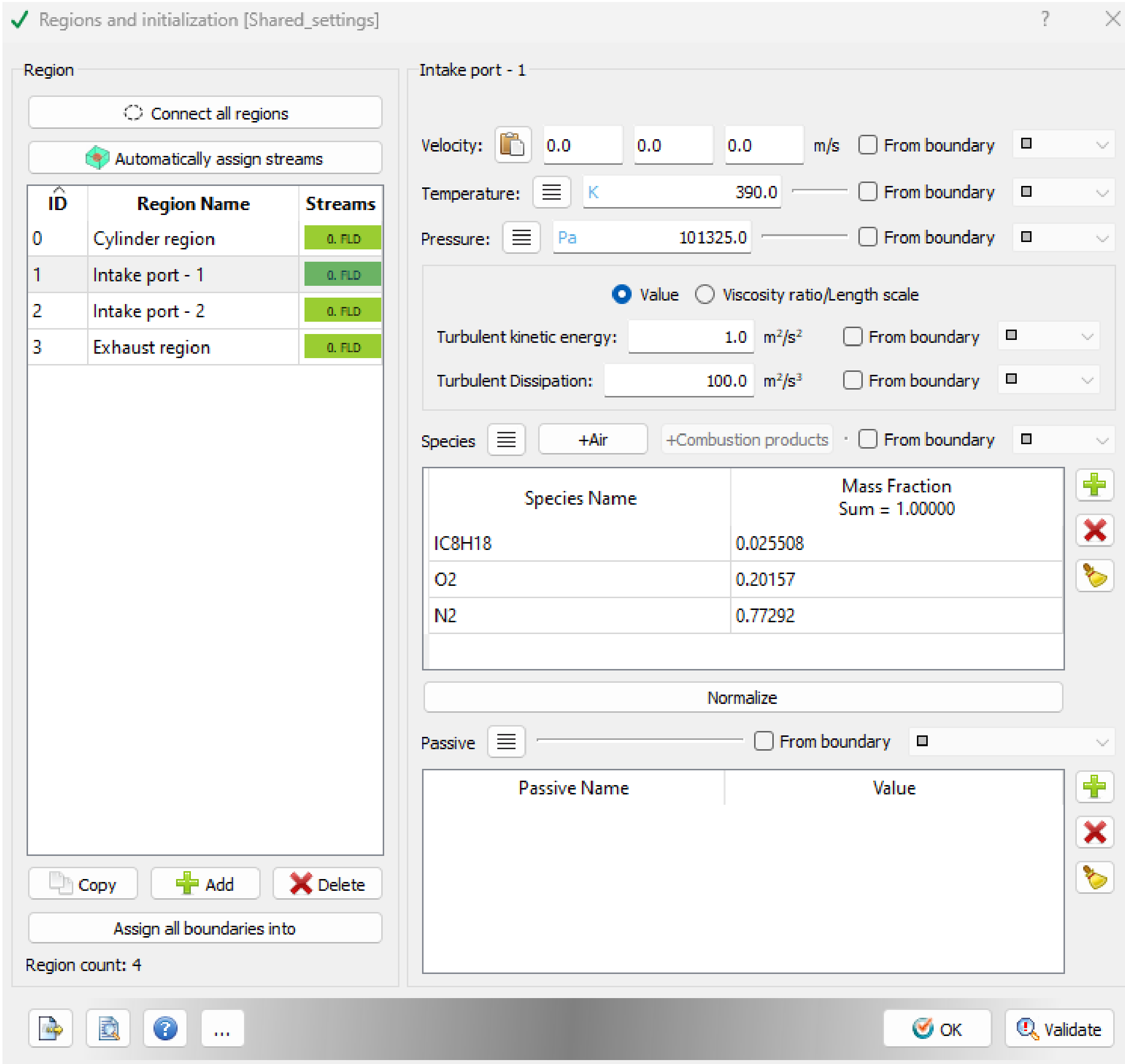

- Intake port - 2

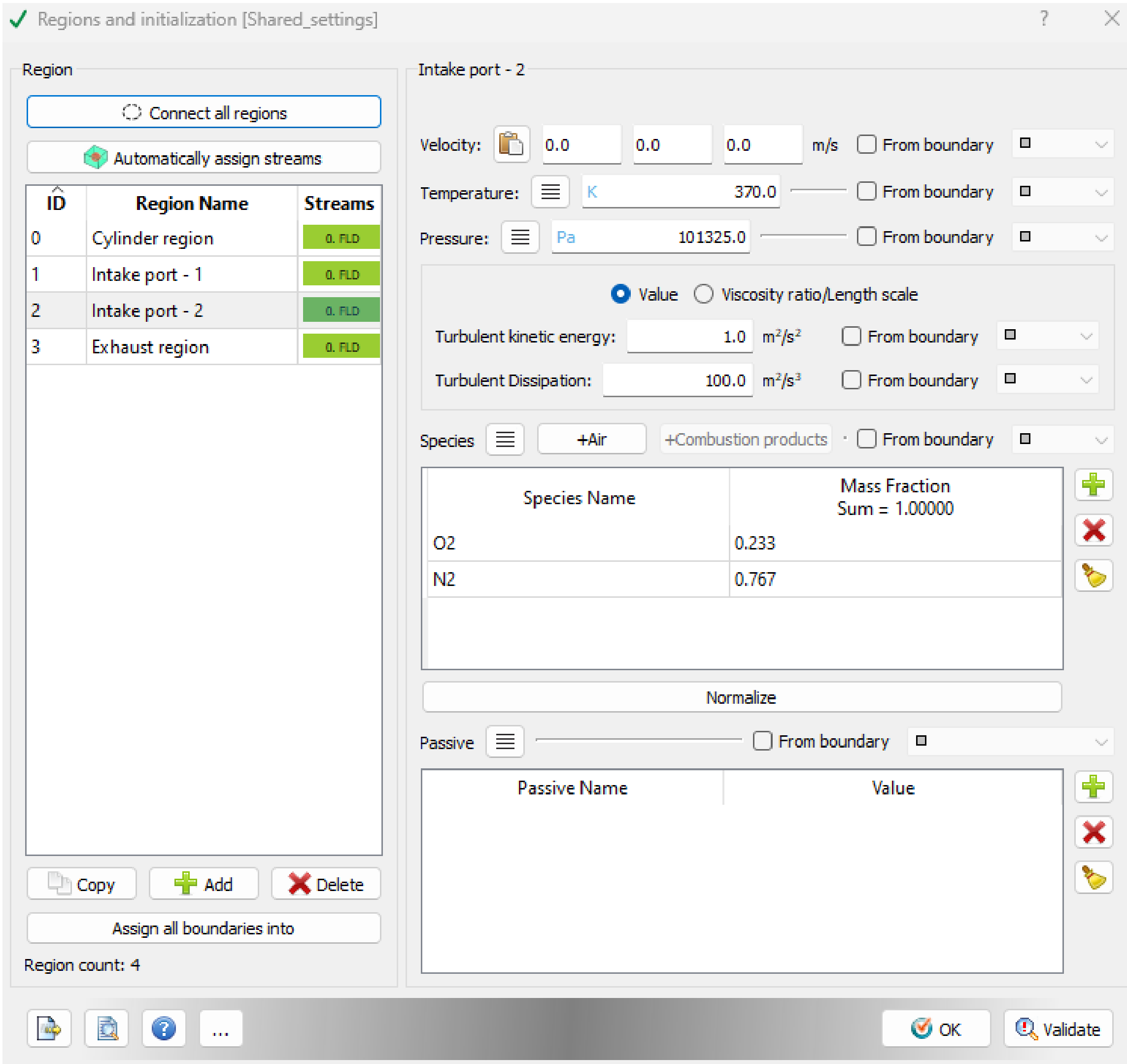

- Exhaust region

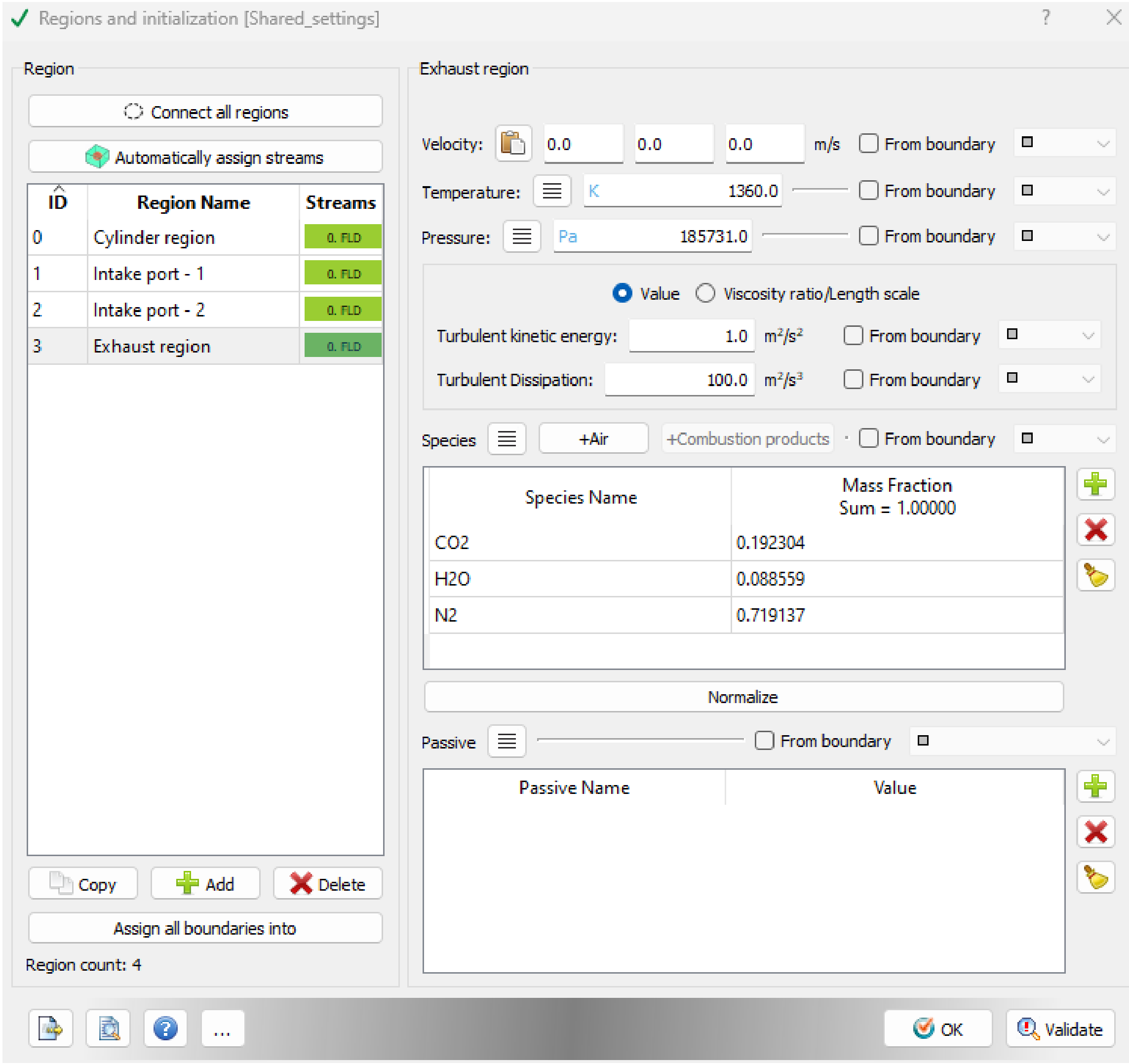

- Events

The cylinder region is linked to the intake port 1 region according to the intake valve motion profile and to the exhaust region based on the exhaust valve motion profile. Additionally, ensure that the intake ports 1 and 2 regions remain permanently open to each other.

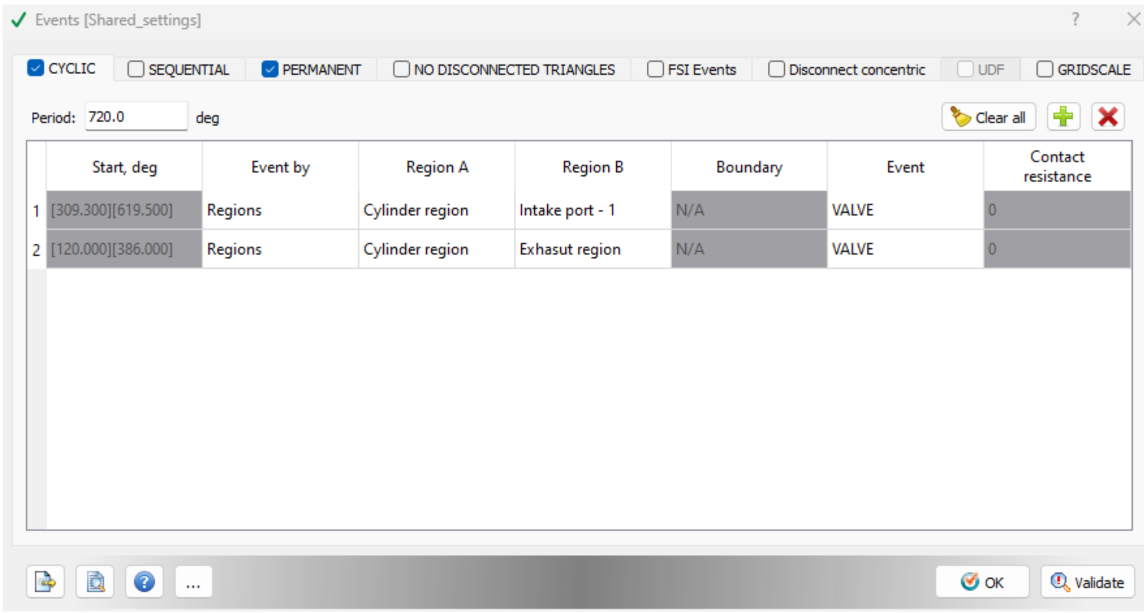

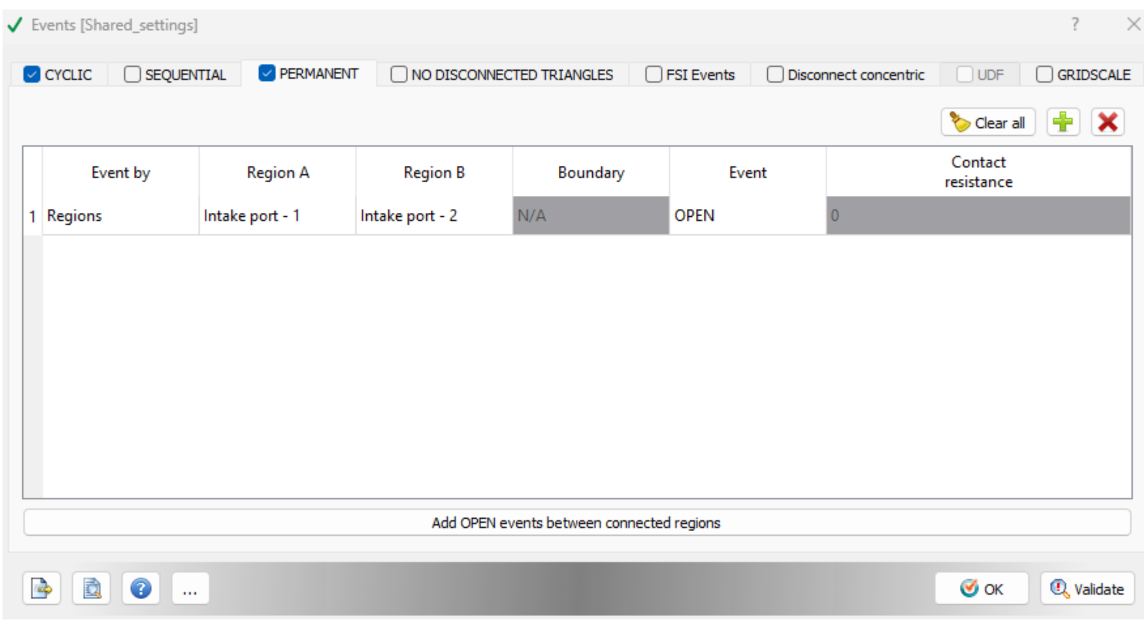

Boundary Conditions

- Boundary

Each boundary is configured with the necessary inputs as follows:

- Piston

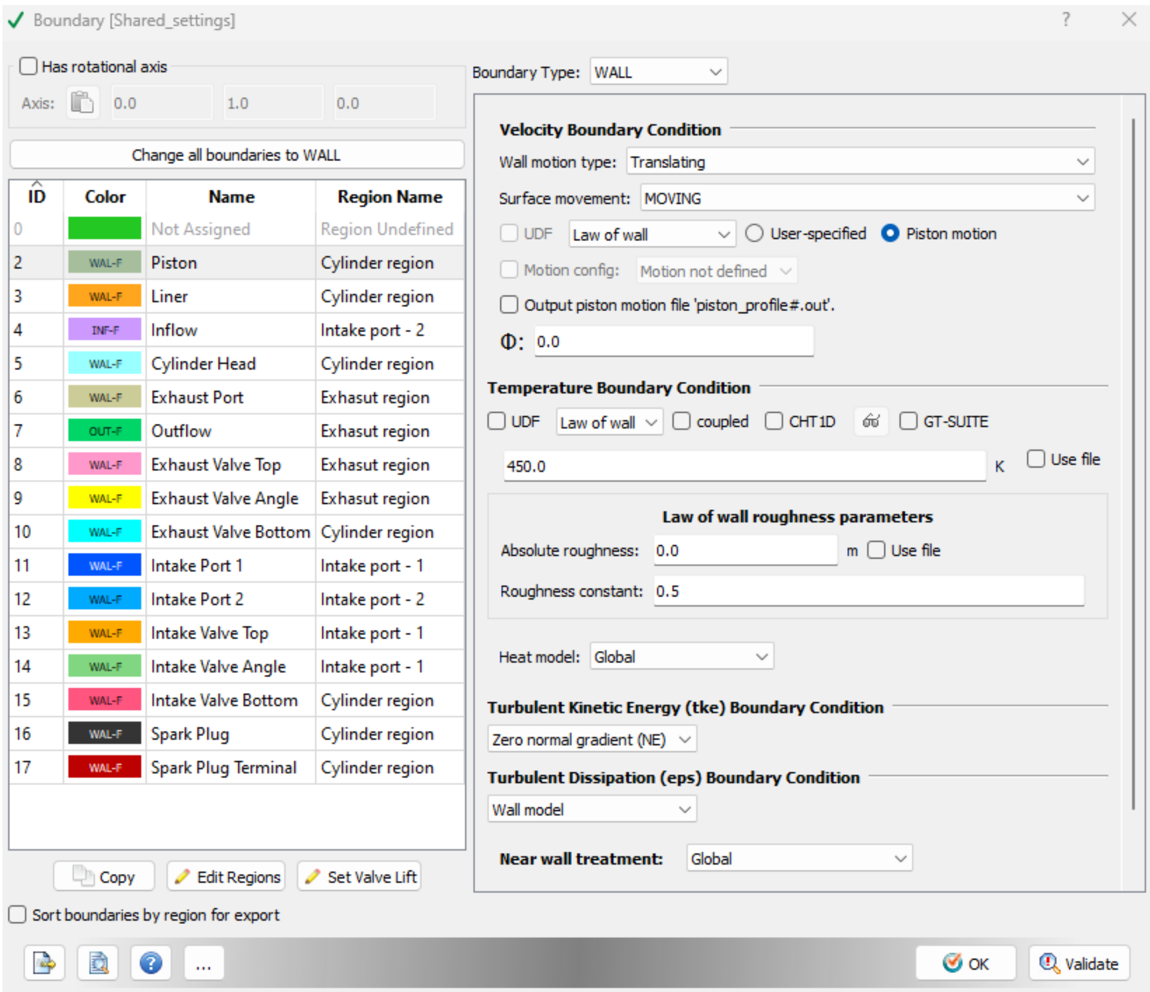

- Liner

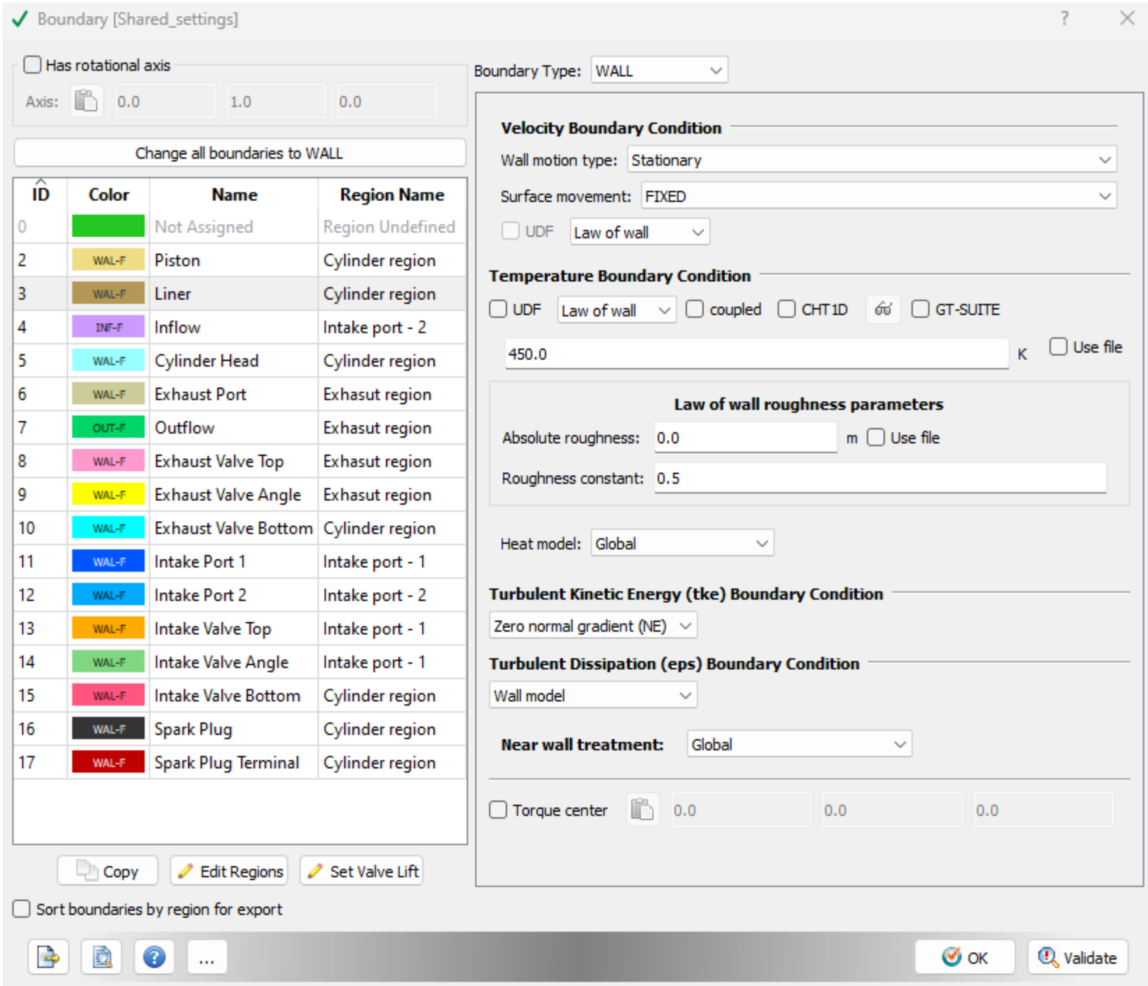

Boundary [Shared_settings]
Has rotational axis
Axis: 0.0 1.0 0.0
Change all boundaries to WALL
ID Color Name Region Name
0 Not Assigned Region Undefined
2 WAL-F Piston Cylinder region
3 WAL-F Liner Cylinder region
4 INF-F Inflow Intake port - 2
5 WAL-F Cylinder Head Cylinder region
6 WAL-F Exhaust Port Exhasut region
7 OUT-F Outflow Exhasut region
8 WAL-F Exhaust Valve Top Exhasut region
9 WAL-F Exhaust Valve Angle Exhasut region
10 WAL-F Exhaust Valve Bottom Cylinder region
11 WAL-F Intake Port 1 Intake port - 1
12 WAL-F Intake Port 2 Intake port - 2
13 WAL-F Intake Valve Top Intake port - 1
14 WAL-F Intake Valve Angle Intake port - 1
15 WAL-F Intake Valve Bottom Cylinder region
16 WAL-F Spark Plug Cylinder region
17 WAL-F Spark Plug Terminal Cylinder region
Copy
Edit Regions
Set Valve Lift
Sort boundaries by region for export
Boundary Type: WALL
Velocity Boundary Condition
Wall motion type: Stationary
Surface movement: FIXED
UDF Law of wall
Temperature Boundary Condition
UDF Law of wall coupled CHT1D GT-SUITE
450.0 K Use file
Law of wall roughness parameters
Absolute roughness: 0.0 m Use file
Roughness constant: 0.5
Heat model: Global
Turbulent Kinetic Energy (tke) Boundary Condition
Zero normal gradient (NE)
Turbulent Dissipation (eps) Boundary Condition
Wall model
Near wall treatment: Global
Torque center 0.0 0.0 0.0
OK
Validate

- Inflow

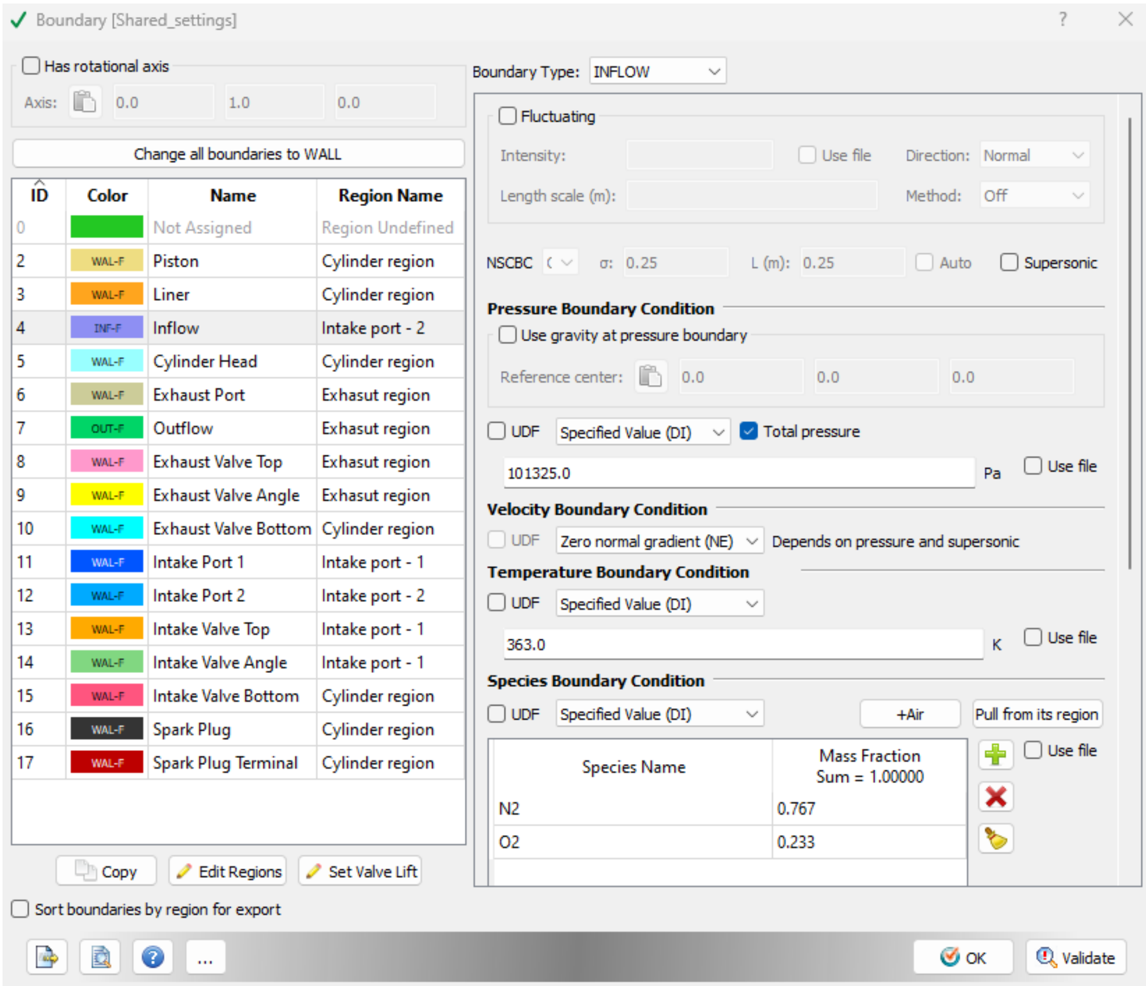
Boundary [Shared_settings]
Has rotational axis
Axis: 0.0 1.0 0.0
Change all boundaries to WALL
ID Color Name Region Name
0 Not Assigned Region Undefined
2 WAL-F Piston Cylinder region
3 WAL-F Liner Cylinder region
4 INF-F Inflow Intake port - 2
5 WAL-F Cylinder Head Cylinder region
6 WAL-F Exhaust Port Exhaust region
7 OUT-F Outflow Exhaust region
8 WAL-F Exhaust Valve Top Exhaust region
9 WAL-F Exhaust Valve Angle Exhausut region
10 WAL-F Exhaust Valve Bottom Cylinder region
11 WAL-F Intake Port 1 Intake port - 1
12 WAL-F Intake Port 2 Intake port - 2
13 WAL-F Intake Valve Top Intake port - 1
14 WAL-F Intake Valve Angle Intake port - 1
15 WAL-F Intake Valve Bottom Cylinder region
16 WAL-F Spark Plug Cylinder region
17 WAL-F Spark Plug Terminal Cylinder region
Copy
Edit Regions
Set Valve Lift
Sort boundaries by region for export
Boundary Type: INFLOW
Fluctuating
Intensity:
Use file
Direction: Normal
Length scale (m):
Method: Off
NSCBC
σ: 0.25
L (m): 0.25
Auto
Supersonic
Pressure Boundary Condition
Use gravity at pressure boundary
Reference center: 0.0 0.0 0.0
UDF Specified Value (DI) Total pressure
101325.0 Pa Use file
Velocity Boundary Condition
UDF Zero normal gradient (NE) Depends on pressure and supersonic
Temperature Boundary Condition
UDF Specified Value (DI)
363.0 K Use file
Species Boundary Condition
UDF Specified Value (DI) +Air Pull from its region
Species Name
Mass Fraction Sum = 1.00000
Use file
N2 0.767
O2 0.233
OK
Validate

- Cylinder Head

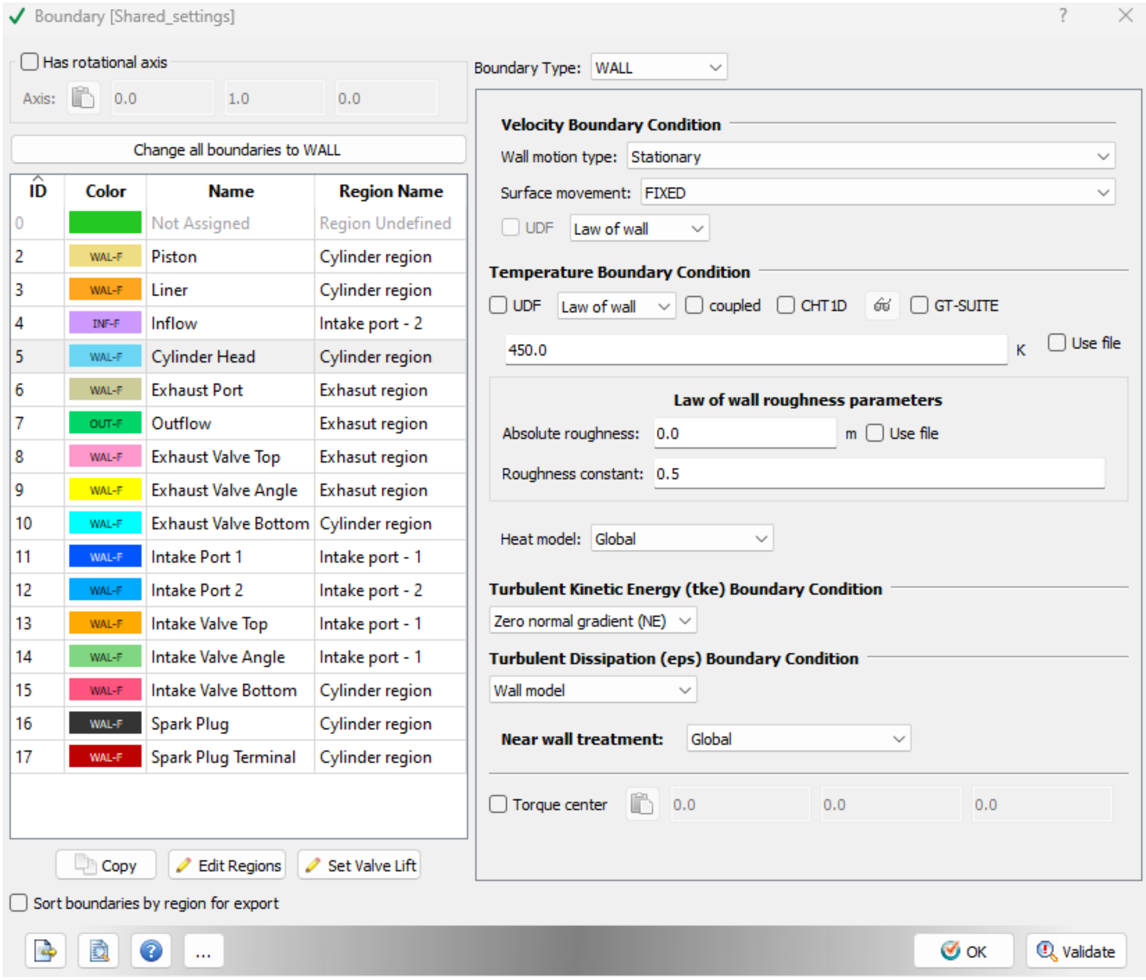

- Exhaust Port

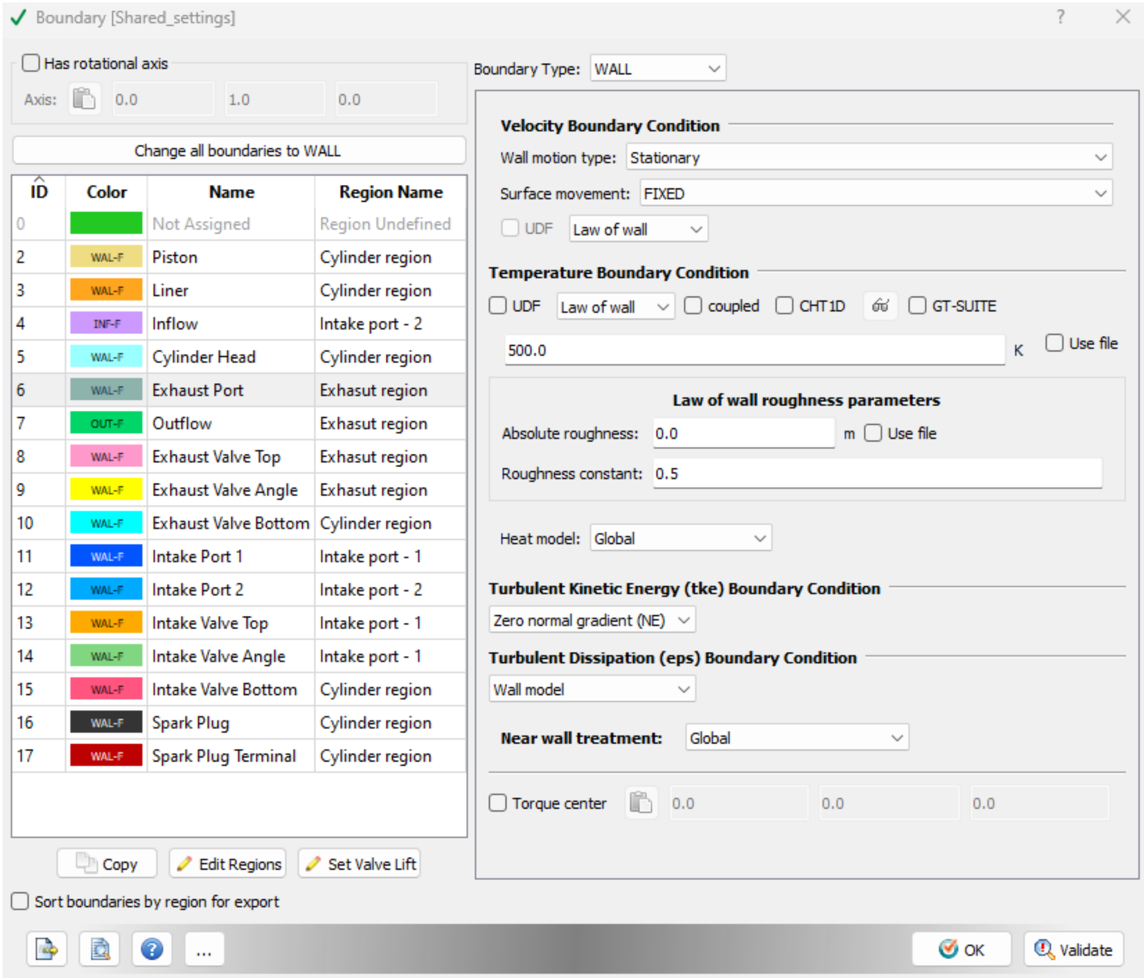

- Outflow

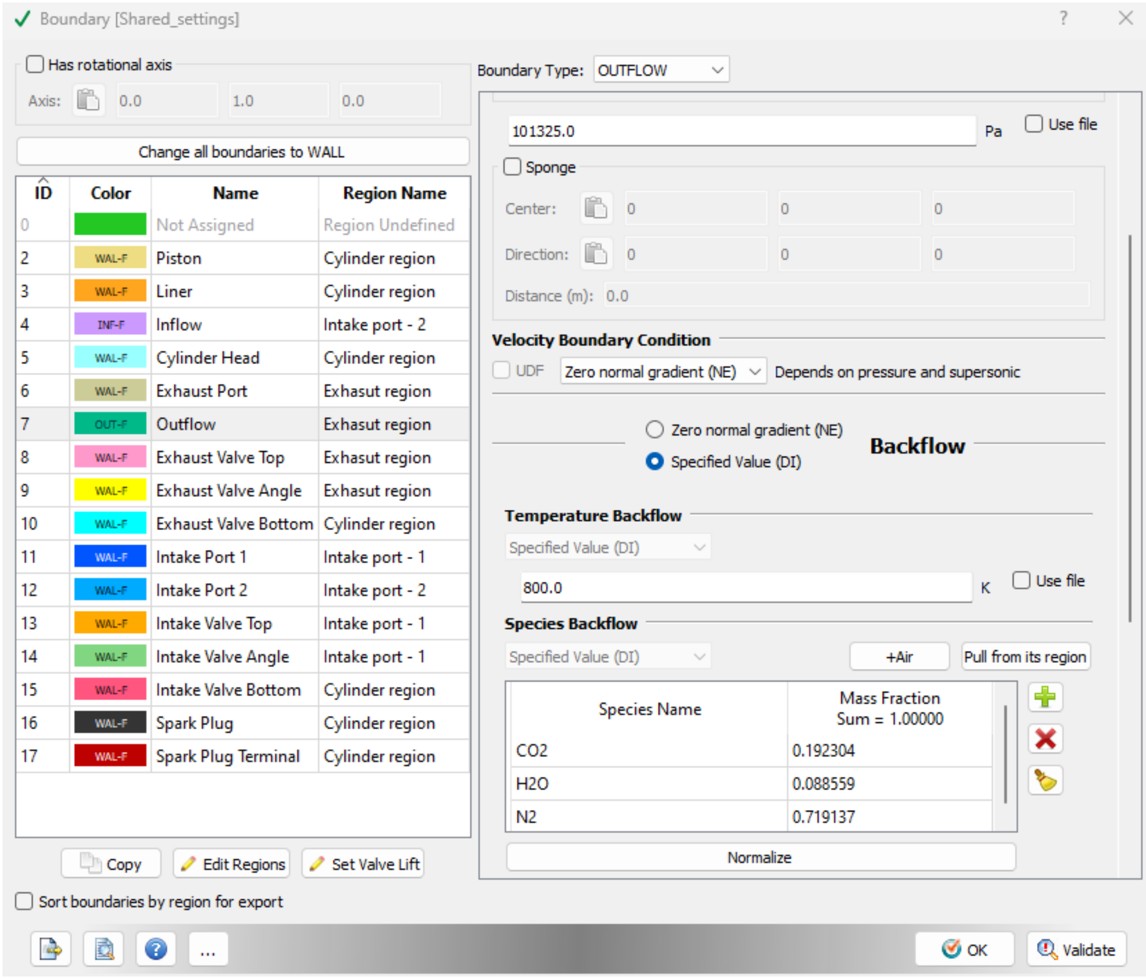

Boundary [Shared_settings]
Has rotational axis
Axis: 0.0 1.0 0.0
Change all boundaries to WALL
ID Color Name Region Name
0 Not Assigned Region Undefined
2 WAL-F Piston Cylinder region
3 WAL-F Liner Cylinder region
4 INF-F Inflow Intake port - 2
5 WAL-F Cylinder Head Cylinder region
6 WAL-F Exhaust Port Exhasut region
7 OUT-F Outflow Exhasut region
8 WAL-F Exhaust Valve Top Exhasut region
9 WAL-F Exhaust Valve Angle Exhasut region
10 WAL-F Exhaust Valve Bottom Cylinder region
11 WAL-F Intake Port 1 Intake port - 1
12 WAL-F Intake Port 2 Intake port - 2
13 WAL-F Intake Valve Top Intake port - 1
14 WAL-F Intake Valve Angle Intake port - 1
15 WAL-F Intake Valve Bottom Cylinder region
16 WAL-F Spark Plug Cylinder region
17 WAL-F Spark Plug Terminal Cylinder region
Copy
Edit Regions
Set Valve Lift
Sort boundaries by region for export
Boundary Type: OUTFLOW
101325.0 Pa
Use file
Sponge
Center: 0 0 0
Direction: 0 0 0
Distance (m): 0.0
Velocity Boundary Condition
UDF
Zero normal gradient (NE)
Depends on pressure and supersonic
Zero normal gradient (NE)
Specified Value (DI)
Backflow
Temperature Backflow
Specified Value (DI)
800.0 K
Use file
Species Backflow
Specified Value (DI)
+Air
Pull from its region
Species Name
Mass Fraction Sum = 1.00000
CO2 0.192304
H2O 0.088559
N2 0.719137
Normalize
OK
Validate

- Exhaust Valve Top, Exhaust Valve Angle, and Exhaust Valve Bottom

They are all configured with the same inputs except for the exhaust valve bottom that is assigned in the cylinder region. For the valve motion profile, use the provided `exhaust_lift.in` file for the three boundaries. The minimum lift is set to 0.000199 m for the three boundaries.

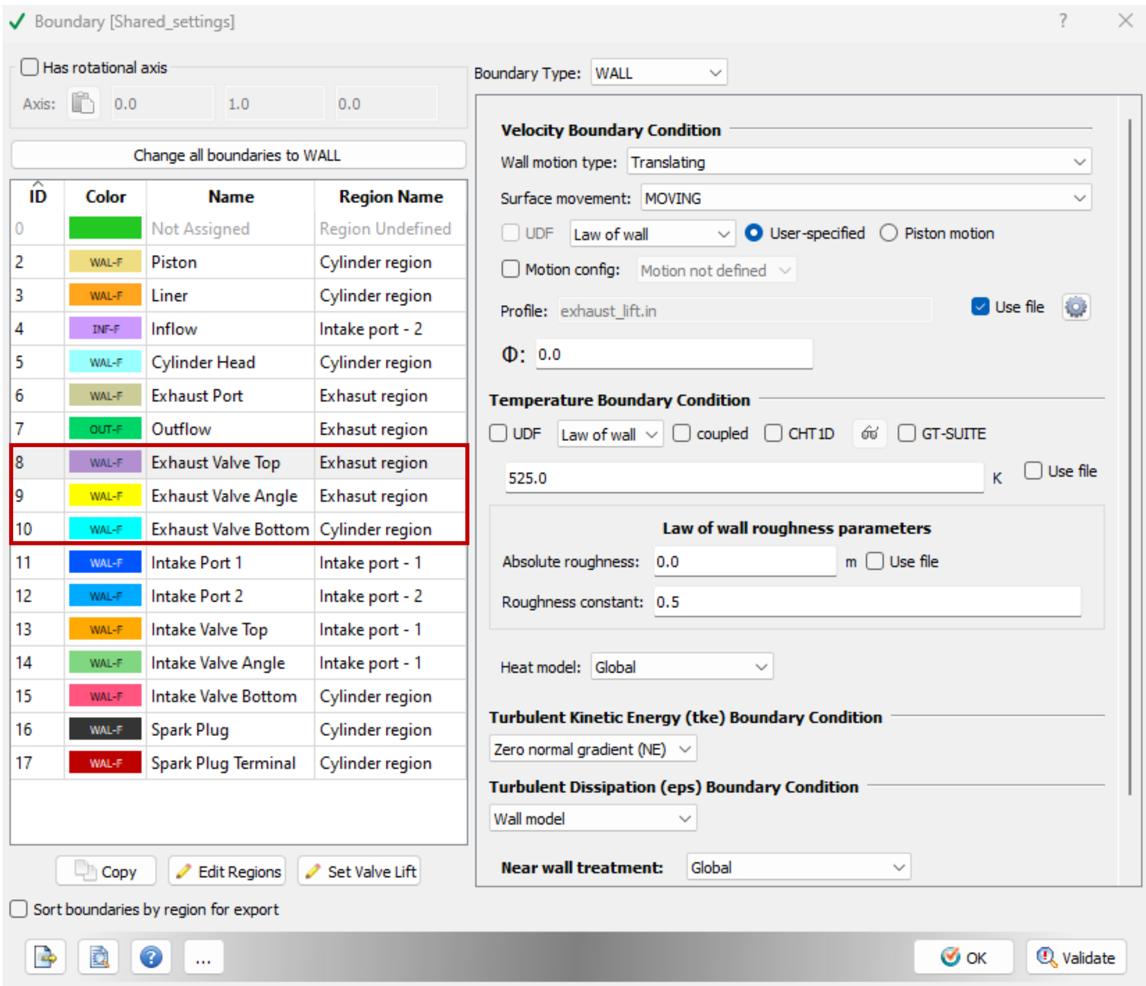

- Intake Port 1

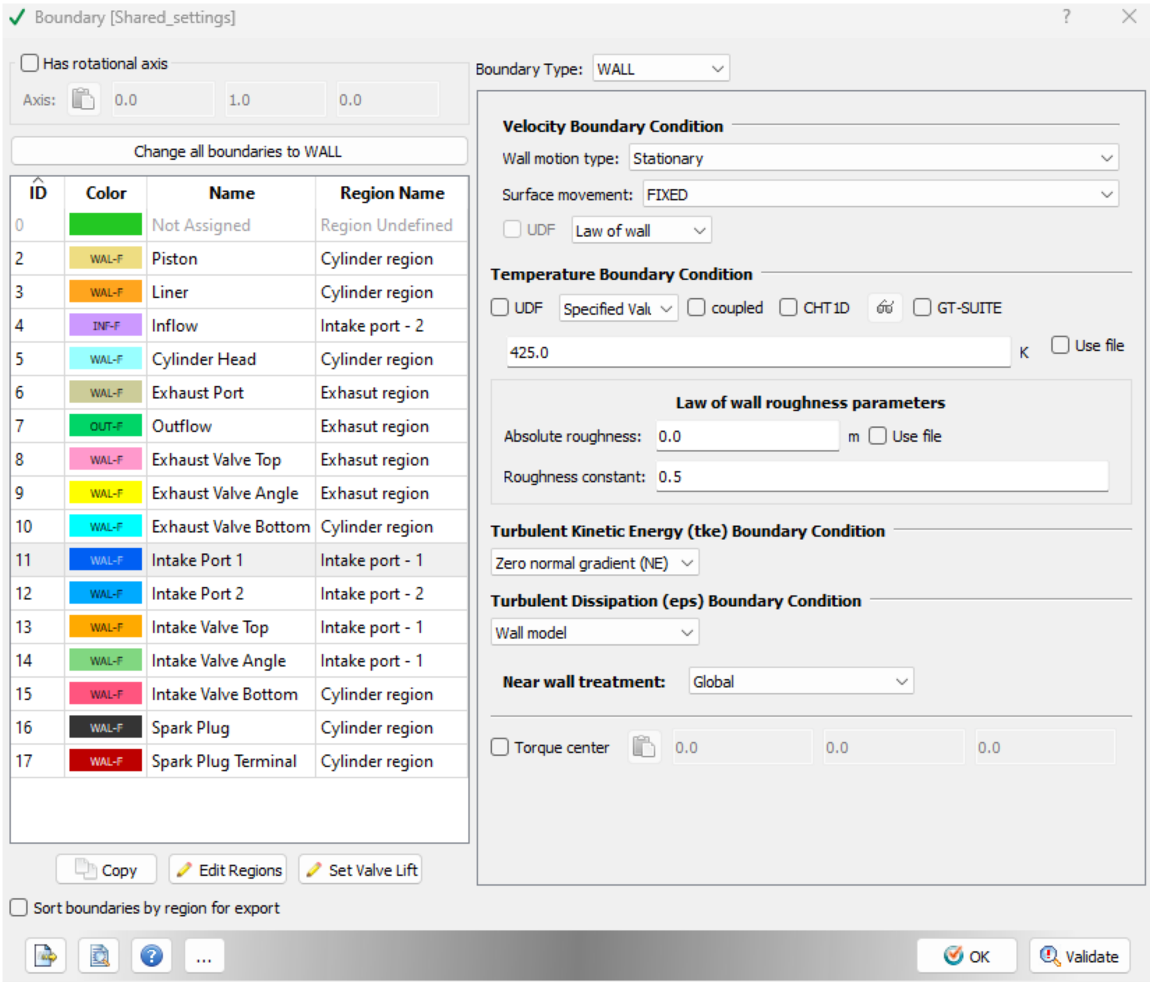

- Intake Port 2

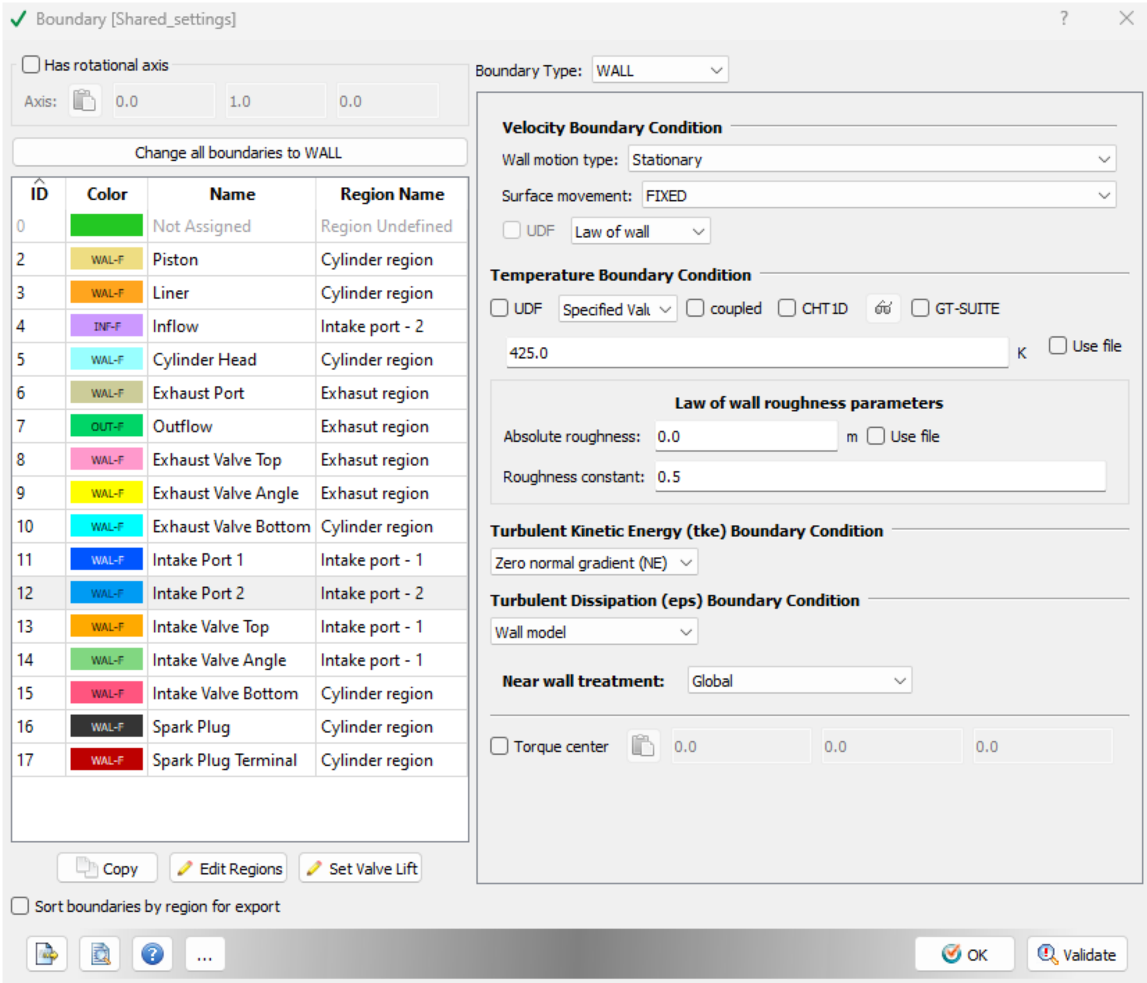

- Intake Valve Top, Intake Valve Angle, and Intake Valve Bottom

They are all configured with the same inputs except for the intake valve bottom that is assigned in the cylinder region. For the valve motion profile, use the provided `intake_lift.in` file for the three boundaries. The minimum lift is set to 0.00188 m for the three boundaries.

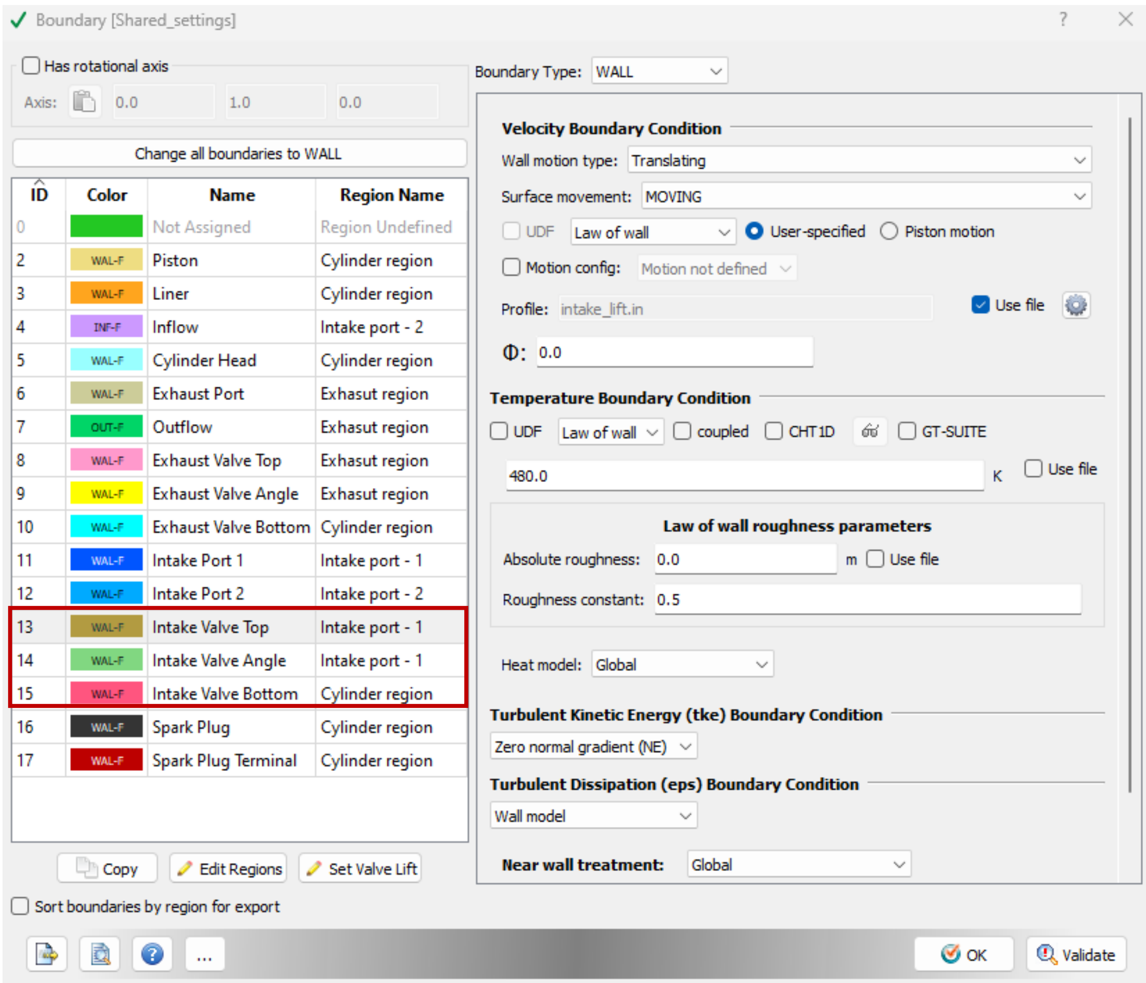

- Spark Plug

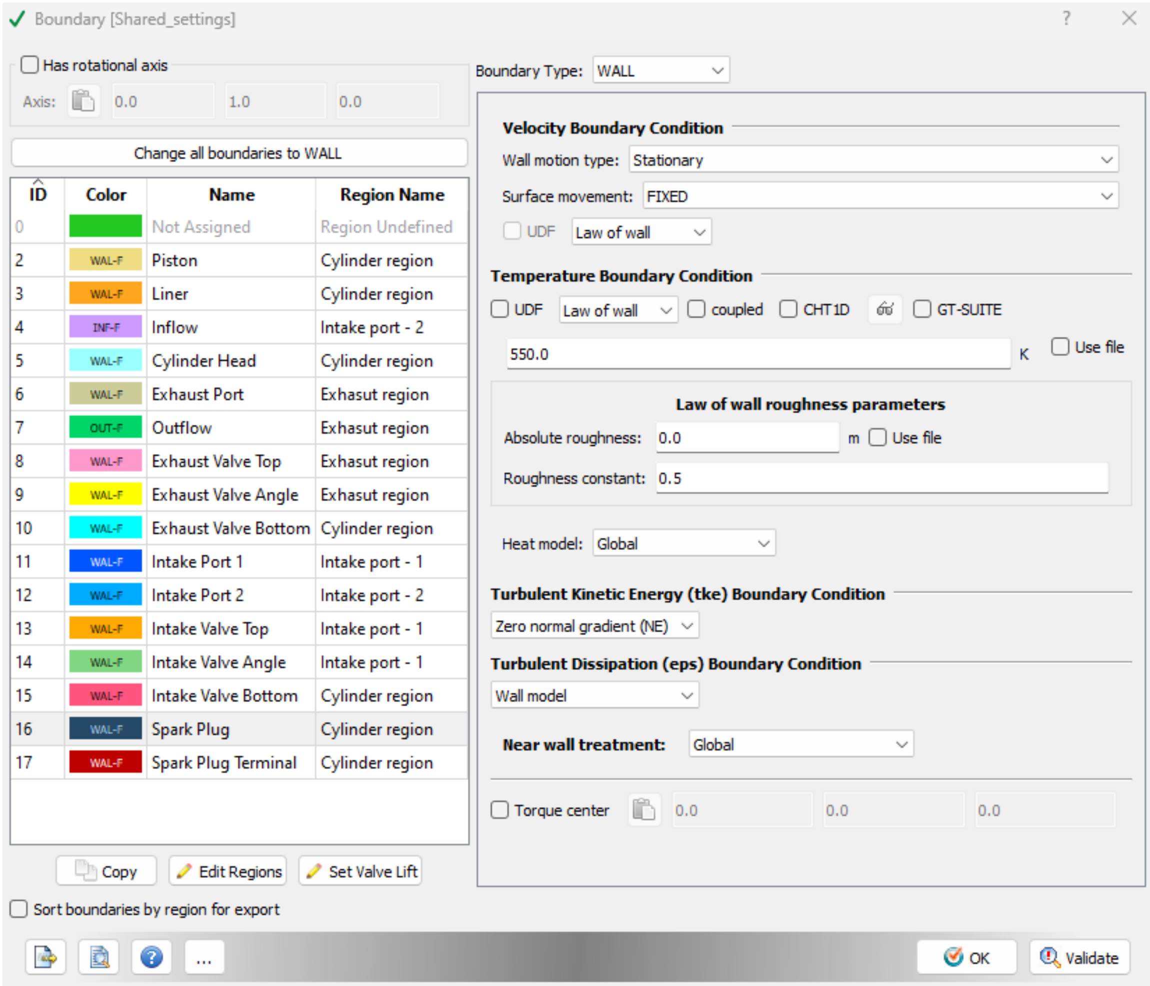

Boundary [Shared_settings]
Has rotational axis
Axis: 0.0 1.0 0.0
Change all boundaries to WALL
ID Color Name Region Name
0 Not Assigned Region Undefined
2 WAL-F Piston Cylinder region
3 WAL-F Liner Cylinder region
4 INF-F Inflow Intake port - 2
5 WAL-F Cylinder Head Cylinder region
6 WAL-F Exhaust Port Exhasut region
7 OUT-F Outflow Exhasut region
8 WAL-F Exhaust Valve Top Exhasut region
9 WAL-F Exhaust Valve Angle Exhasut region
10 WAL-F Exhaust Valve Bottom Cylinder region
11 WAL-F Intake Port 1 Intake port - 1
12 WAL-F Intake Port 2 Intake port - 2
13 WAL-F Intake Valve Top Intake port - 1
14 WAL-F Intake Valve Angle Intake port - 1
15 WAL-F Intake Valve Bottom Cylinder region
16 WAL-F Spark Plug Cylinder region
17 WAL-F Spark Plug Terminal Cylinder region
Copy
Edit Regions
Set Valve Lift
Sort boundaries by region for export
Boundary Type: WALL
Velocity Boundary Condition
Wall motion type: Stationary
Surface movement: FIXED
UDF Law of wall
Temperature Boundary Condition
UDF Law of wall coupled CHT1D GT-SUITE
550.0 K Use file
Law of wall roughness parameters
Absolute roughness: 0.0 m Use file
Roughness constant: 0.5
Heat model: Global
Turbulent Kinetic Energy (tke) Boundary Condition
Zero normal gradient (NE)
Turbulent Dissipation (eps) Boundary Condition
Wall model
Near wall treatment: Global
Torque center 0.0 0.0 0.0
OK
Validate

- Spark Plug Terminal

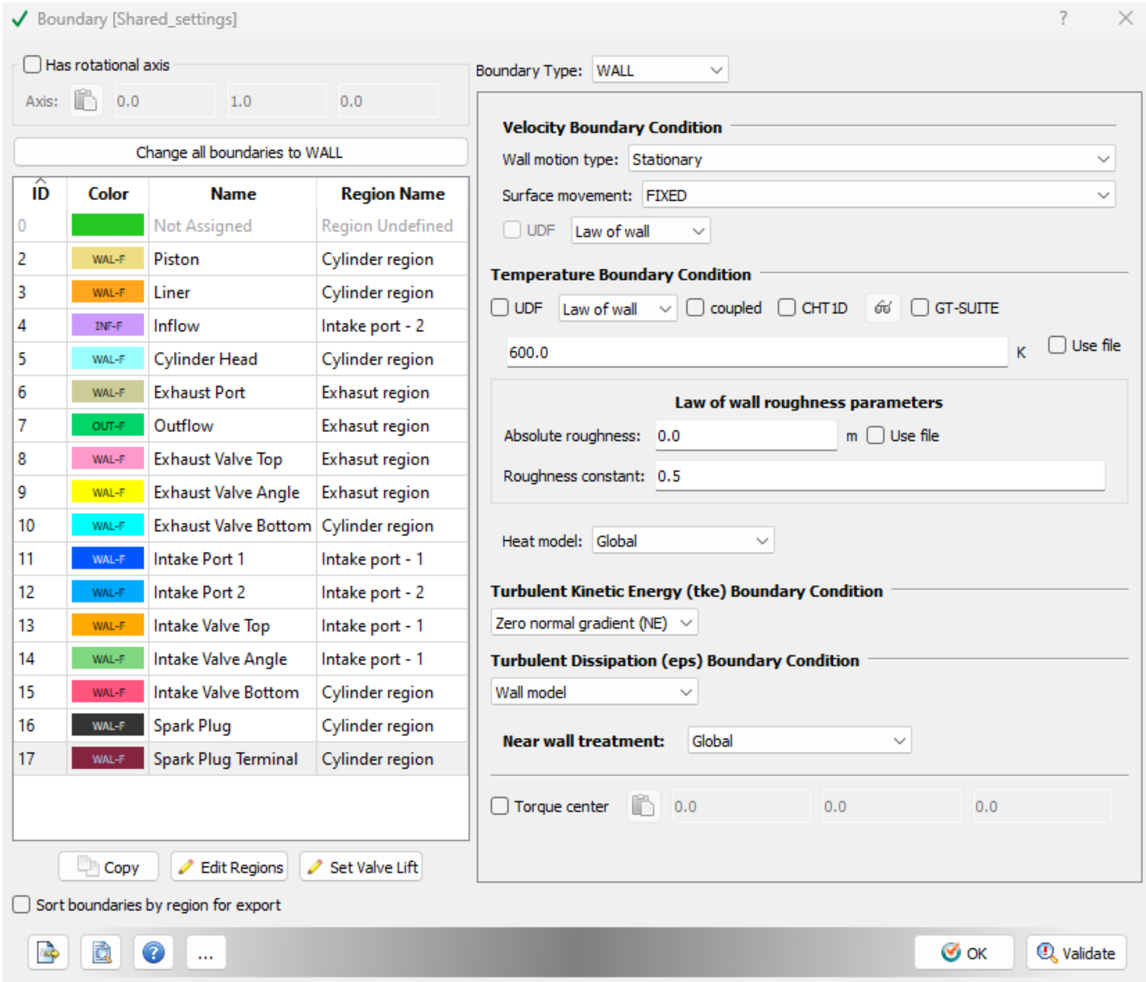

Physical Models

Check the combustion, turbulence, and the source/sink modeling boxes.

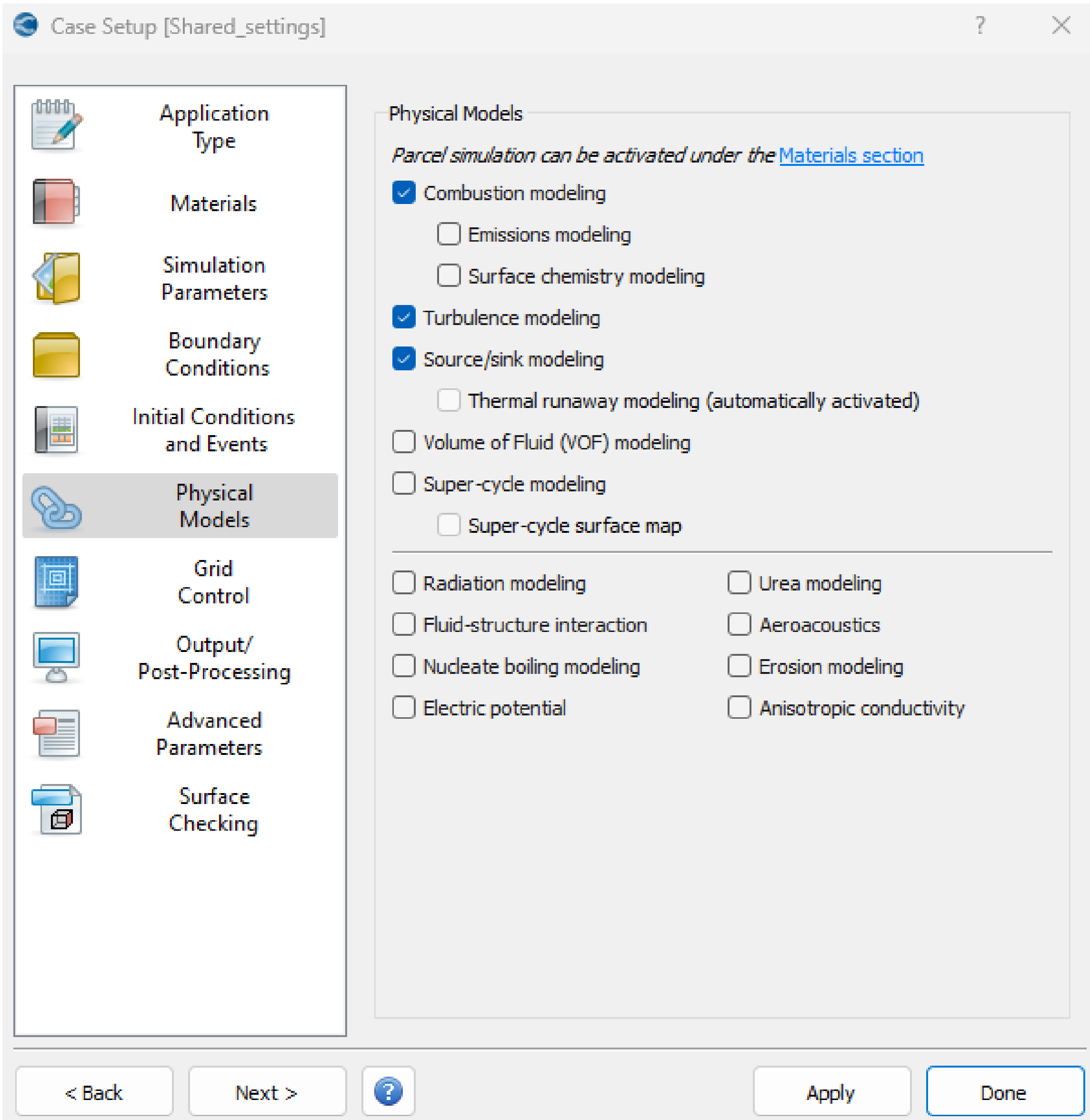

- Parcels configuration

In the parcel configuration setup, the NTC collision model is selected for efficient and accurate droplet interaction simulation, with collision outcomes set to predict post-collision behaviors like merging or bouncing. The wall interaction model, defined as "parcel_wall_interaction.in," simulates droplet behavior upon surface impact, including splashing and evaporation, essential for capturing realistic wall heat transfer. The Kelvin-Helmholtz (KH) and Rayleigh-Taylor (RT) breakup model (KH-RT model) is employed to accurately simulate primary atomization and secondary breakup of fuel droplets, ensuring realistic spray dynamics [4]. The parcel species is defined as IC_8H_{18}, representing iso-octane, with all interactions tied to this fuel type, enabling a detailed and accurate representation of the fuel injection and combustion processes.

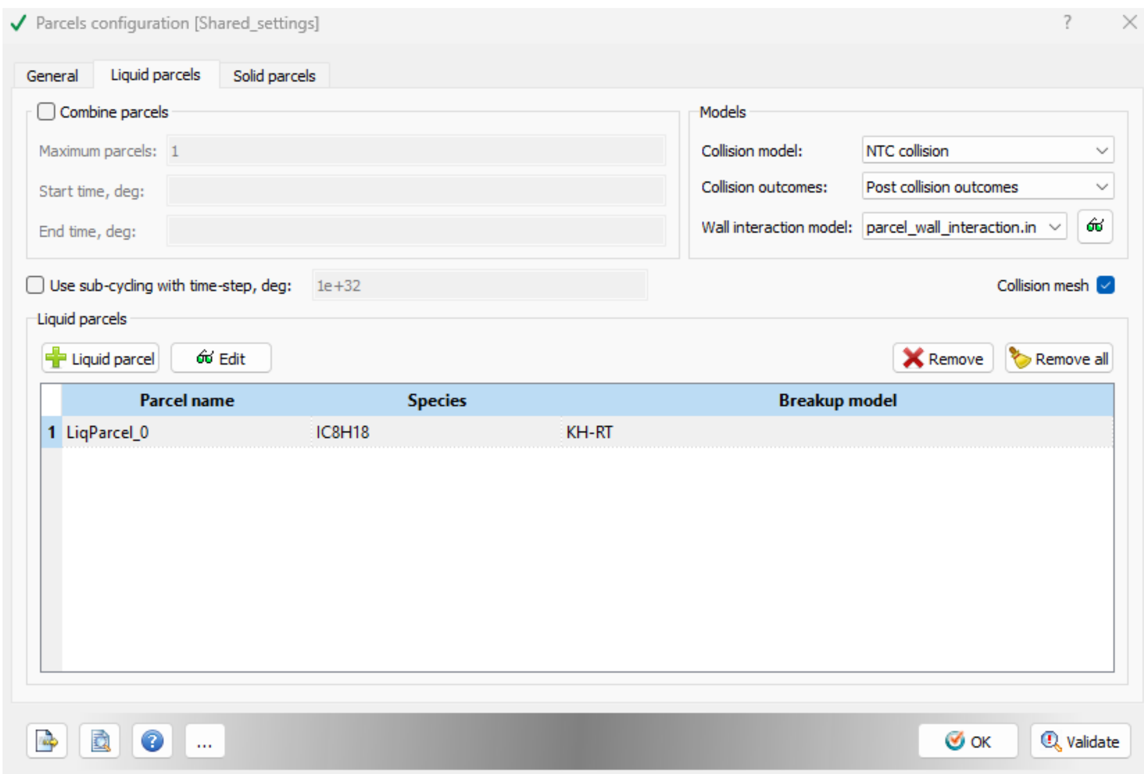

IC_8H_{18} is selected as the parcel species with a mass fraction of 1.0, signifying that the injected fuel is pure iso-octane. This aligns with the simulation's focus on accurately modeling gasoline combustion in the PFI system. The parcel cutoff parameters, specifically the mass ratio (0.001) and radius ($1e^{-20}$ m), are configured to define the minimum size and mass of liquid parcels considered in the simulation. These values help ensure that computational resources are allocated to significant droplets, avoiding unnecessary tracking of negligibly small parcels that would not meaningfully impact the simulation dynamics.

The O'Rourke model is applied for turbulent dispersion, which provides a realistic representation of how droplets interact and disperse under turbulence [5]. This model considers the stochastic nature of turbulence to predict droplet trajectories, promoting an accurate simulation of droplet distribution within the combustion chamber. These parameters collectively ensure a detailed simulation of fuel injection, droplet behavior, and subsequent combustion, while maintaining computational efficiency.

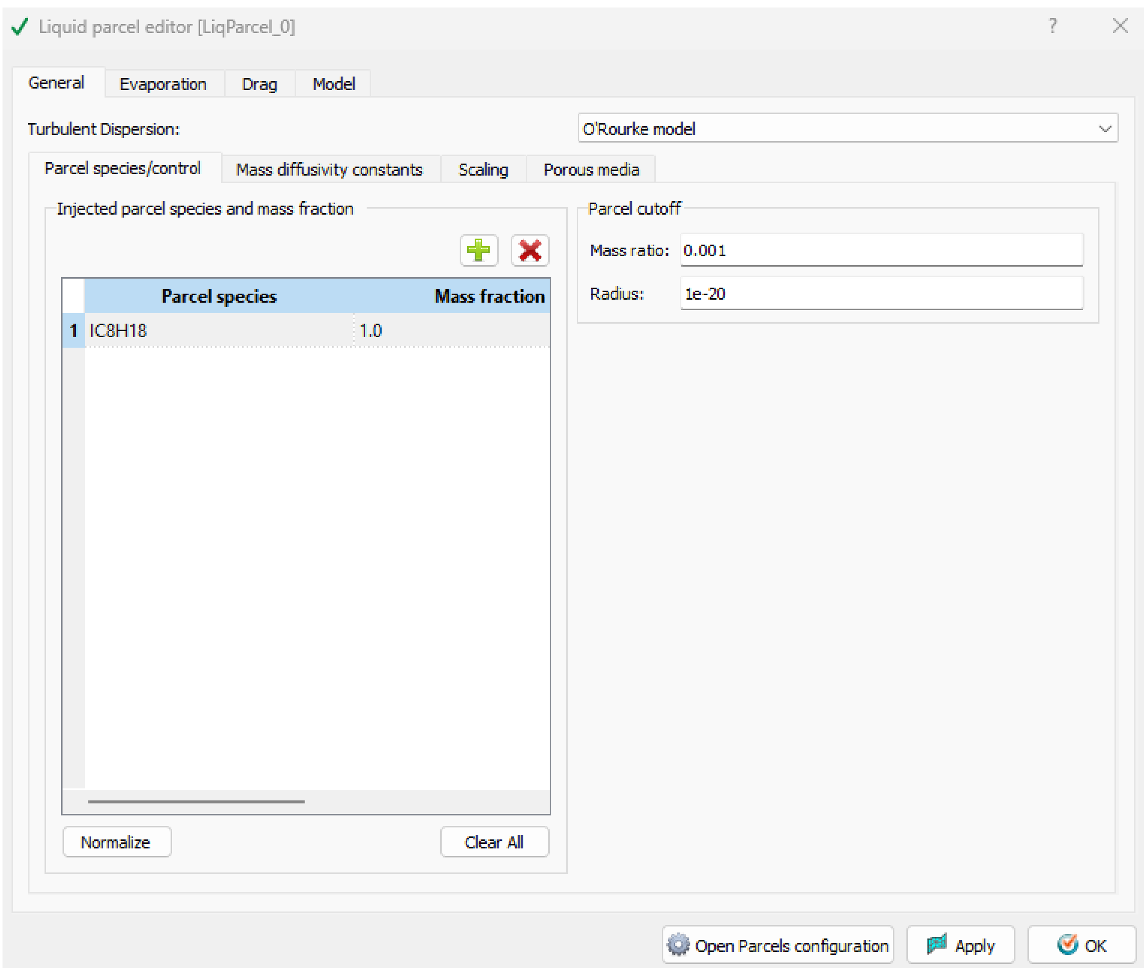

The Frossling model is used to simulate droplet radius reduction over time due to heat and mass transfer, capturing evaporation dynamics in high-temperature, turbulent environments like internal combustion engines [6]. The evaporation model actively simulates fuel droplet vaporization throughout the combustion process.

The evaporation source is set to "2 - Source all base parcel species," enabling all base species to contribute to vaporization for accurate mass transfer tracking. Temperature discretization is enabled to refine thermal calculations, and advanced heat diffusion is applied to droplets larger than 1000.0 m.

The setup uses 15 finite volume cells per spray parcel for high-resolution evaporation and heat transfer modeling. Thermal conductivity is defined as "Physical" to ensure realistic fuel properties. These settings improve the accuracy of droplet vaporization simulations and fuel-air mixture preparation.

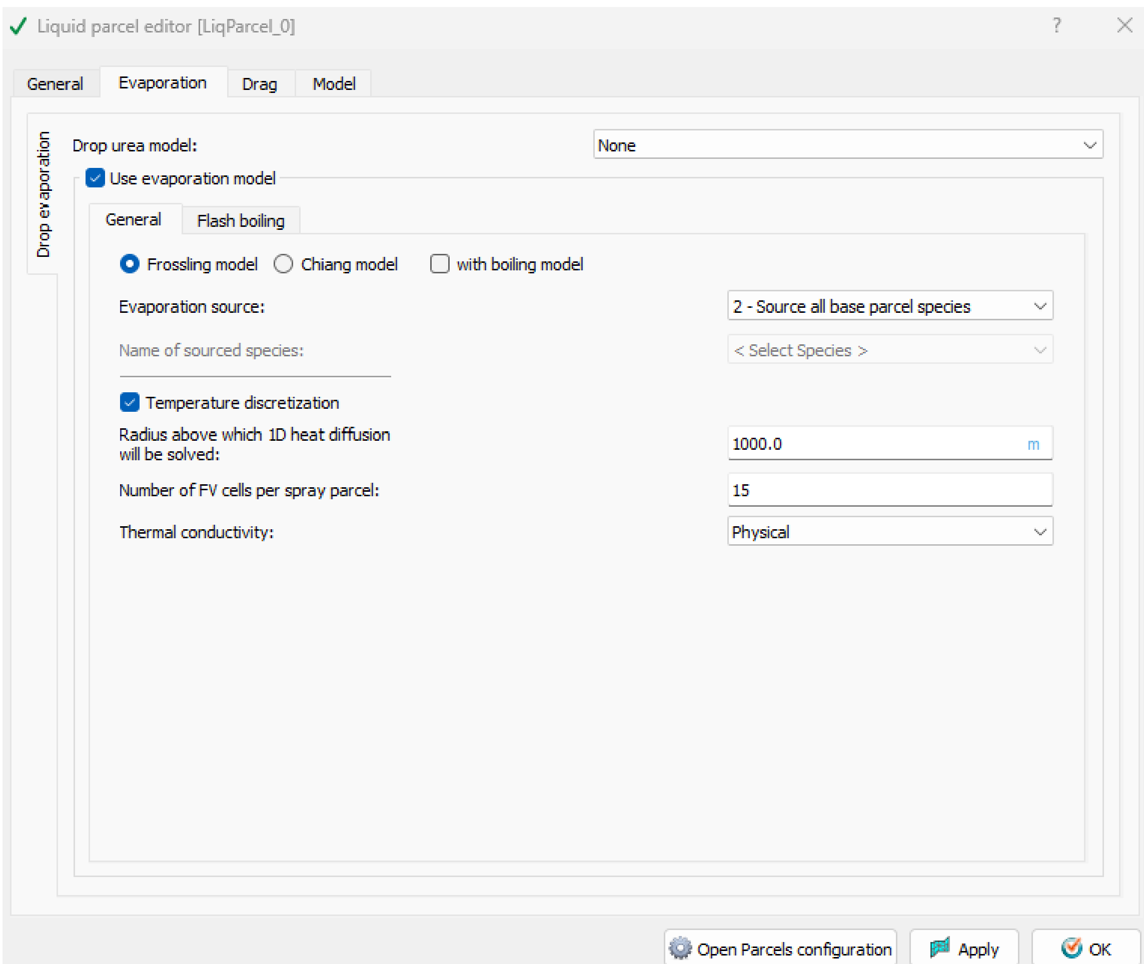

The dynamic drop drag model is employed to accurately simulate the drag forces acting on the fuel droplets during injection and combustion. Unlike static drag models, this approach dynamically adjusts the drag coefficient to account for changes in droplet shape, velocity, and surrounding flow conditions. This adaptability ensures a more precise calculation of droplet trajectories as they interact with the turbulent flow field within the combustion chamber.

The drag model parameters are finely tuned to represent the droplet dynamics accurately. The TAB/Dynamic drag var 1 is set to 0.08333, controlling the response of the droplet to aerodynamic forces and its oscillatory behavior during deformation. The TAB/Dynamic drag var 2, set to 10.0, determines the damping of these oscillations, ensuring stable simulations under high turbulence. Finally, TAB/Dynamic drag var 3, set to 8.0, governs the critical Weber number, a dimensionless ratio of aerodynamic forces to surface tension forces, influencing the conditions under which droplets break up due to aerodynamic stress [7].

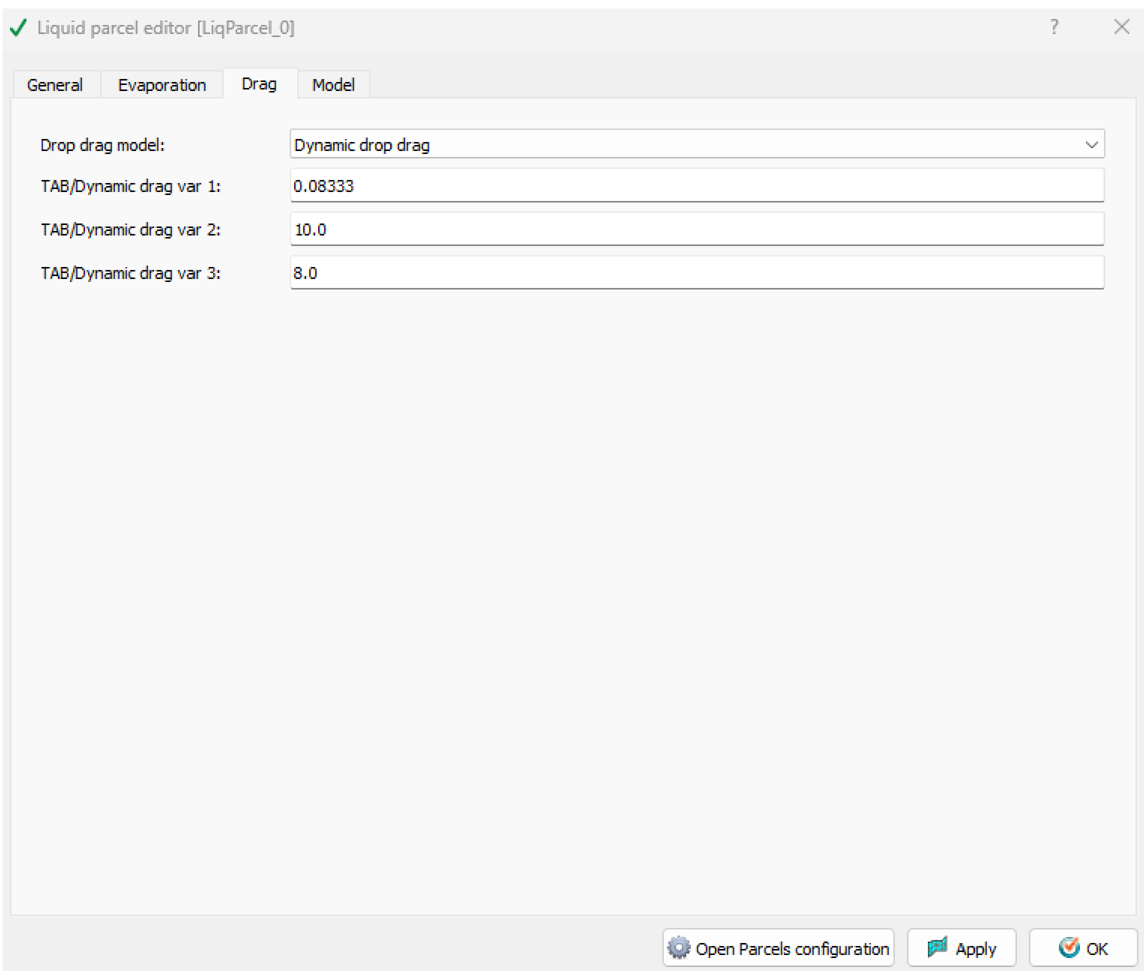

The KH and RT models are selected for predicting the atomization and breakup of liquid fuel. The KH model handles the initial breakup of droplets due to aerodynamic forces, while the RT model captures further disintegration due to instabilities in the fuel surface. This combination ensures a realistic simulation of fuel spray, improving the prediction of combustion dynamics.

The `Create child parcels` option is enabled to simulate the breakup of large parent droplets into smaller child droplets, which is essential for achieving a more refined spray pattern.

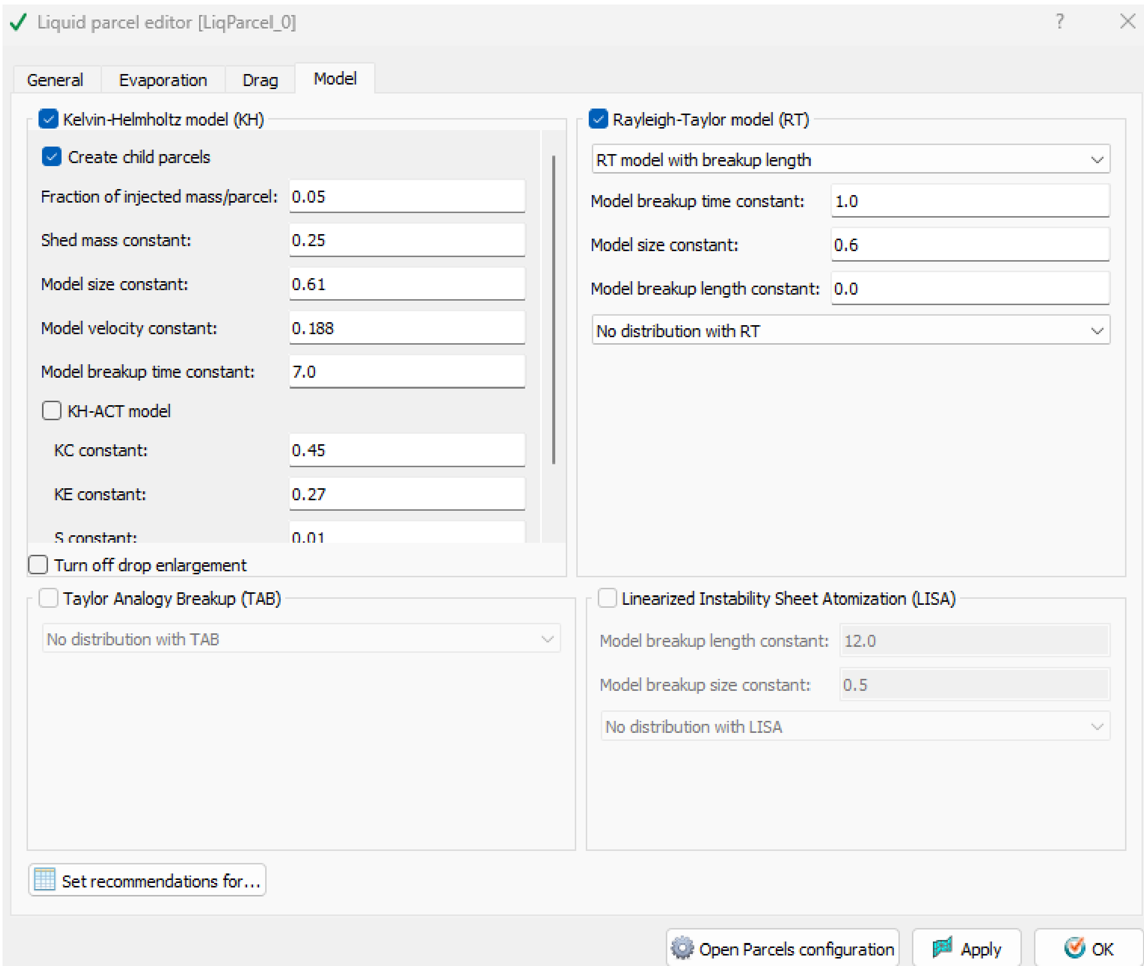

- Parcels introduction

The injector configuration involves setting up the injector name, stream ID, parcel type, and corresponding parcel reference. Here, `Injector_0` is defined with a stream ID of 0, referencing the `LiqParcel_0` parcel type, which is specifically configured for liquid fuel injections.

The injector utilizes the `BLOB` injection distribution, which simulates the initial fuel droplet size and distribution based on the specified nozzle characteristics [8]. This distribution is suitable for capturing the initial droplet formation and subsequent breakup during the injection process.

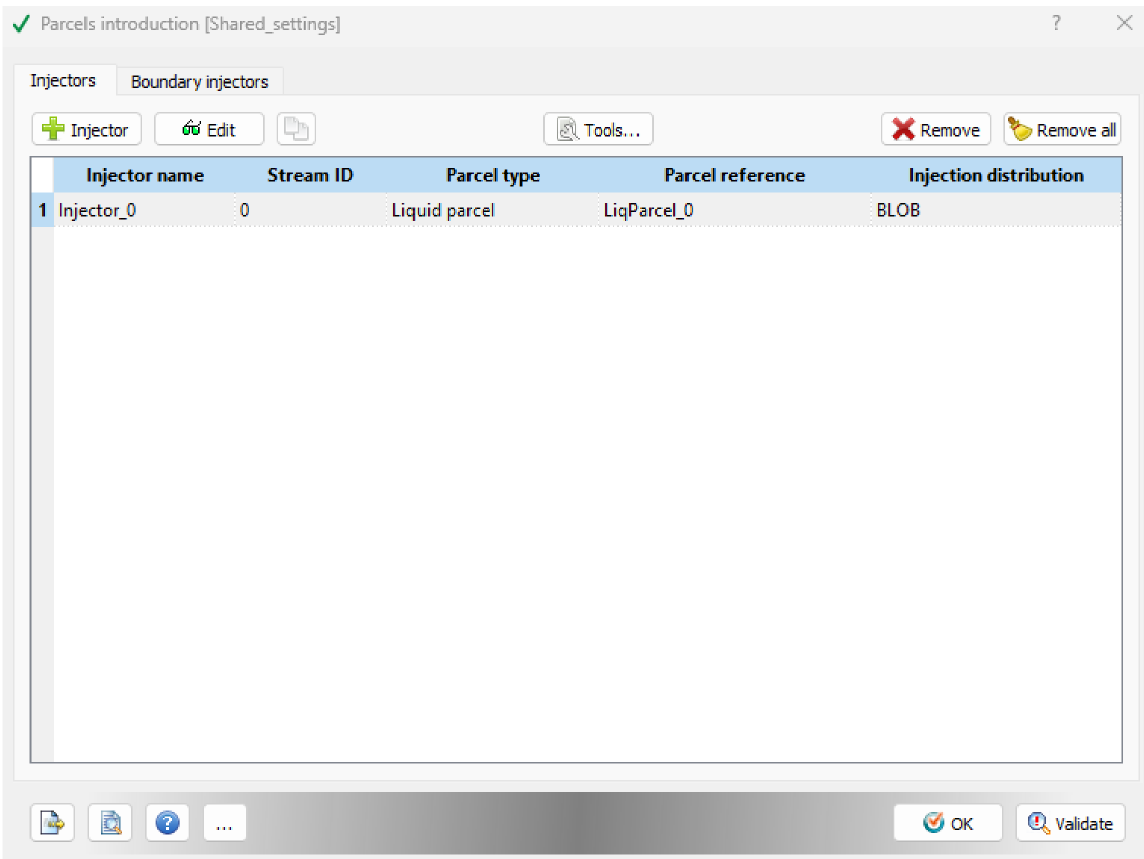

The `VOF-Spray coupling` is left unchecked, as this setup does not require volume-of-fluid (VOF) interactions with the spray. Instead, the injection is defined through a constant rate-shape, which simplifies the simulation while maintaining accuracy in the fuel delivery characteristics.

The parcel distribution is set to distribute parcels evenly throughout the injection cone, ensuring that fuel droplets are uniformly spread, mimicking real-world injector behavior.

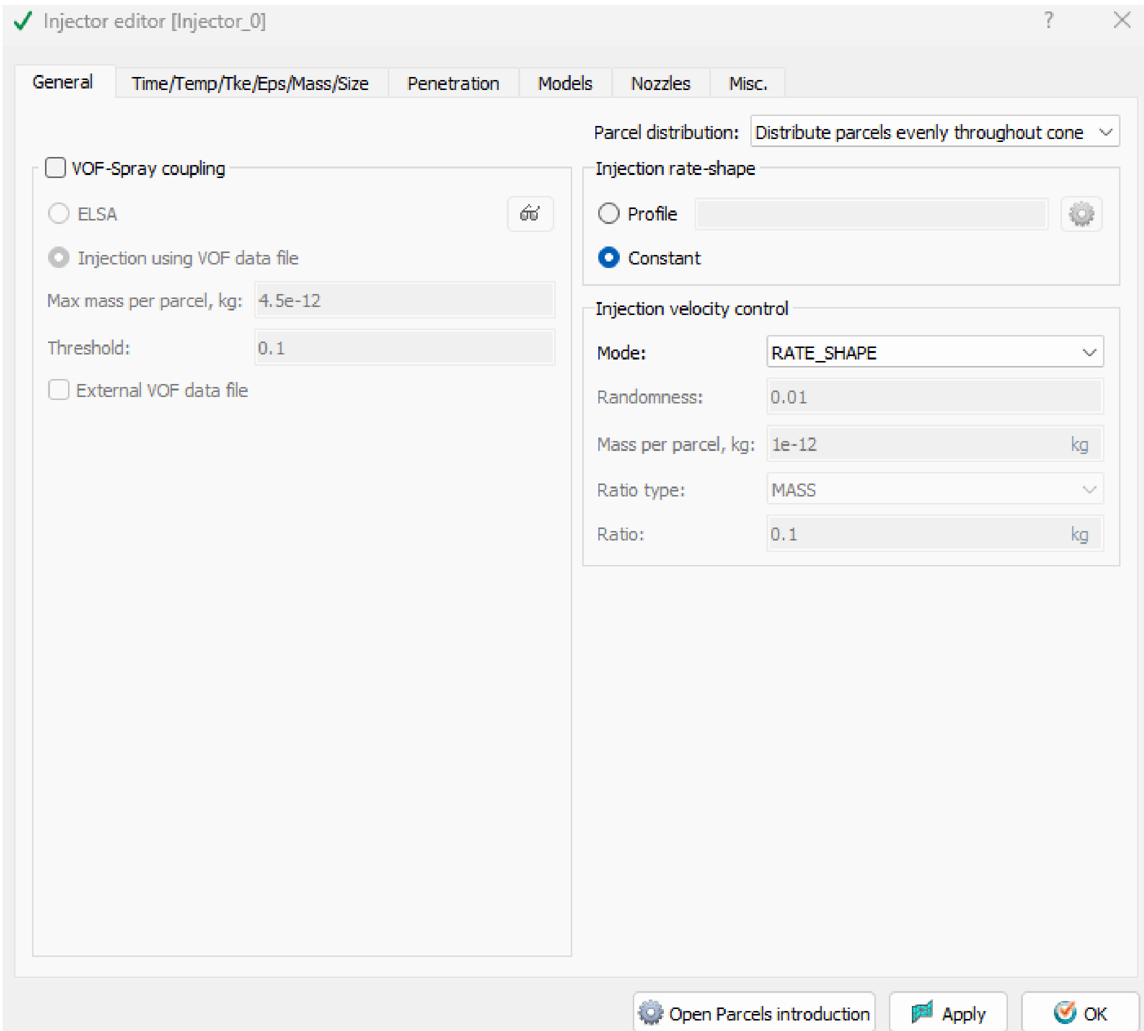

The injection temporal type is set to `CYCLIC` with a cyclic period of 720 degrees, matching the operating cycle of a 4-stroke engine. The start of injection is specified at -480 degrees, with an injection duration of 191.2 degrees, accurately modeling the timing of fuel delivery within the engine cycle.

The total injected mass is configured as 3e^{-05} kg per cycle, corresponding to the specified mass flow rate of the injector and ensuring consistent fuel delivery during each engine cycle.

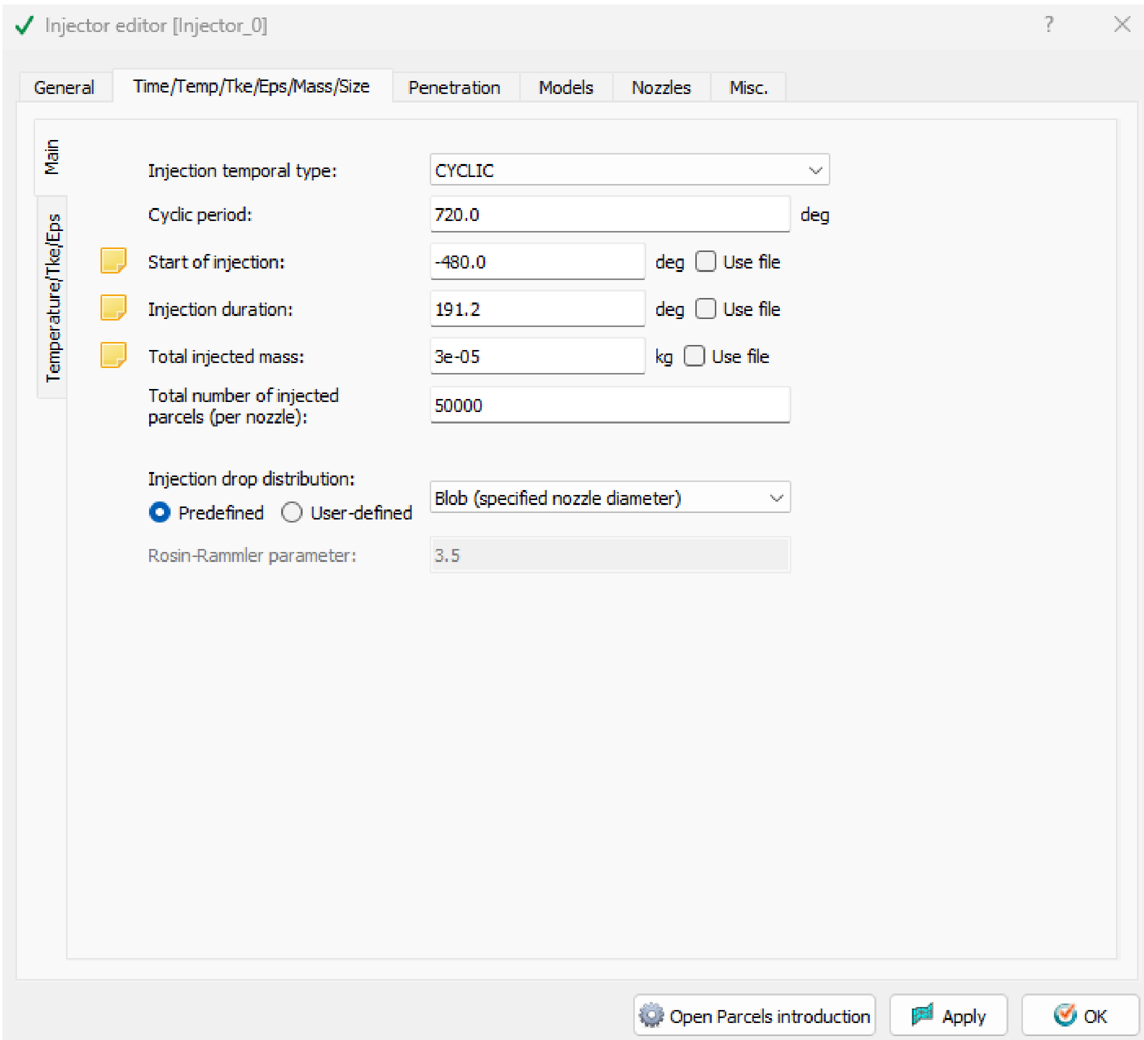

The injector temperature is set to a constant value of 330 K, reflecting the initial fuel temperature as it enters the cylinder. Turbulent kinetic energy (tke) and dissipation (eps) values are also defined to characterize the fuel-air mixing and spray dynamics, critical for accurate combustion modeling.

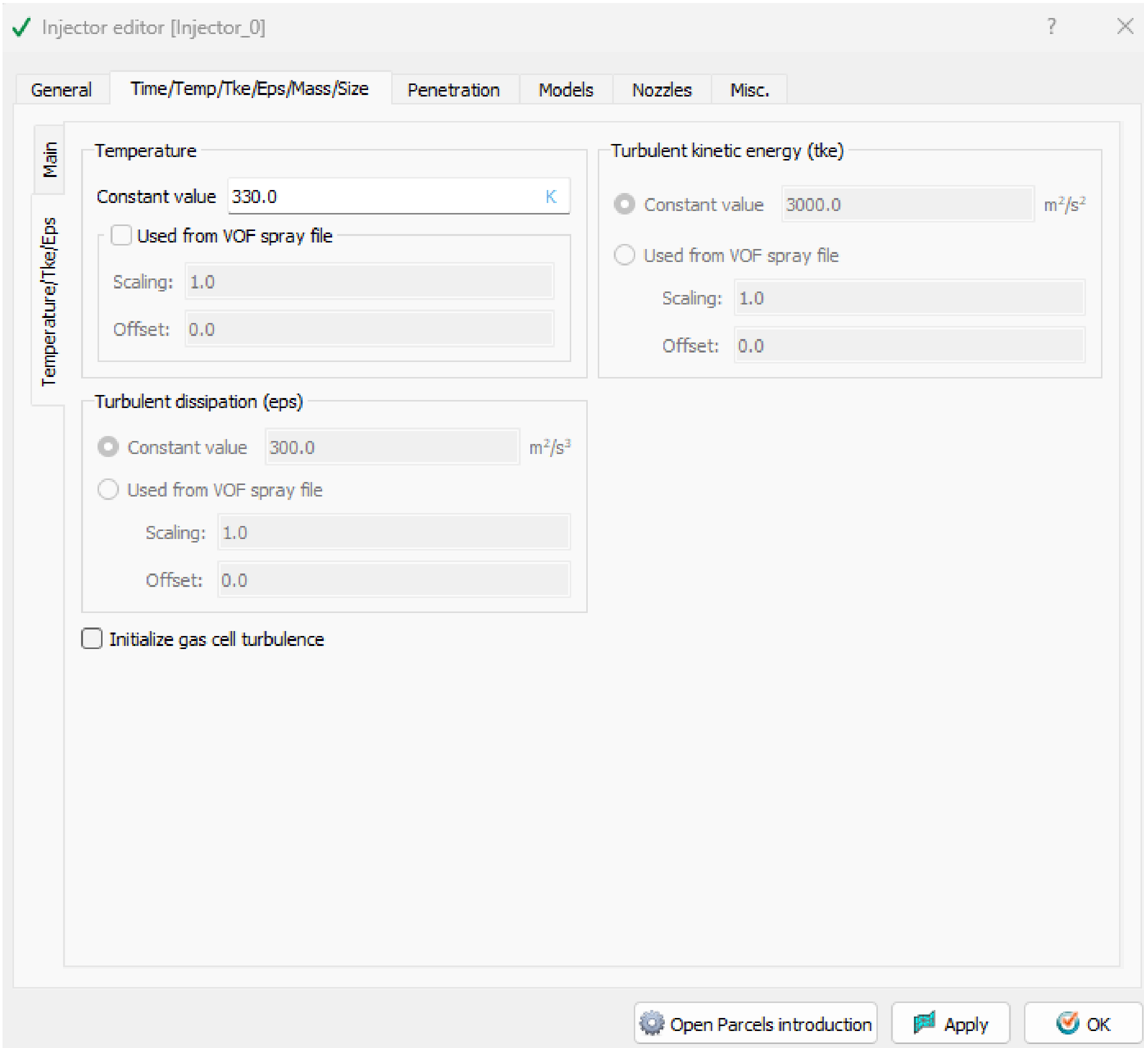

Parameters for liquid and vapor penetration are configured to ensure accurate calculation of spray characteristics, critical for determining combustion efficiency and emissions in the engine. The liquid fuel mass fraction for calculating spray penetration is set to 0.95, indicating that the spray penetration length is determined based on the region where the liquid phase of the fuel constitutes 95% of its mass. This ensures precise identification of the liquid spray's extent within the combustion chamber.

The bin size for calculating vapor penetration is set to 0.001 m, providing a high spatial resolution for analyzing the vapor phase's penetration depth. This resolution is particularly important for capturing the transition of fuel from liquid to vapor as it mixes with air, significantly influencing ignition and flame propagation.

Similarly, the fuel vapor mass fraction for calculating vapor penetration is set to 0.001, specifying the threshold at which the vapor phase is considered in the penetration calculation. These parameters are carefully tuned to capture both the liquid and vapor phases' behavior, ensuring accurate predictions of spray penetration, mixing efficiency, and the subsequent combustion dynamics in the engine.

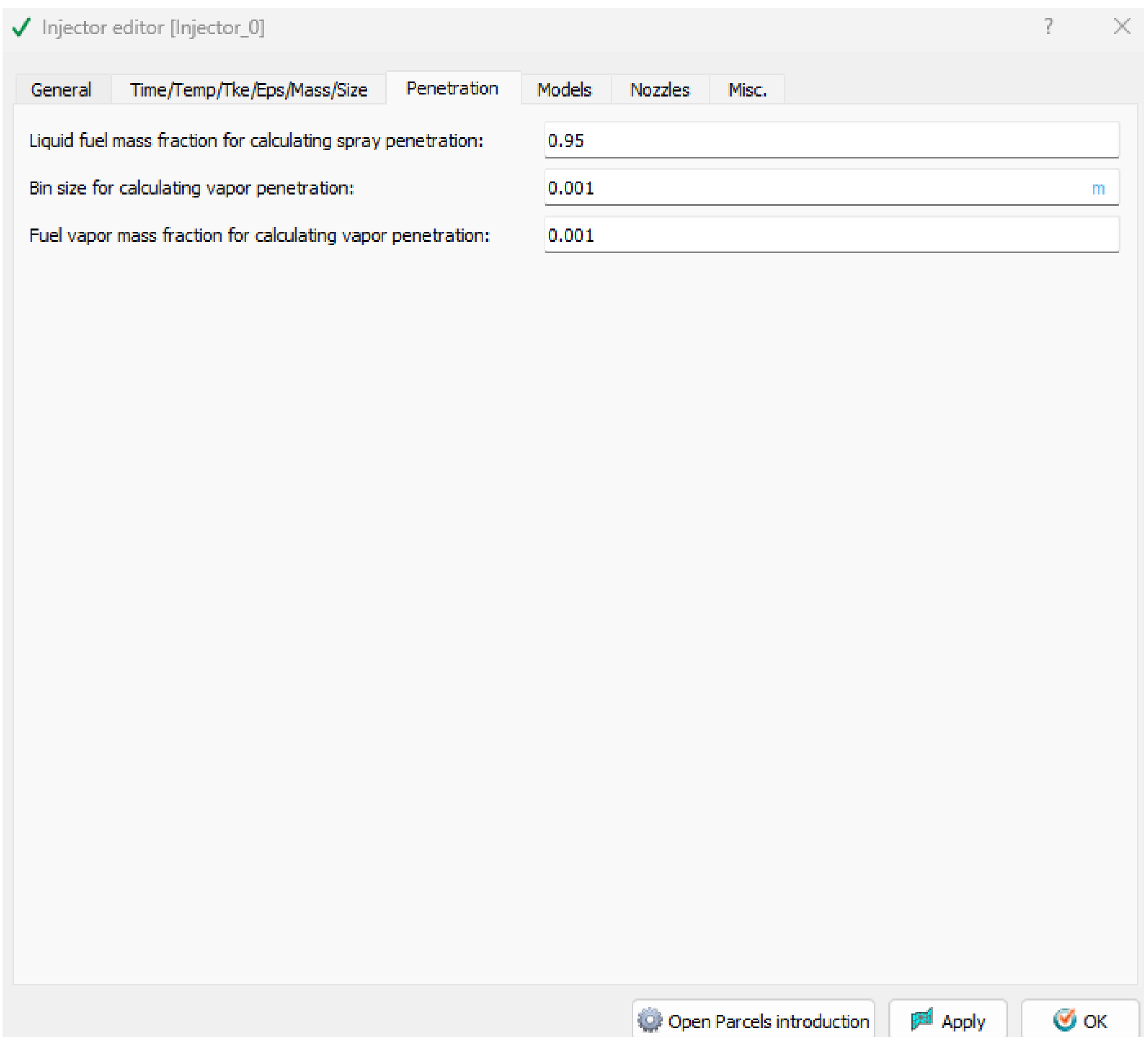

The `Discharge coefficient model` is enabled with a coefficient value of 0.8, representing the flow characteristics of the injector nozzles [9]. This model helps in determining the velocity and distribution of fuel droplets as they exit the nozzles, crucial for accurate spray representation.

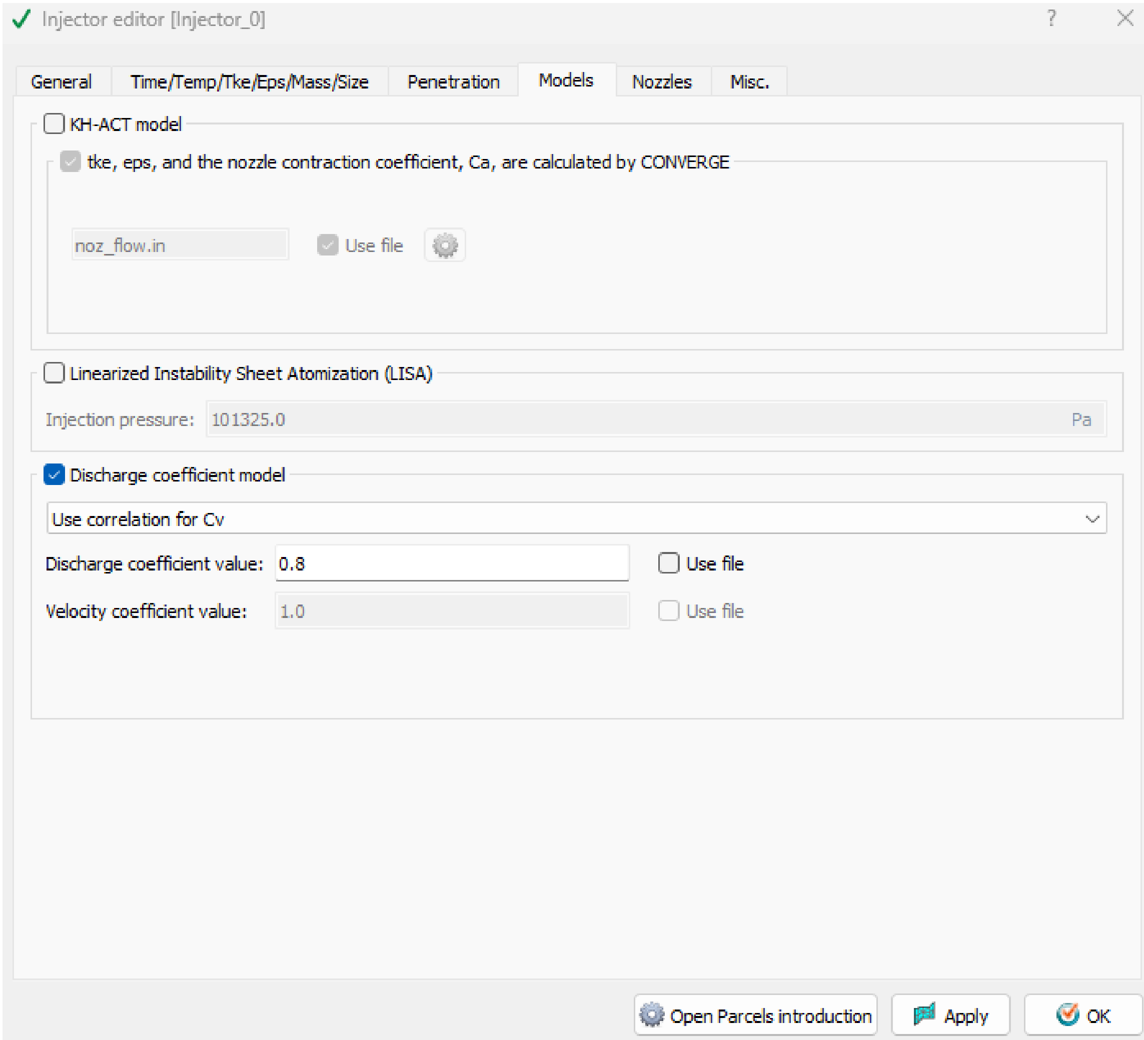

For `Injector 0`, four nozzles are defined to simulate the fuel spray accurately. The configuration of each nozzle, including its position, orientation, and spray characteristics, is crucial for replicating the real-world injection conditions specified by the manufacturer. Each nozzle is individually configured with specific properties such as diameter, cone angle, and location to ensure precise representation of the spray pattern.

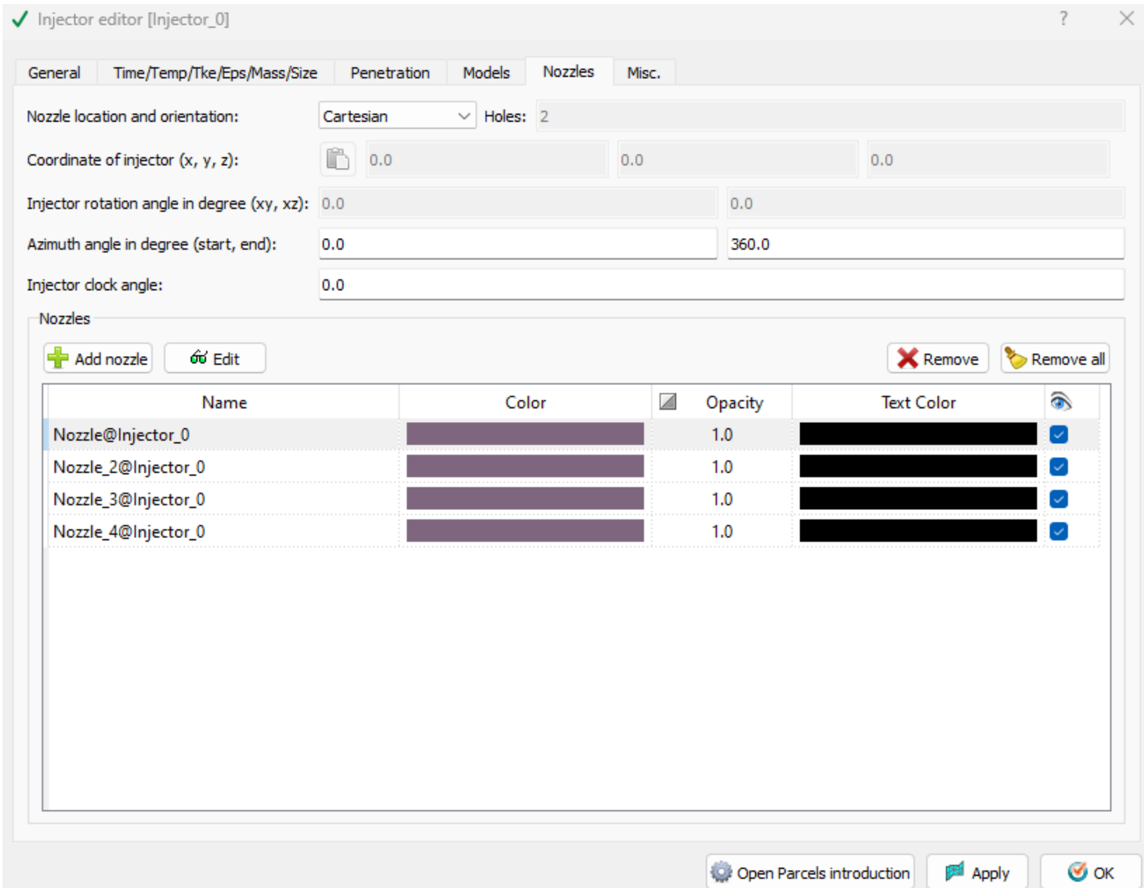

The nozzle diameter is set to 0.00025 m with a circular injection radius of 0.000125 m. The spray cone angle is 10 degrees, consistent with the specified fuel injection dynamics.

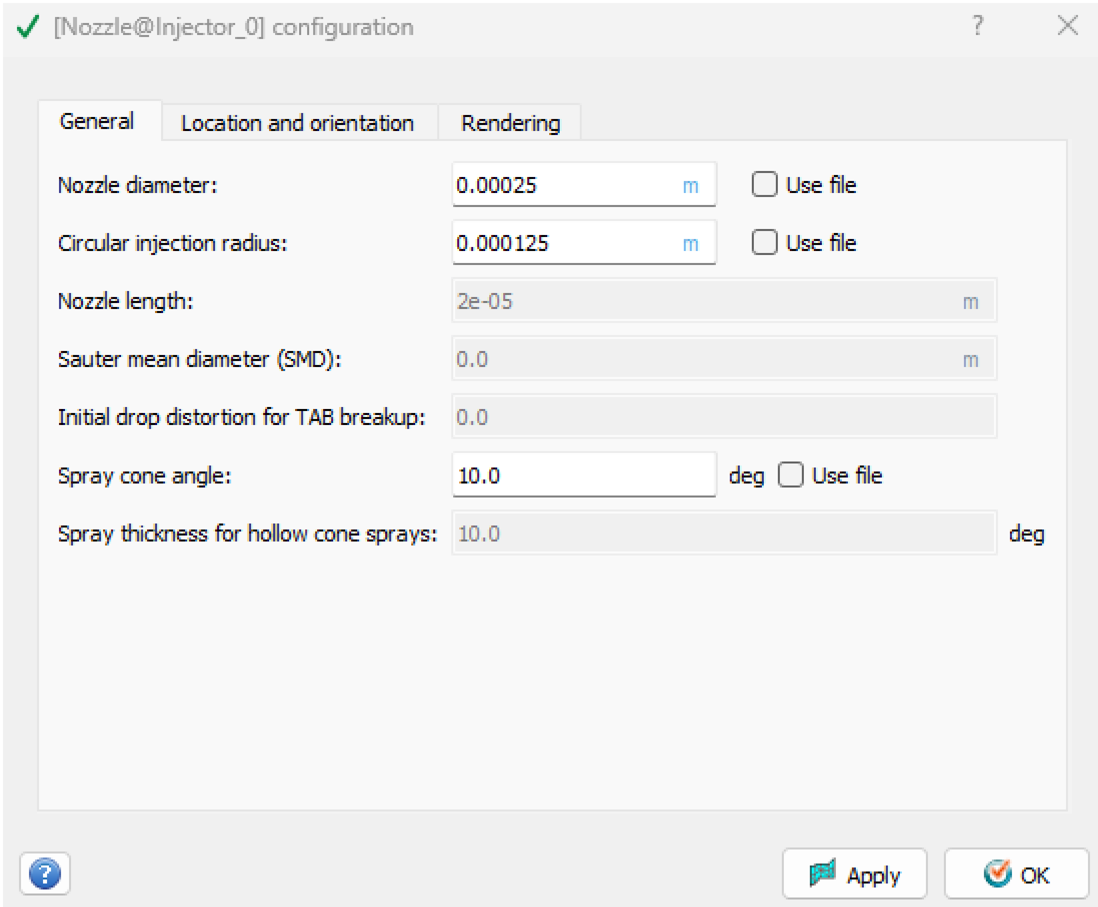

The coordinates for nozzle no.1 (given in the problem statement) are defined as (0.0823357, 0.00100001, 0.07019) with an orientation vector of (-0.732501, 0.210489, -0.647408), reflecting the manufacturer's specifications for accurate placement and direction of the fuel spray. Other nozzles are set similarly.

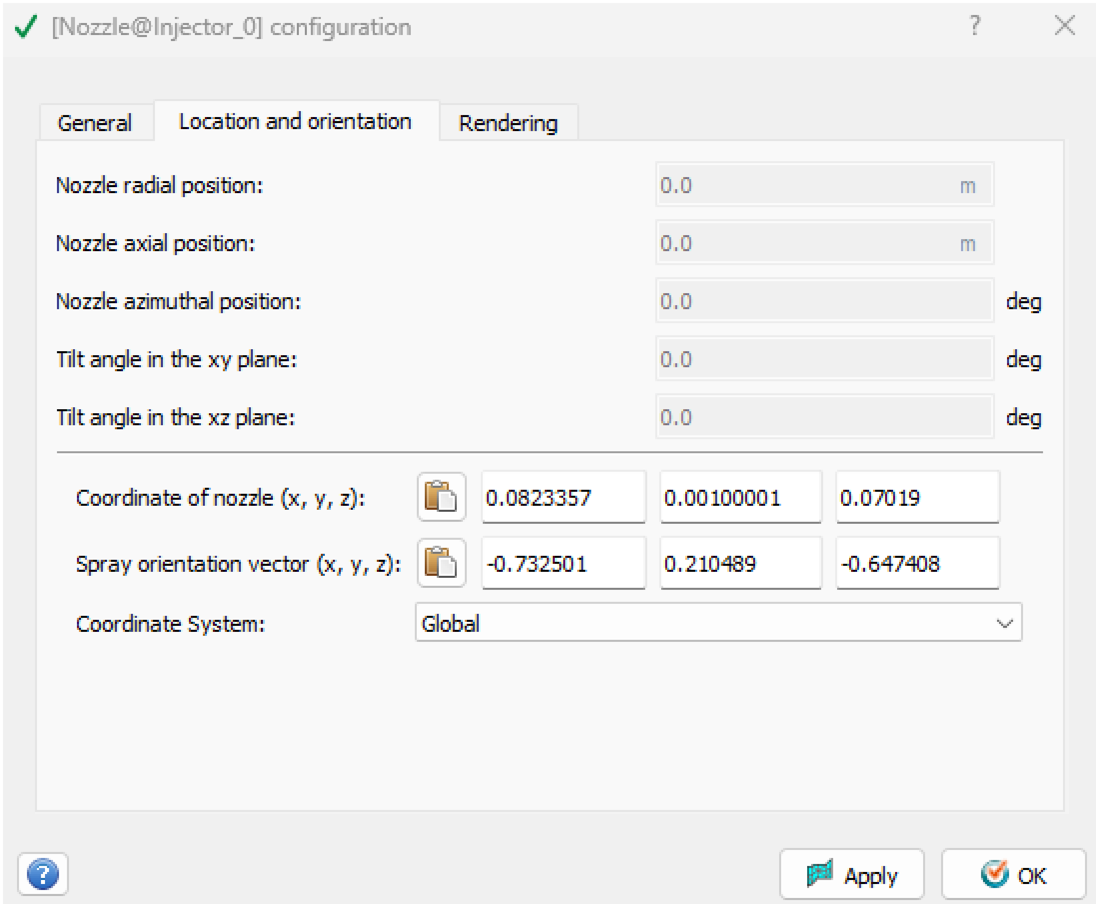

The nozzle spray cone is visualized to ensure correct alignment and opacity settings, which aids in verifying the spray distribution within the engine simulation.

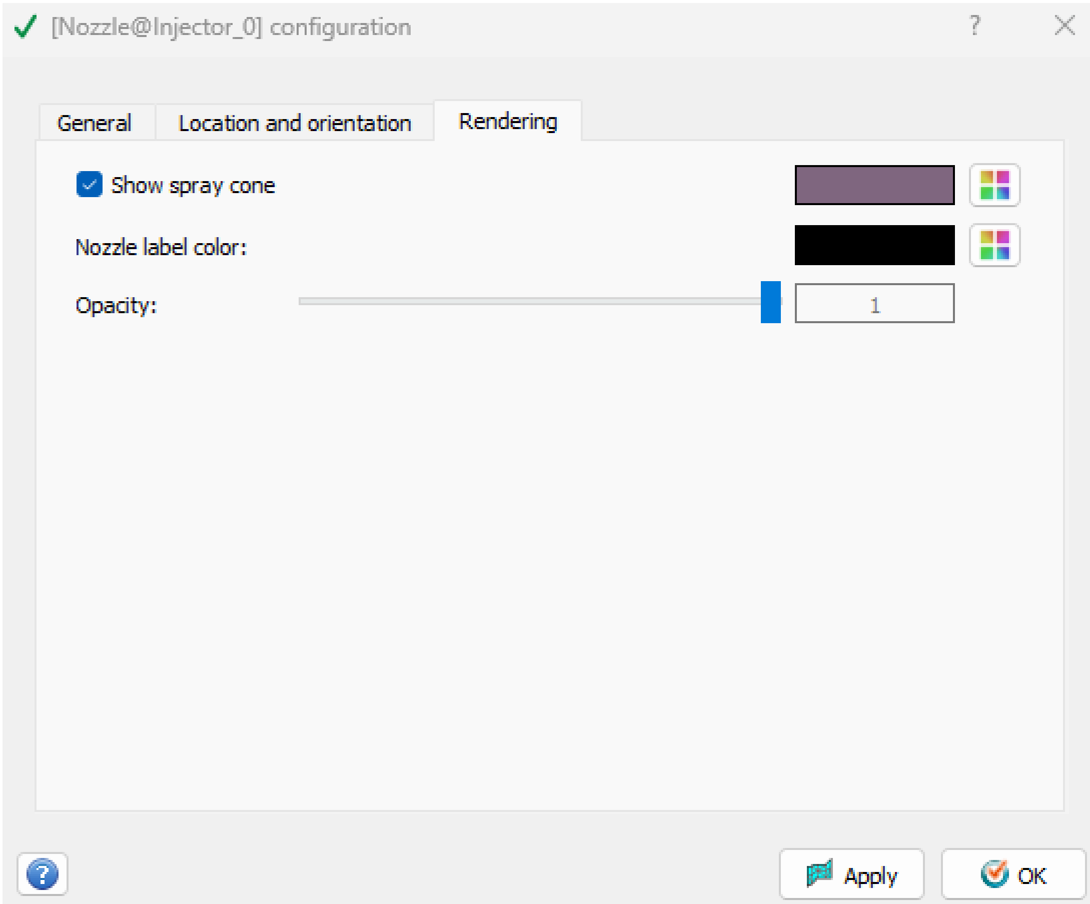

The `Injector 0` setup utilizes a Solid Cone Spray type, which is suitable for accurately simulating the injection of fuel in a concentrated and controlled manner.

- The Dynamic Cone Angle option is disabled, and the spray cone angle is set to a fixed value of 10 degrees (shown in a previous step), ensuring a consistent and repeatable spray pattern throughout the injection event.
- The Swirl Fraction is set to 0.0, indicating no swirl effect on the injected fuel, which is appropriate for this specific injector design and operational conditions.

This configuration helps maintain the stability of the spray cone and ensures that the fuel is evenly distributed into the combustion chamber, optimizing the air-fuel mixture for effective combustion.

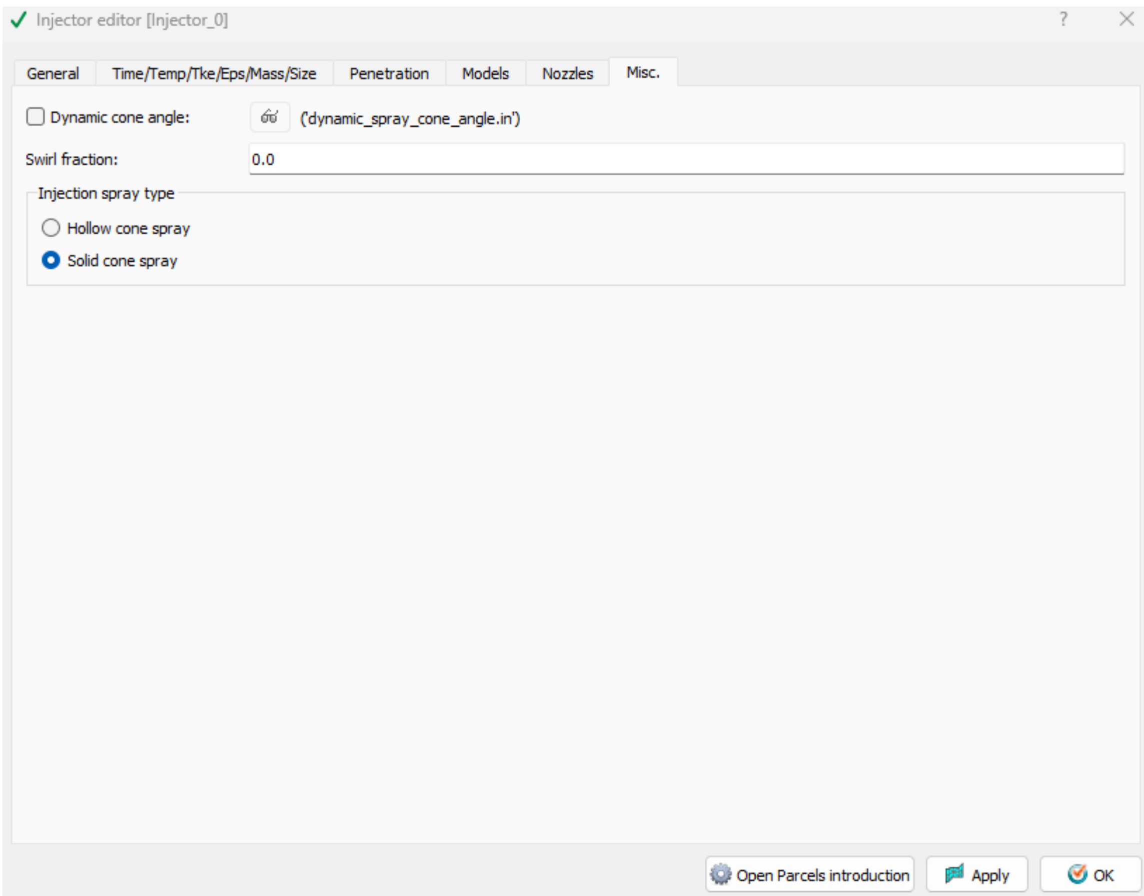

- Parcel-wall interaction

The parcel-wall interaction settings define how liquid parcels behave when they impact engine surfaces, influencing fuel spray dynamics, film formation, and combustion [10].

The wall film model simulates droplet interactions with surfaces, while the O'Rourke film splash model estimates splash behavior based on Weber number, film thickness, and viscosity, providing realistic splash and film formation dynamics [5], [7].

Key parameters include a critical splashing value of 3330, fraction splashed at 1.0 and rebound Weber number of 5.0. These settings control how fuel droplets either splash back or form a film on surfaces.

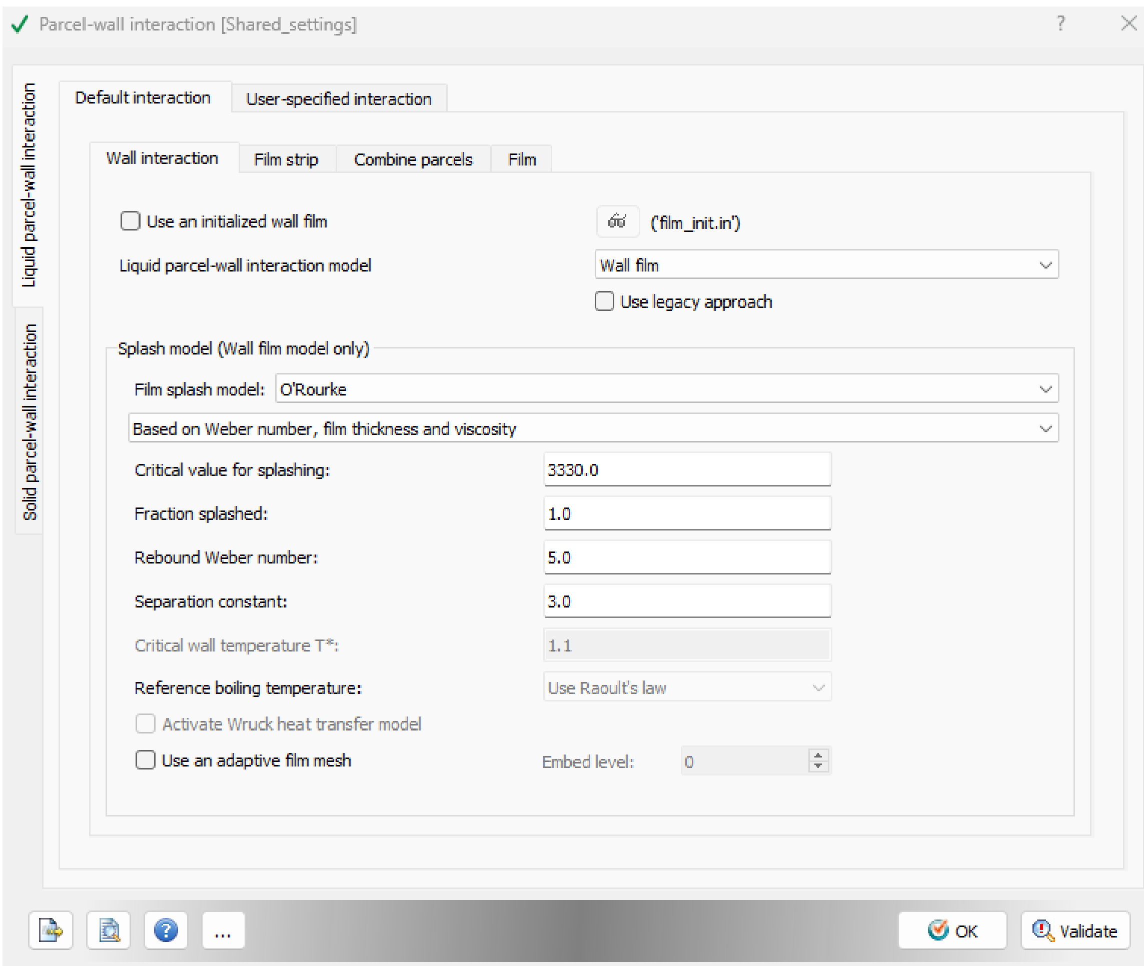

Enable the film evaporation model to simulate the evaporation of fuel films on surfaces, using IC_8H_{18} as the evaporating species, which helps in accurately modeling heat transfer and fuel-air mixing in the engine.

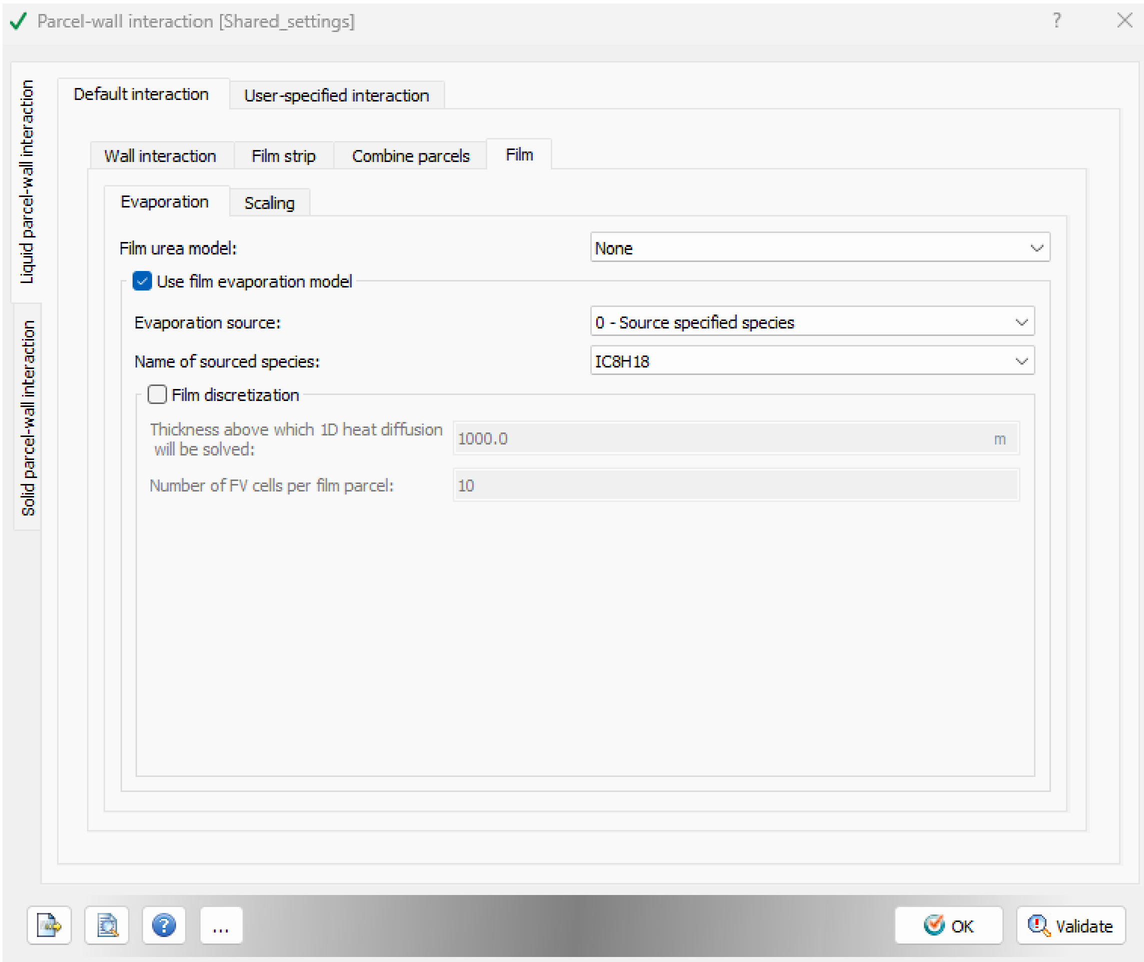

- Combustion modeling

Combustion modeling employs the SAGE detailed chemistry solver with adaptive zoning to capture chemical reactions and combustion processes accurately [11]. The fuel species, defined as IC_8H_{18}, ensures precise representation of combustion chemistry, including intermediate reactions and product formation. The temporal type is set to CYCLIC, with a 720-degree cycle period for a full 4-stroke engine cycle, simulating ignition, flame propagation, and energy release from -17 to 130 degrees.

A combustion temperature cutoff of 600 K prevents processing reactions in non-viable zones, and a minimum hydrocarbon mole fraction of $1e^{-08}$ ensures trace fuel amounts are considered without excessive computation. The solver operates uniformly across regions, with optional features like surface chemistry and emissions models available for detailed analyses. These settings ensure efficient and accurate simulation of engine performance and emissions.

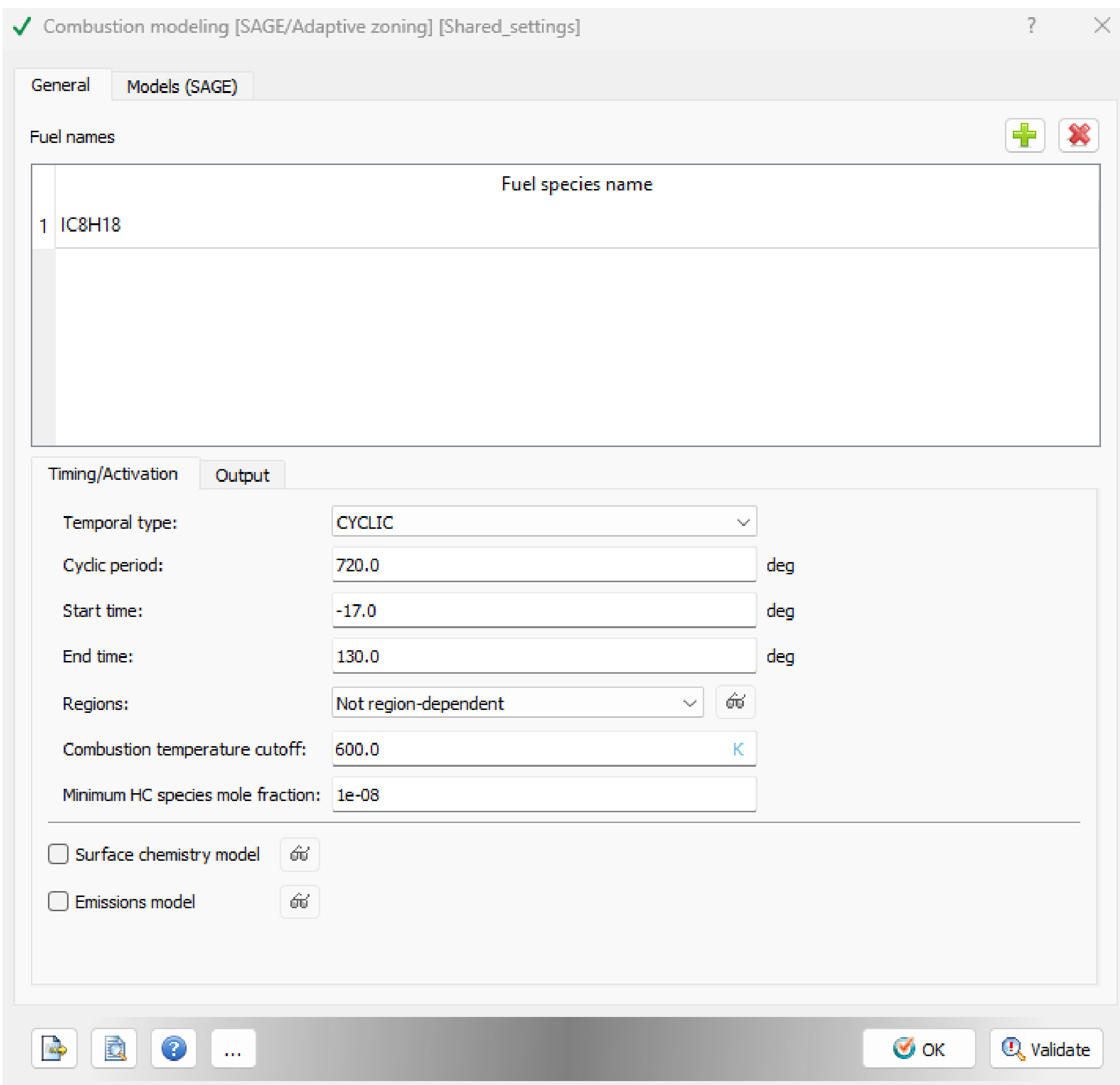

- Adaptive zoning is enabled to optimize computational efficiency by dynamically adjusting the mesh in response to temperature and reaction conditions. This helps focus computational resources on critical zones, enhancing the accuracy of the simulation.
- Key parameters include a temperature bin size of 5 K and a reaction ratio bin size of 0.05, allowing fine control over combustion dynamics.
- NO_x Conservation is enabled during species remap, ensuring that NO_x are accurately accounted for in combustion chemistry.

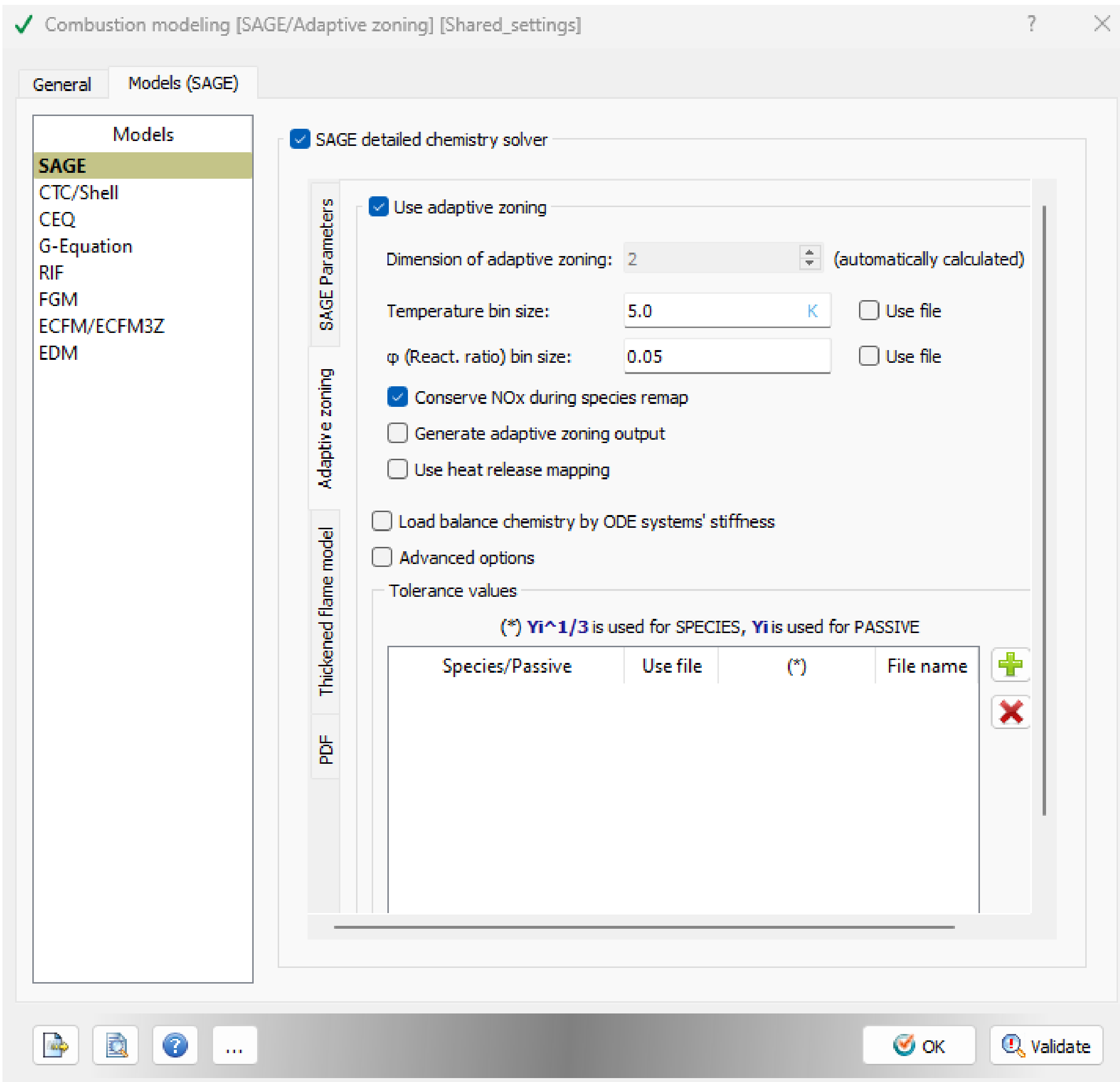

- Turbulence modeling

The RNG k-ε model is selected as the turbulence model, and the turbulence parameters appearing in the window are left unchanged.

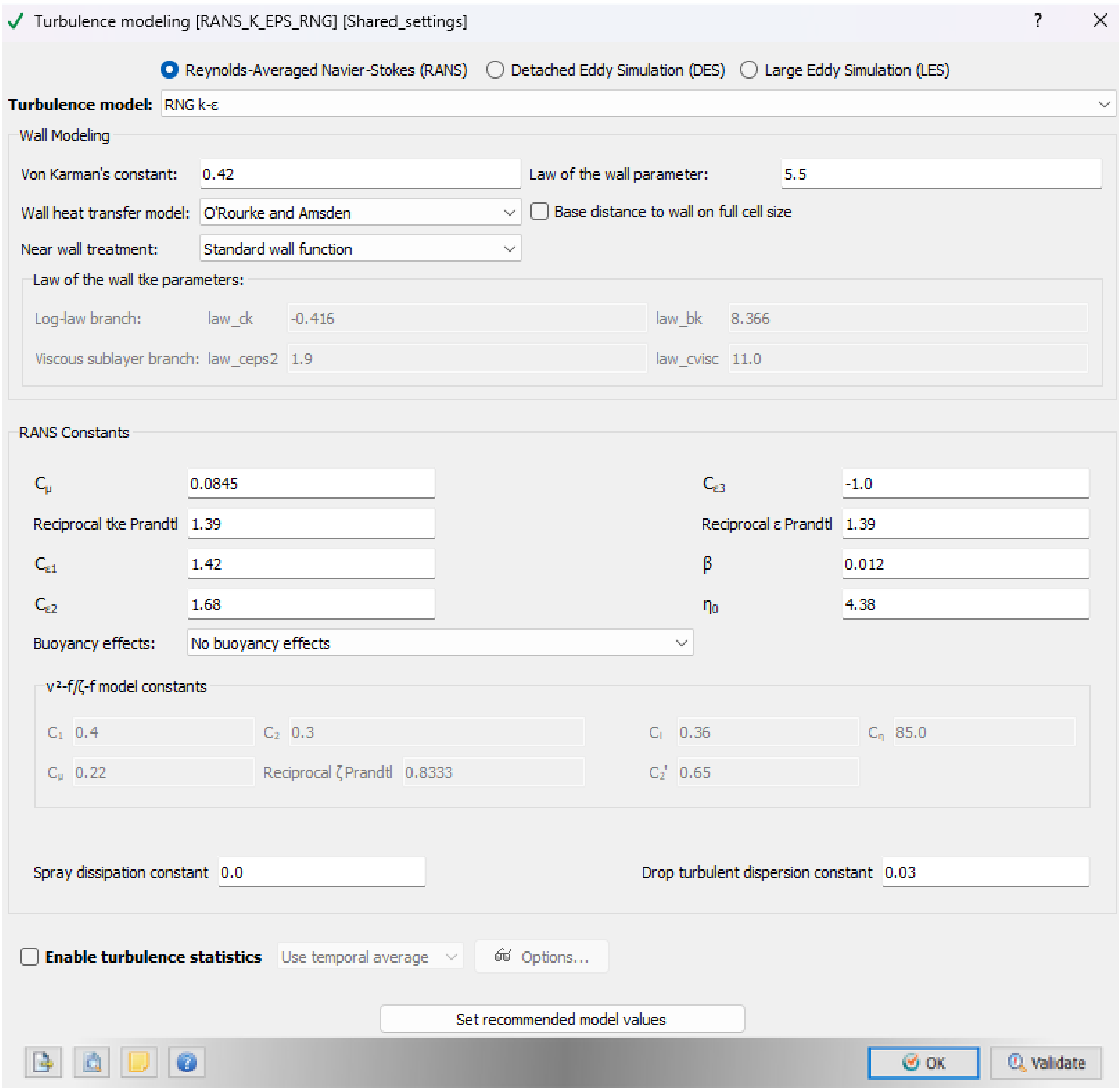

- Source/sink modeling

The source/sink modeling defines the spark plug energy sources critical for initiating combustion in the engine simulation. Two energy sources are configured to represent the ignition process:

▪ Source 1 Configuration

Mode: Set to Cyclic to match the engine cycle, starting at -15.0 degrees and ending at -14.5 degrees, aligning with the early stage of spark ignition.

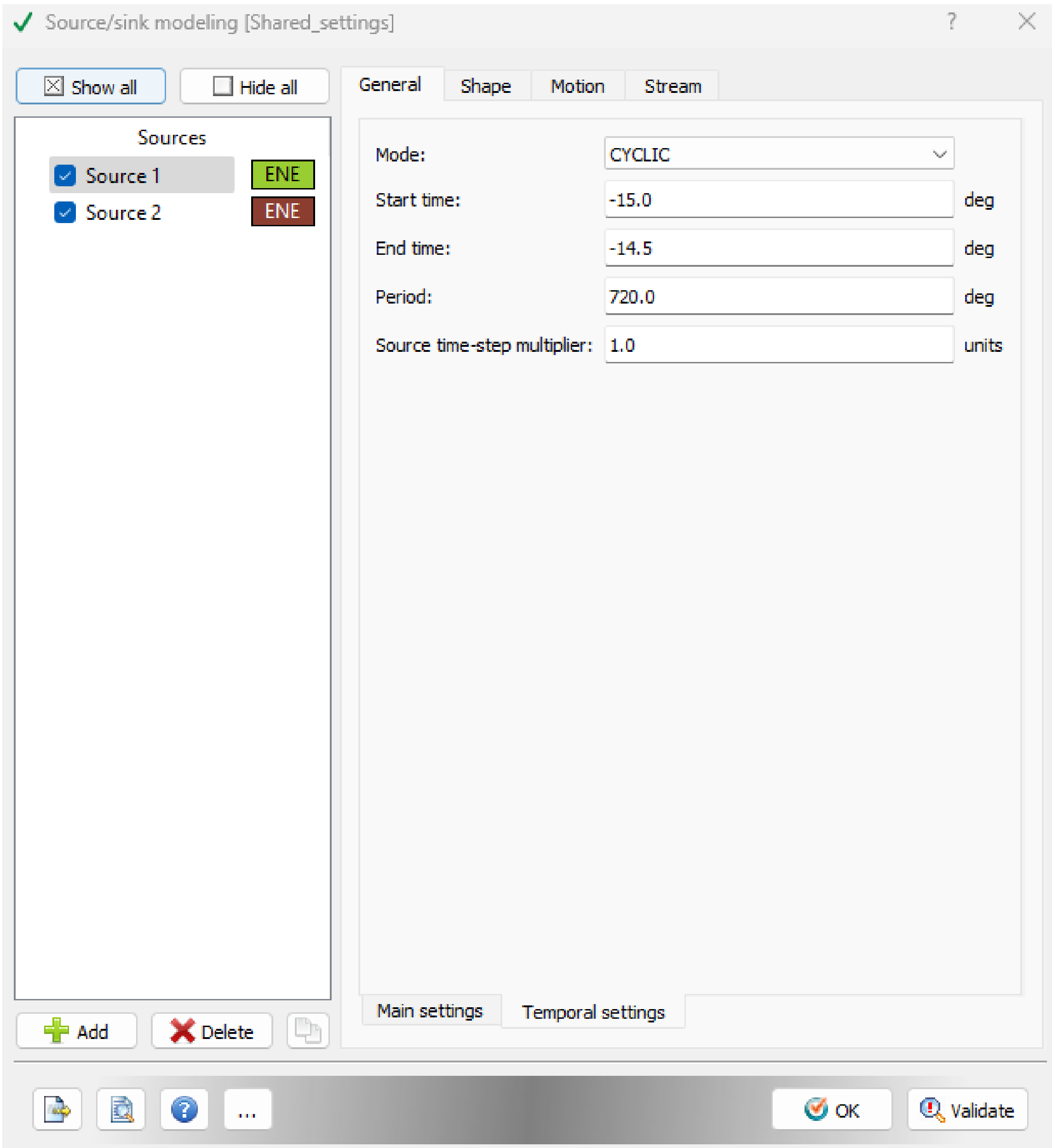

Shape: Defined as a Sphere with a radius of 0.0005 m, centered at coordinates (-0.003, 0.0, 0.0091). This spherical shape simulates the propagation of spark energy in a radial manner, replicating the real-world ignition characteristics of a spark plug [12].

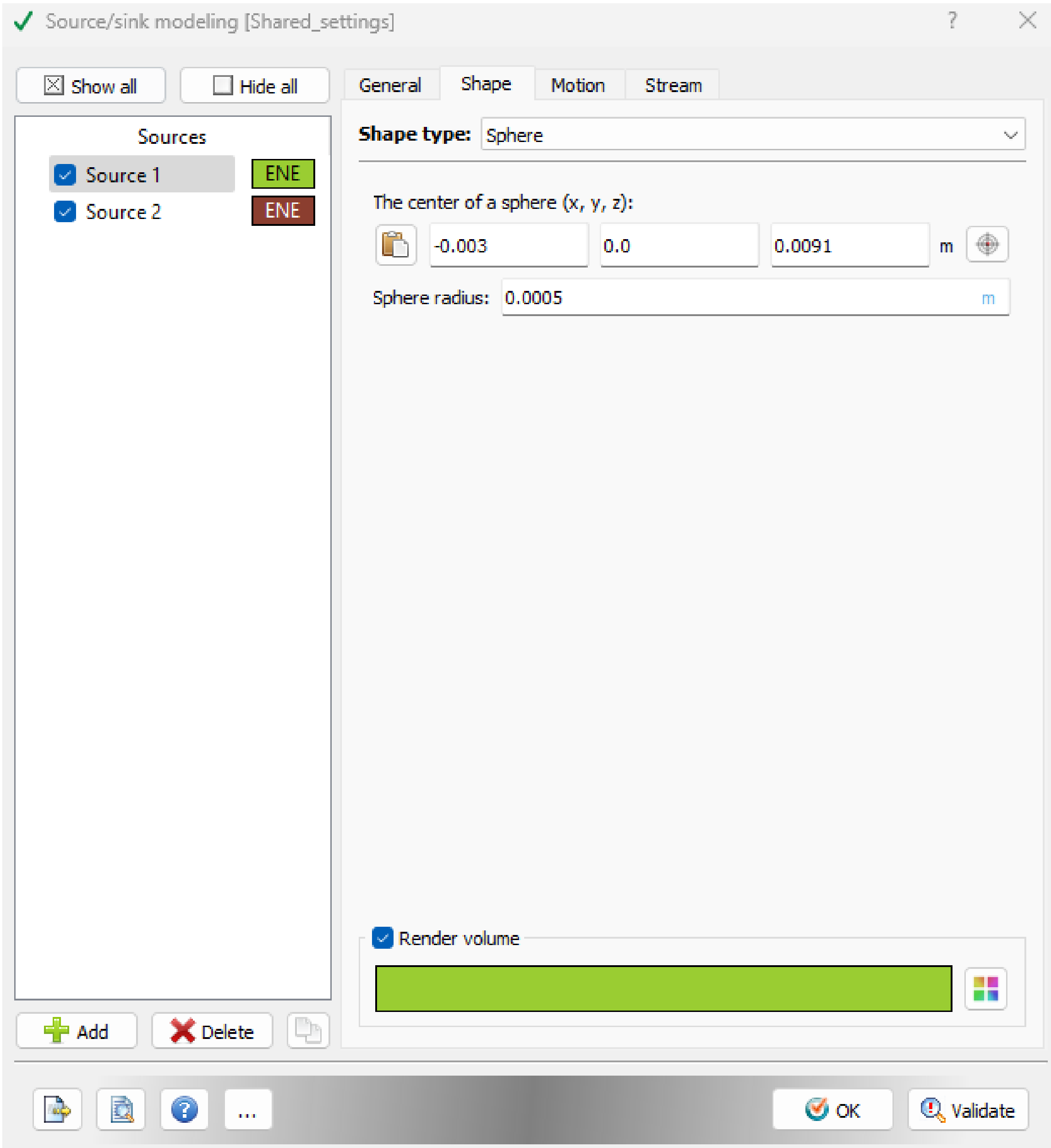

- Source 2 Configuration

Mode: Also set to `**CYCLIC**`, with a start time of -15.0 degrees and an extended end time of -5.0 degrees to cover the complete ignition duration.

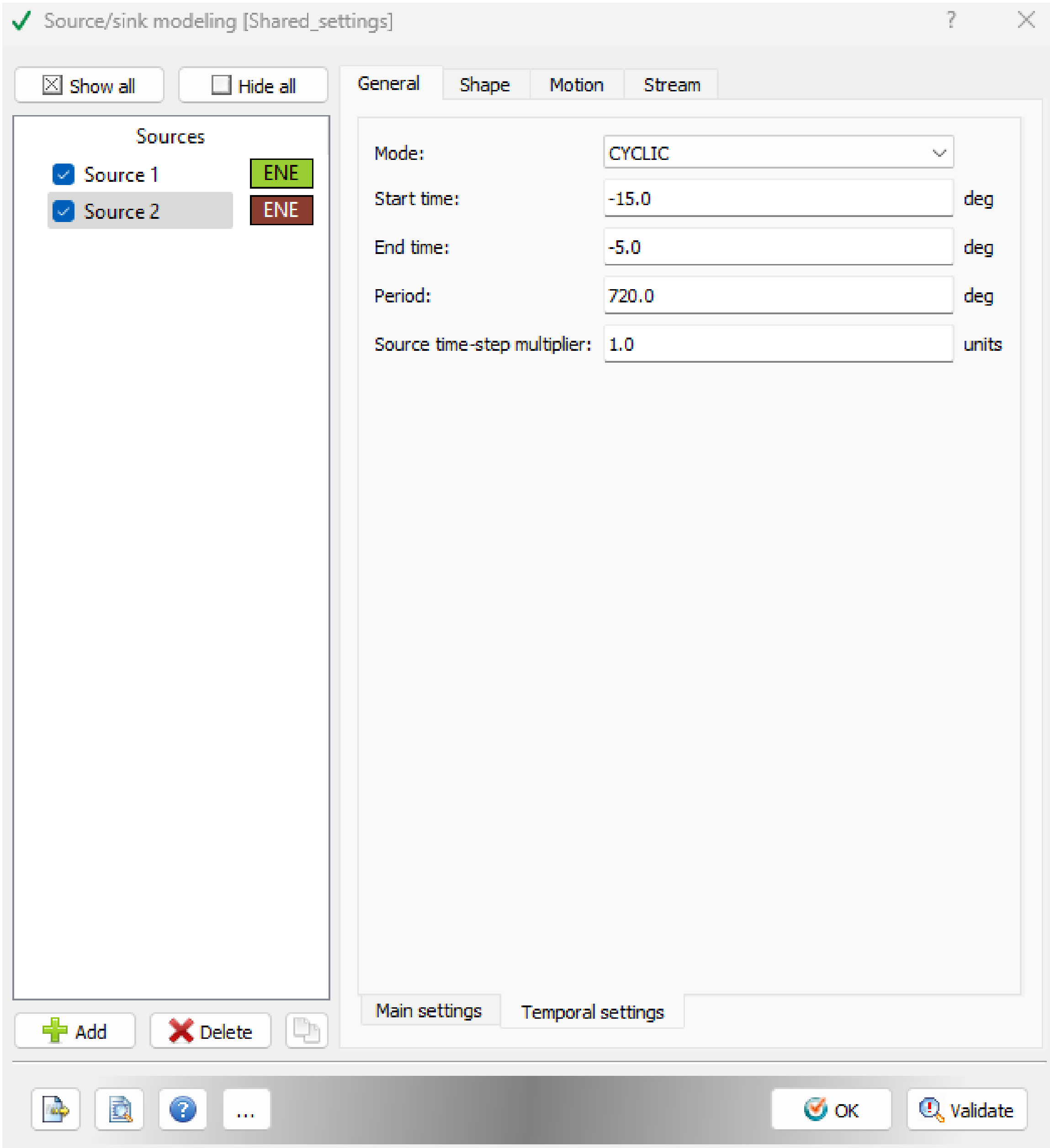

Shape: Similarly defined as a `Sphere` with the same radius and location as Source 1, ensuring consistent ignition energy distribution throughout the ignition phase.

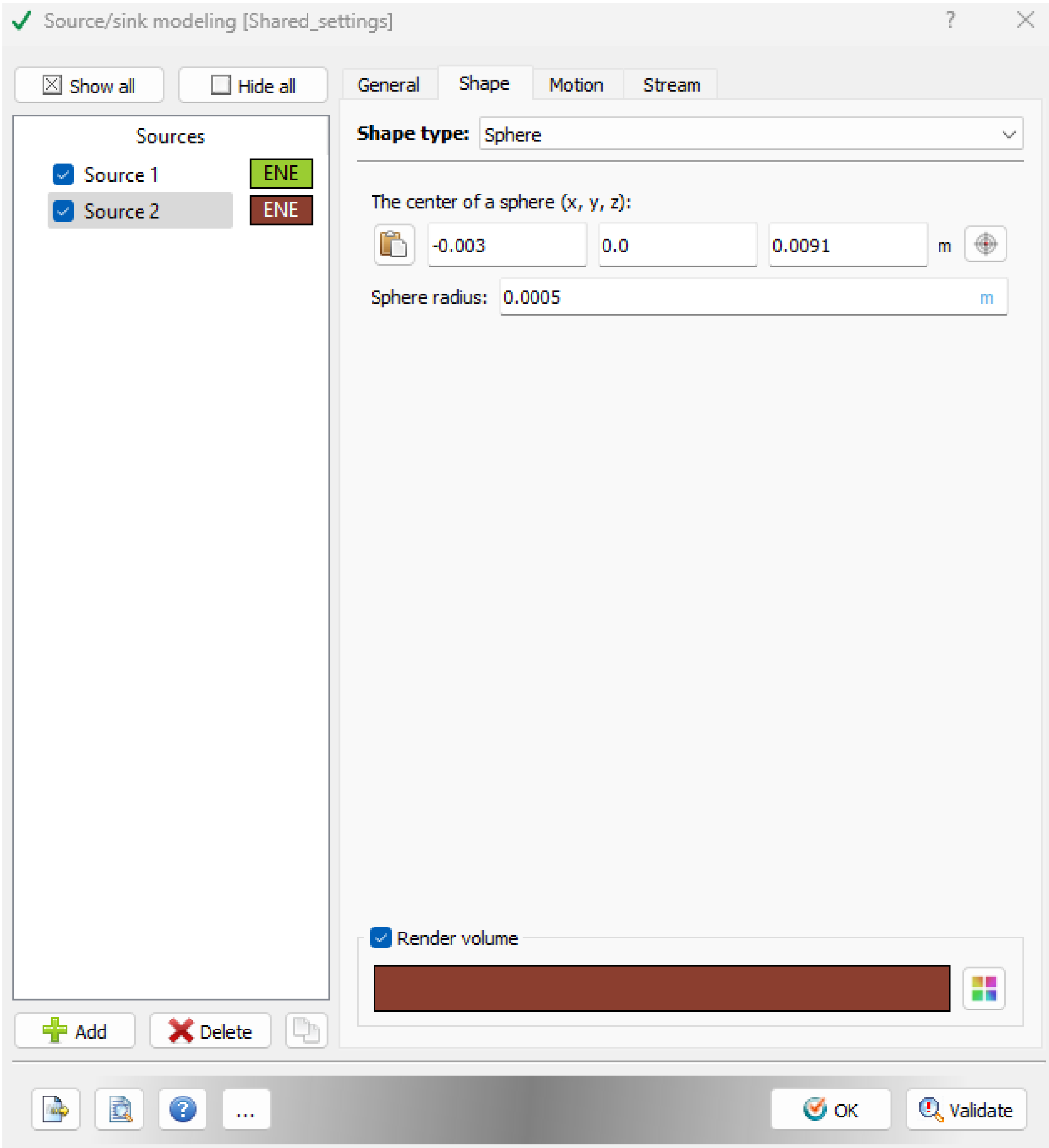

The energy source settings are configured identically for both Source 1 and Source 2 to represent the ignition energy provided by the spark plug.

- **Source Type:** Set to Energy with the source units specified as Energy.
- **Limit Temperature:** Set at 50,000 K, which acts as the upper temperature threshold for the energy release, preventing excessive heating beyond realistic ignition conditions.
- **Energy Value:** Each source releases an energy value of 0.02 J during its activation phase, effectively simulating the energy required to initiate combustion in the engine.

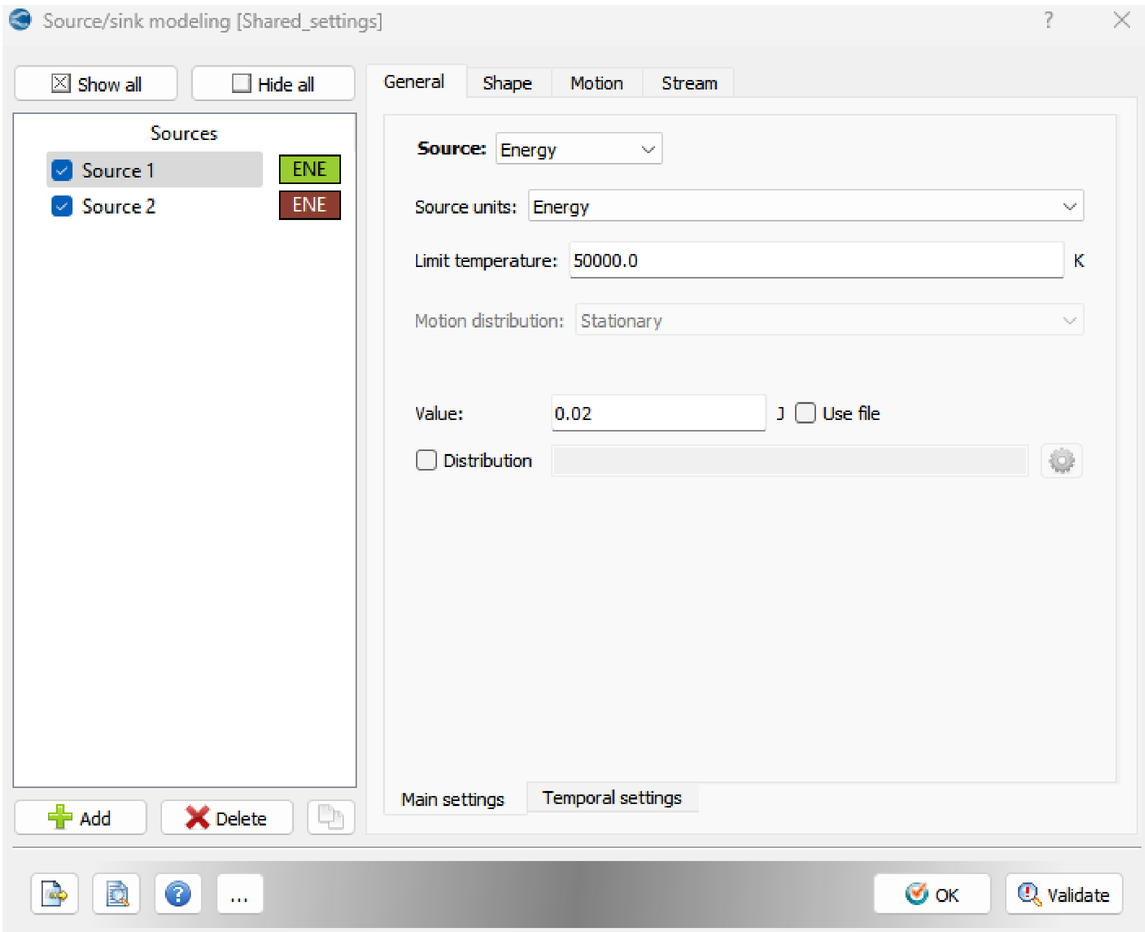

The two energy sources are shown in the image below:

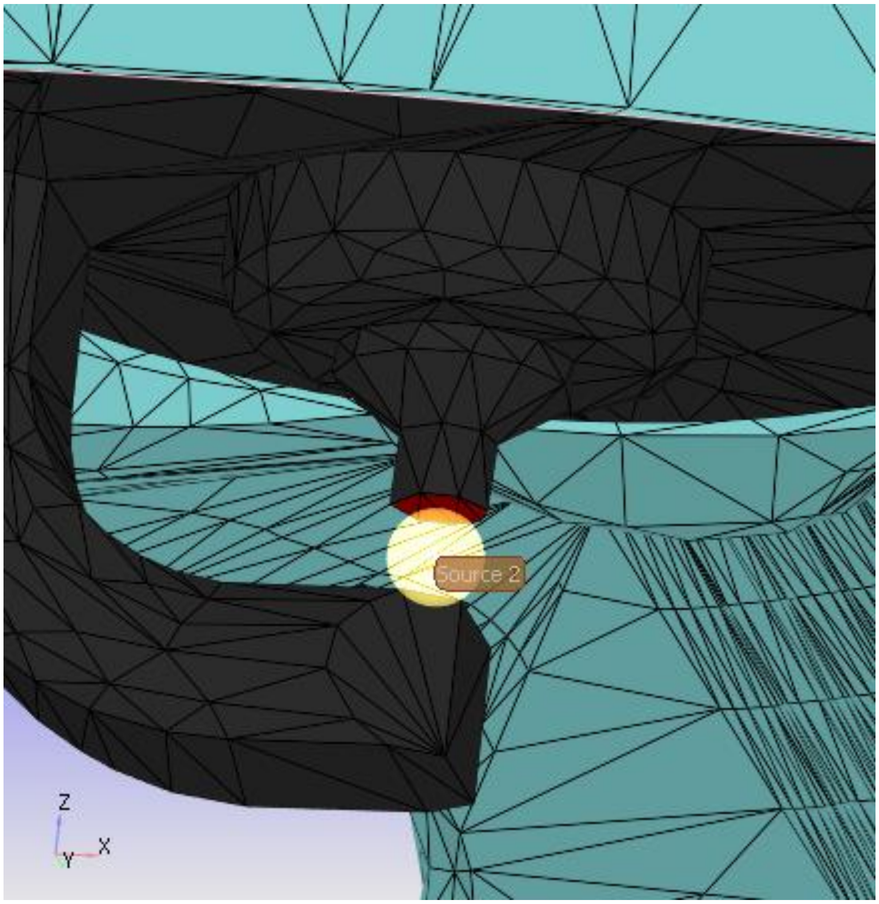

Grid Control

- Base grid

In the Base grid dialog box, the values for dx, dy, and dz are set to 0.005 m.

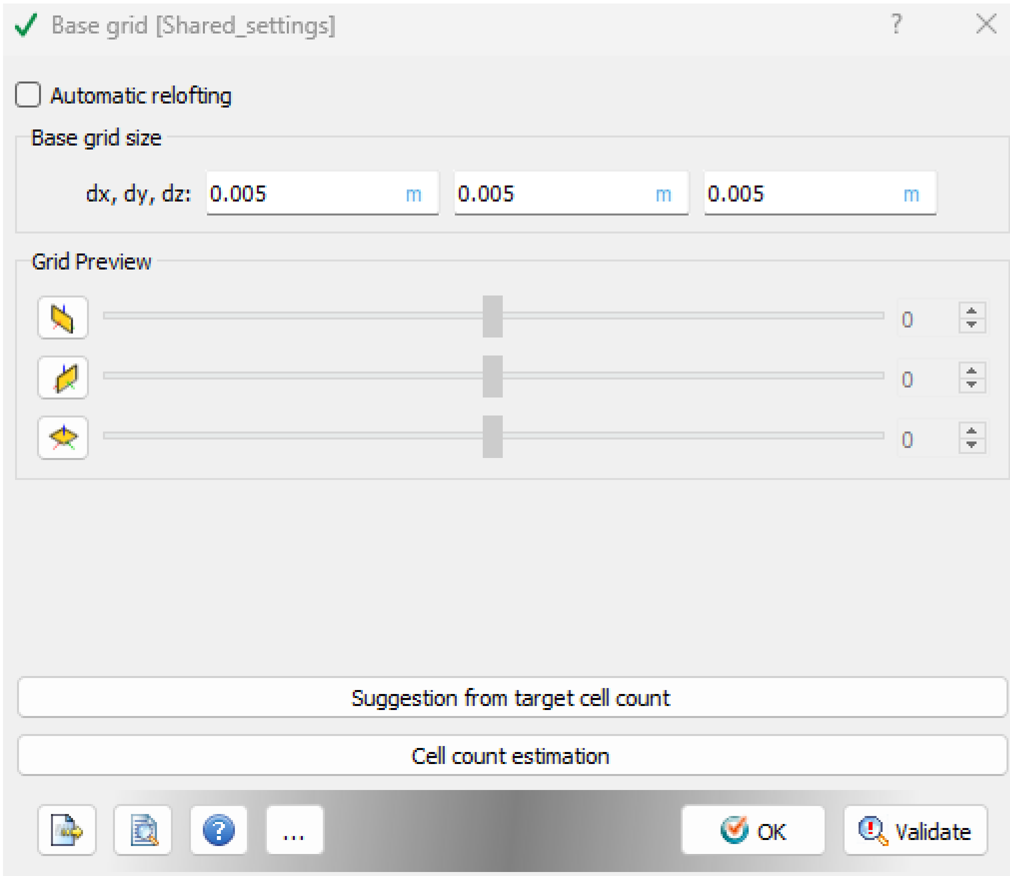

- Adaptive Mesh Refinement

The Adaptive Mesh Refinement (AMR) settings are crucial for achieving higher accuracy in critical regions of the simulation [13]. By refining the mesh selectively, AMR enhances the resolution only in areas where significant changes occur, such as near the intake and exhaust valves or around the cylinder region.

Configuration Overview:

1. **Velocity-Based AMR:** The velocity criterion is set with a sub-grid scale (SGS) where any velocity above 1 m/s triggers mesh refinement. The maximum embedding level is set to 3, meaning the cells can be refined up to 8 times finer. This refinement remains permanent throughout the simulation to ensure accurate capture of high-speed flows within the engine.

2. **Temperature-Based AMR:** The temperature criterion activates when the temperature exceeds 2.5 K. This setting ensures that areas with significant thermal gradients, especially during combustion events between -17 and 135 crank degrees, receive

enhanced mesh resolution. The AMR operates in a cyclic mode with a cycle period of 720 degrees, matching the engine's operational cycle.

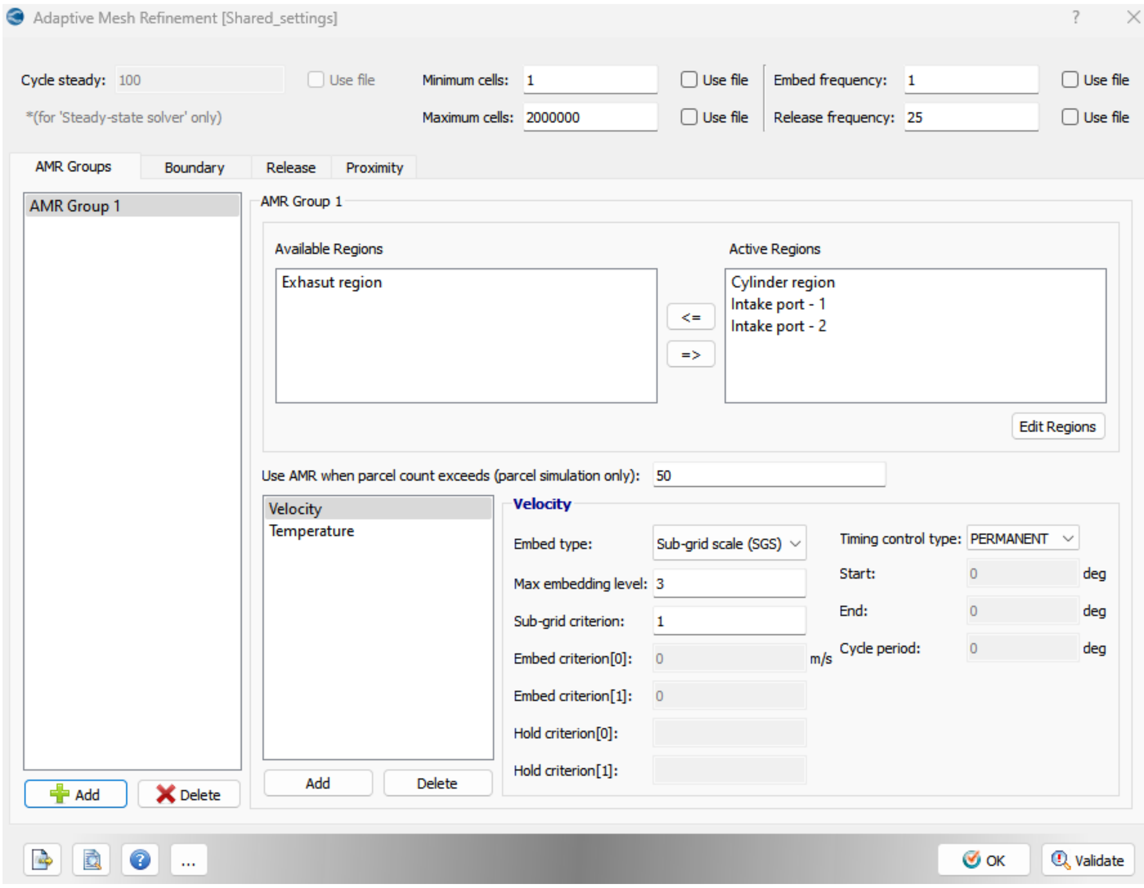

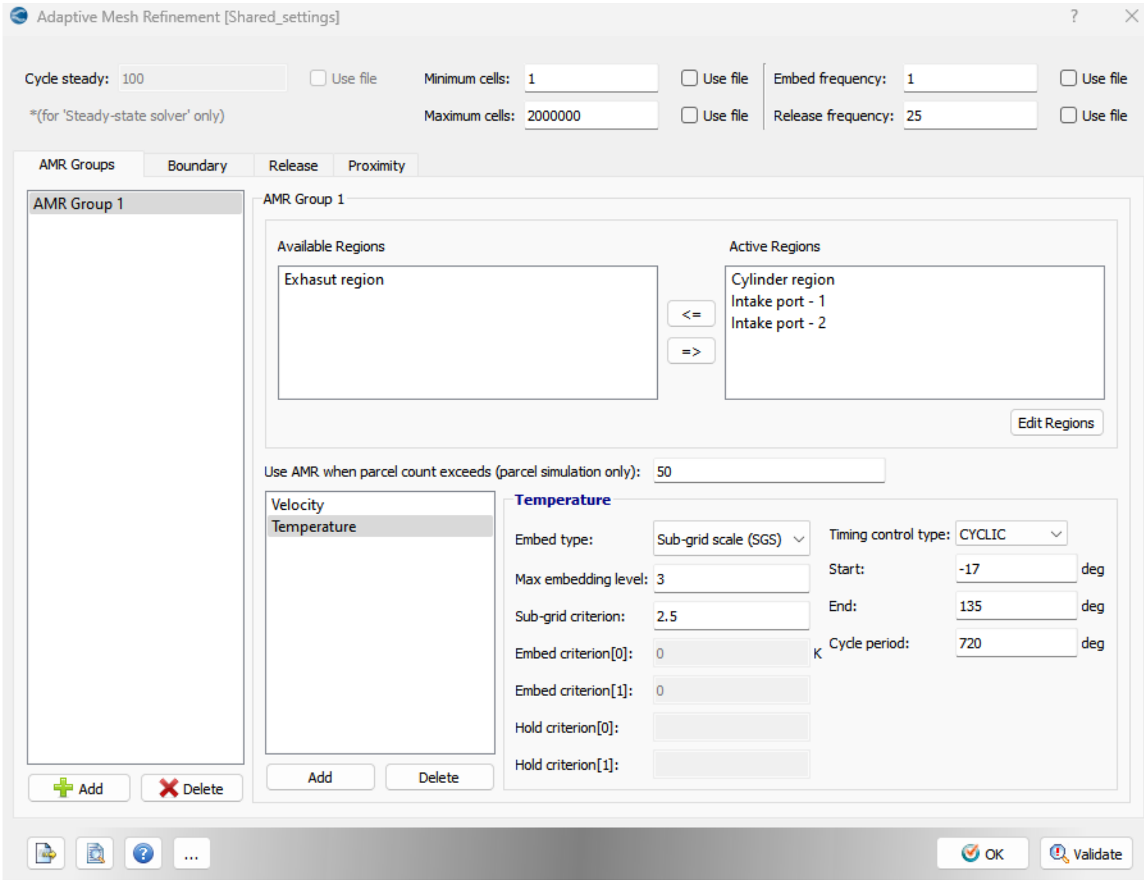

These AMR configurations enable the simulation to maintain computational efficiency while capturing critical flow and thermal phenomena accurately.

- Fixed Embedding

The following zones are covered with fixed embedding:

- Intake Valve Angle

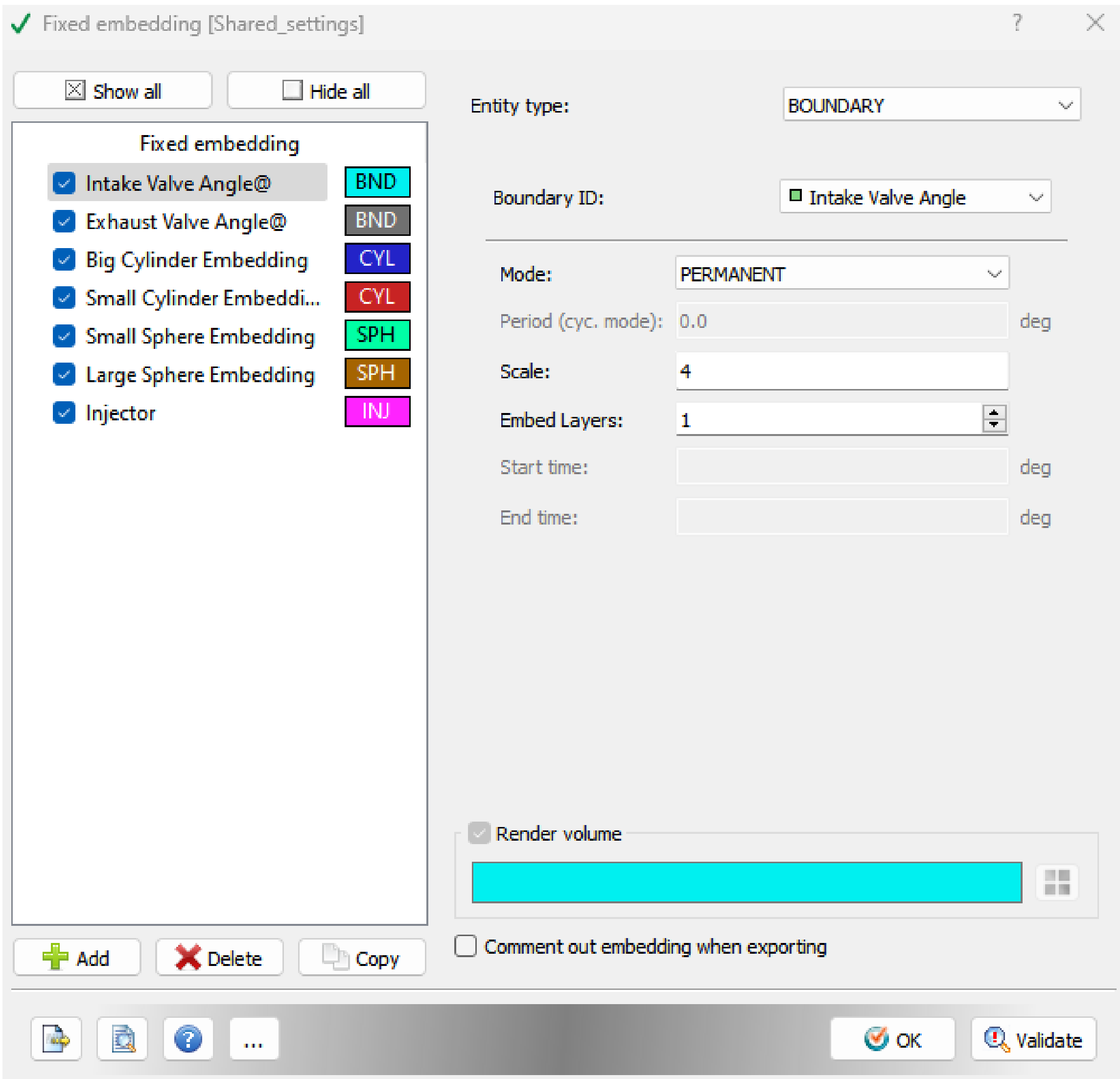

- Exhaust Valve Angle

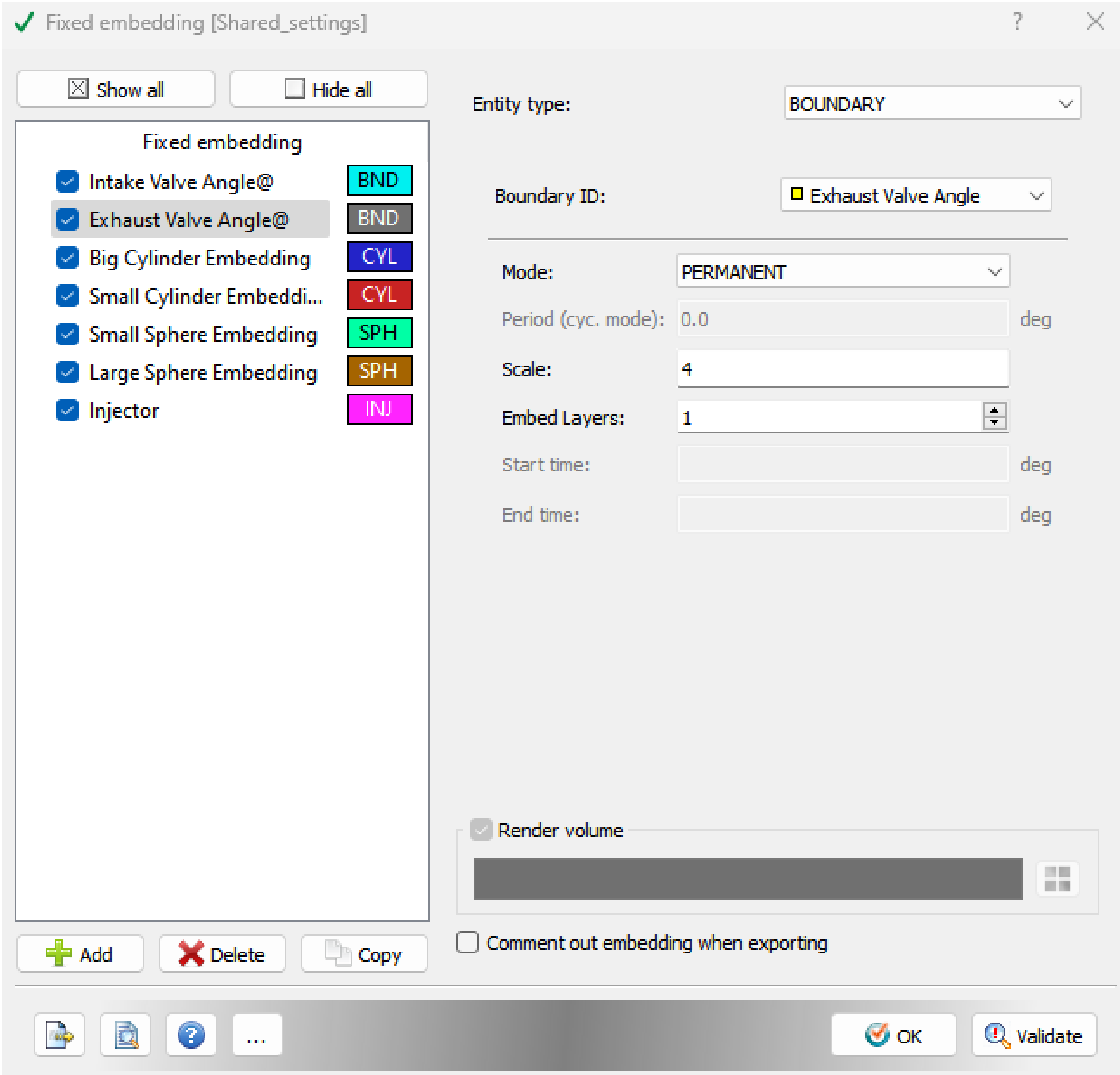

- Cylinder

It is covered with two types of embedding of different sizes: (1) big cylinder embedding and (2) small cylinder embedding.

(1) Big cylinder embedding

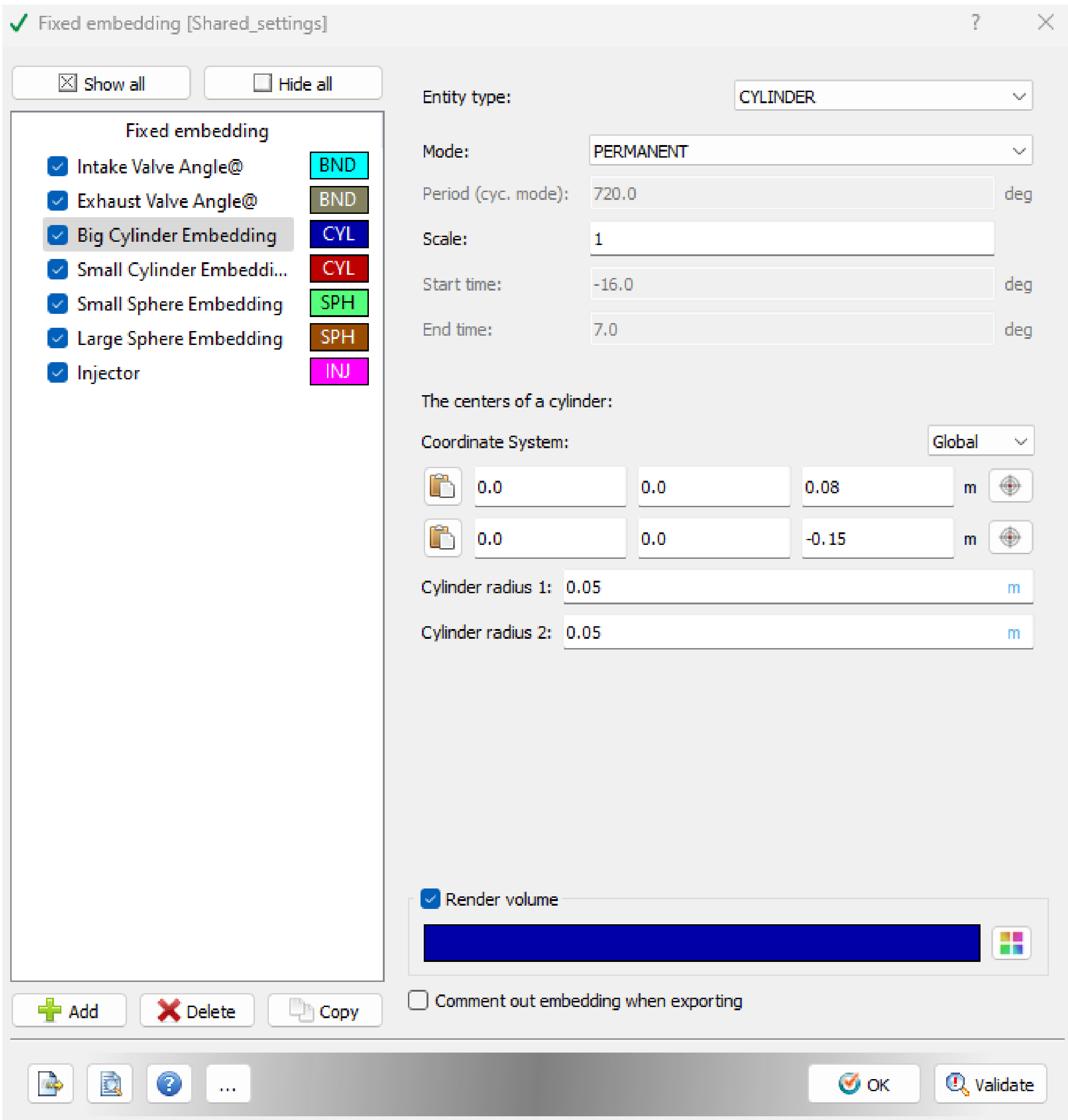

(2) Small cylinder embedding

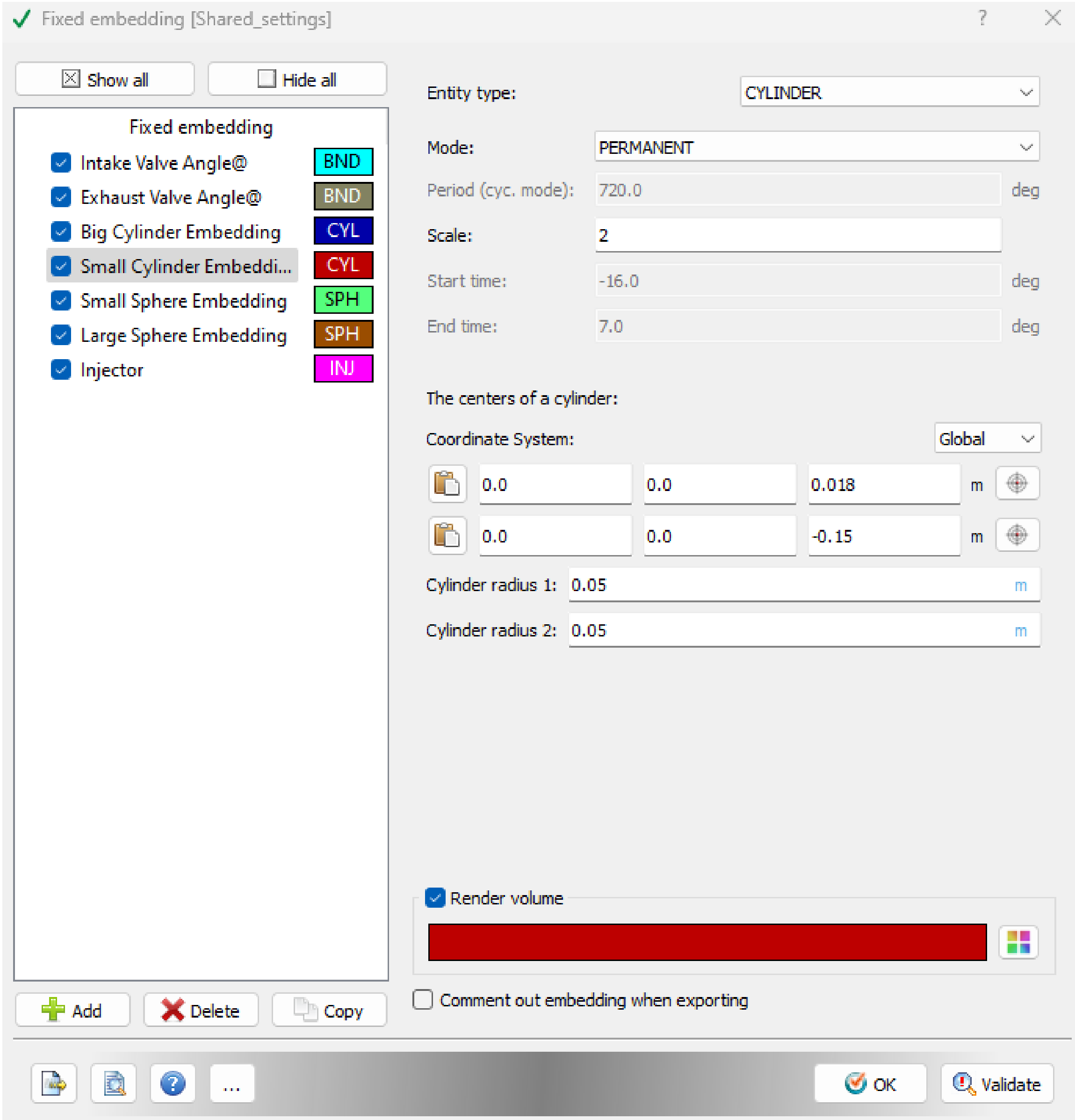

The two covered cylinder zones are illustrated in the image below:

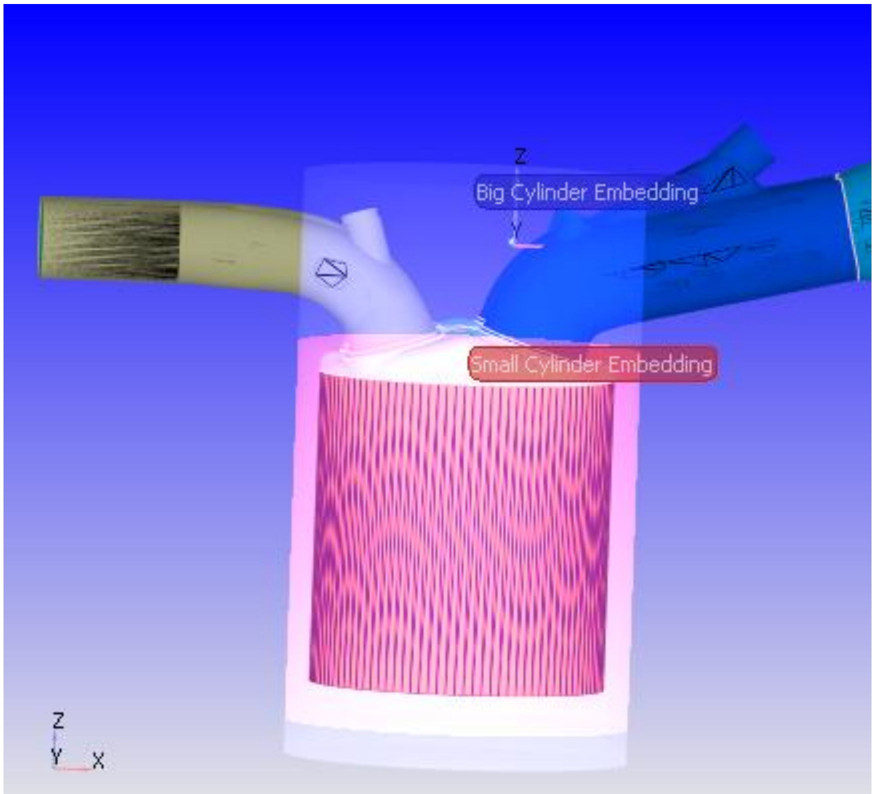

- Energy source/sink

It is covered with two types of embedding of different sizes: (1) small sphere embedding and (2) large sphere embedding.

(1) Small sphere embedding

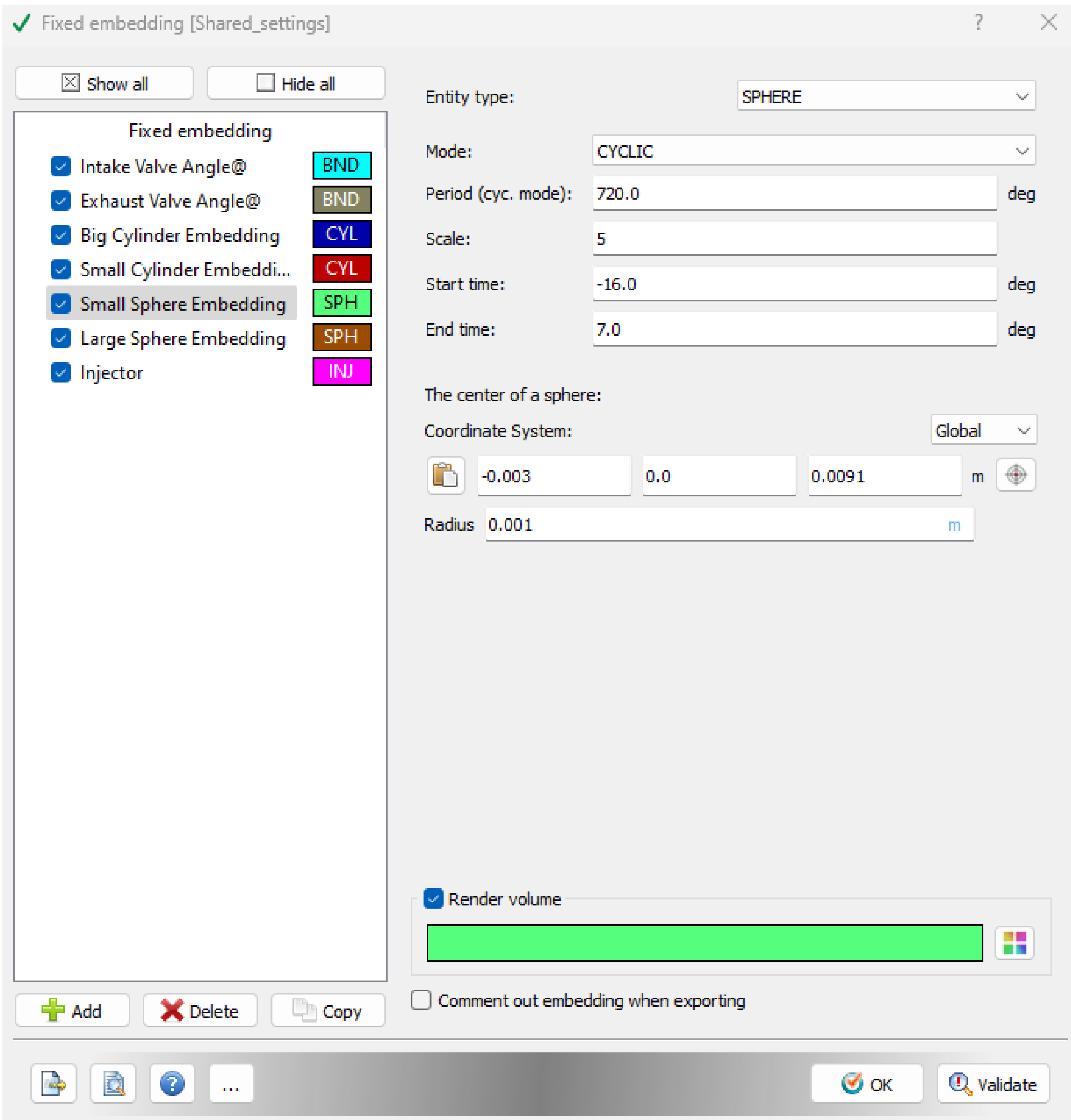

(2) Large sphere embedding

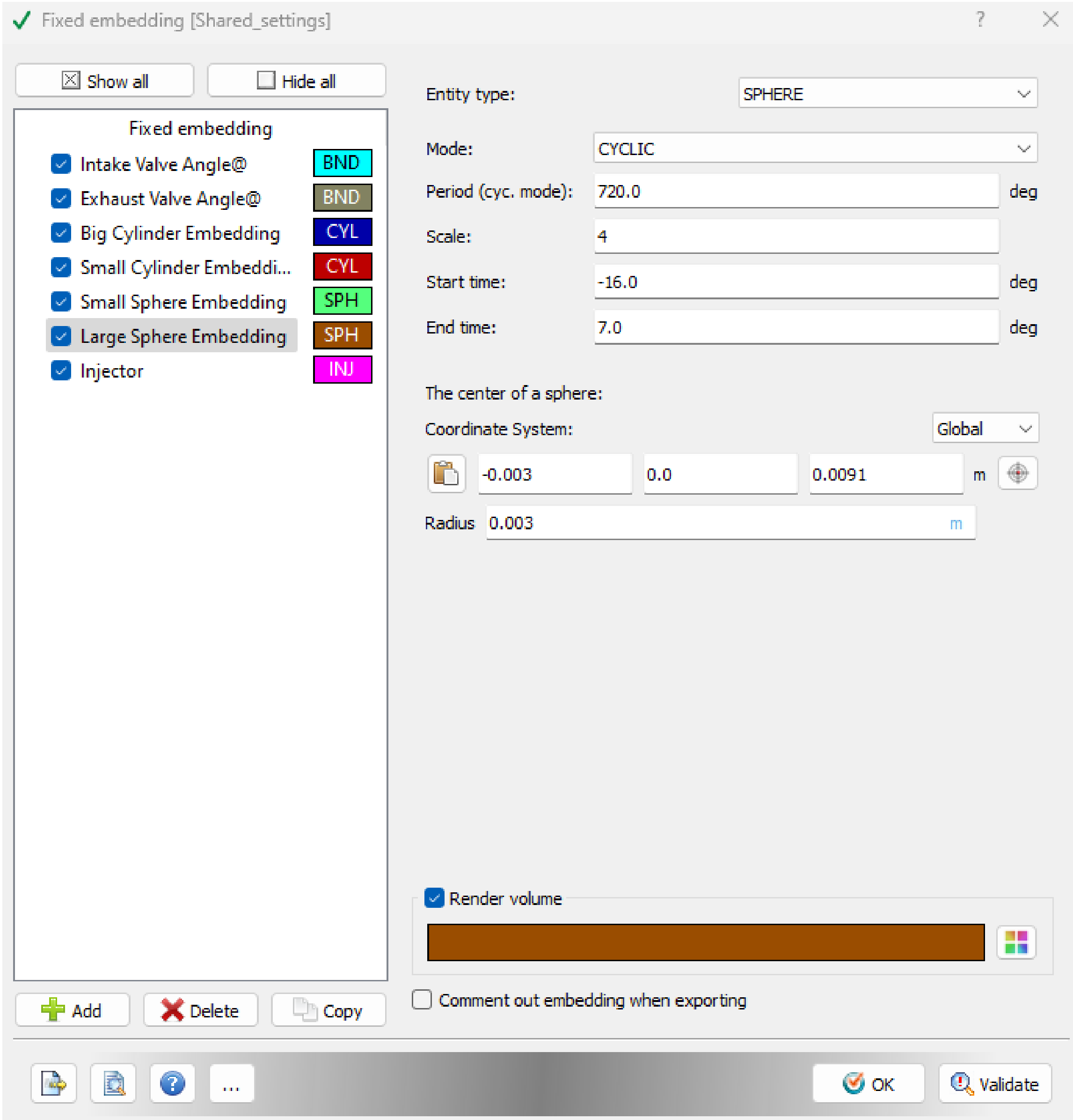

The two covered spherical zones are illustrated in the image below:

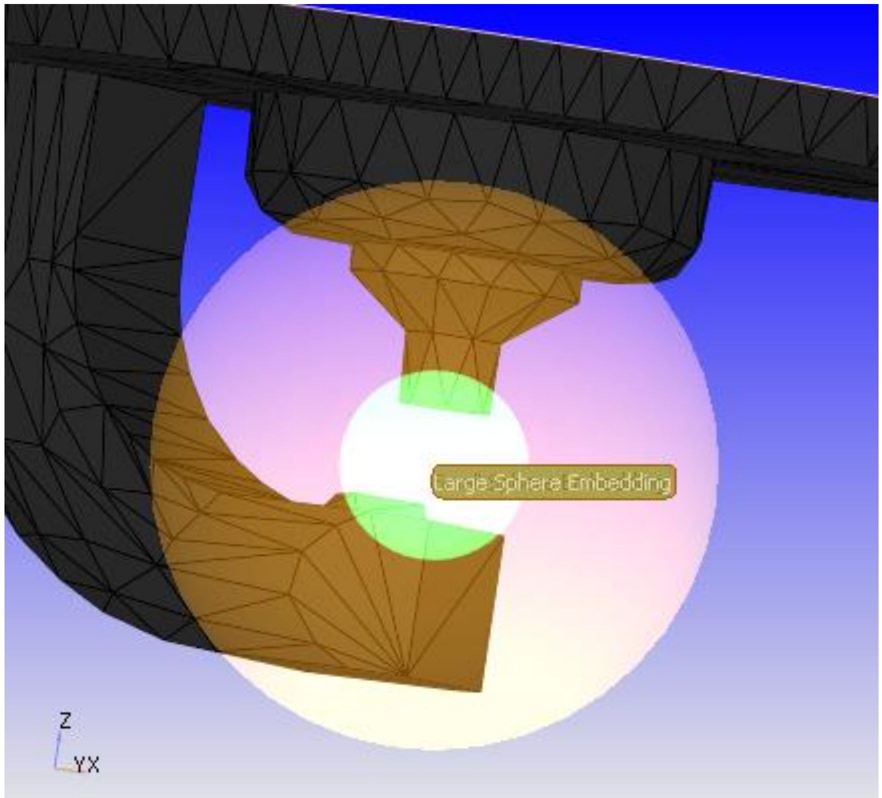

- Injector

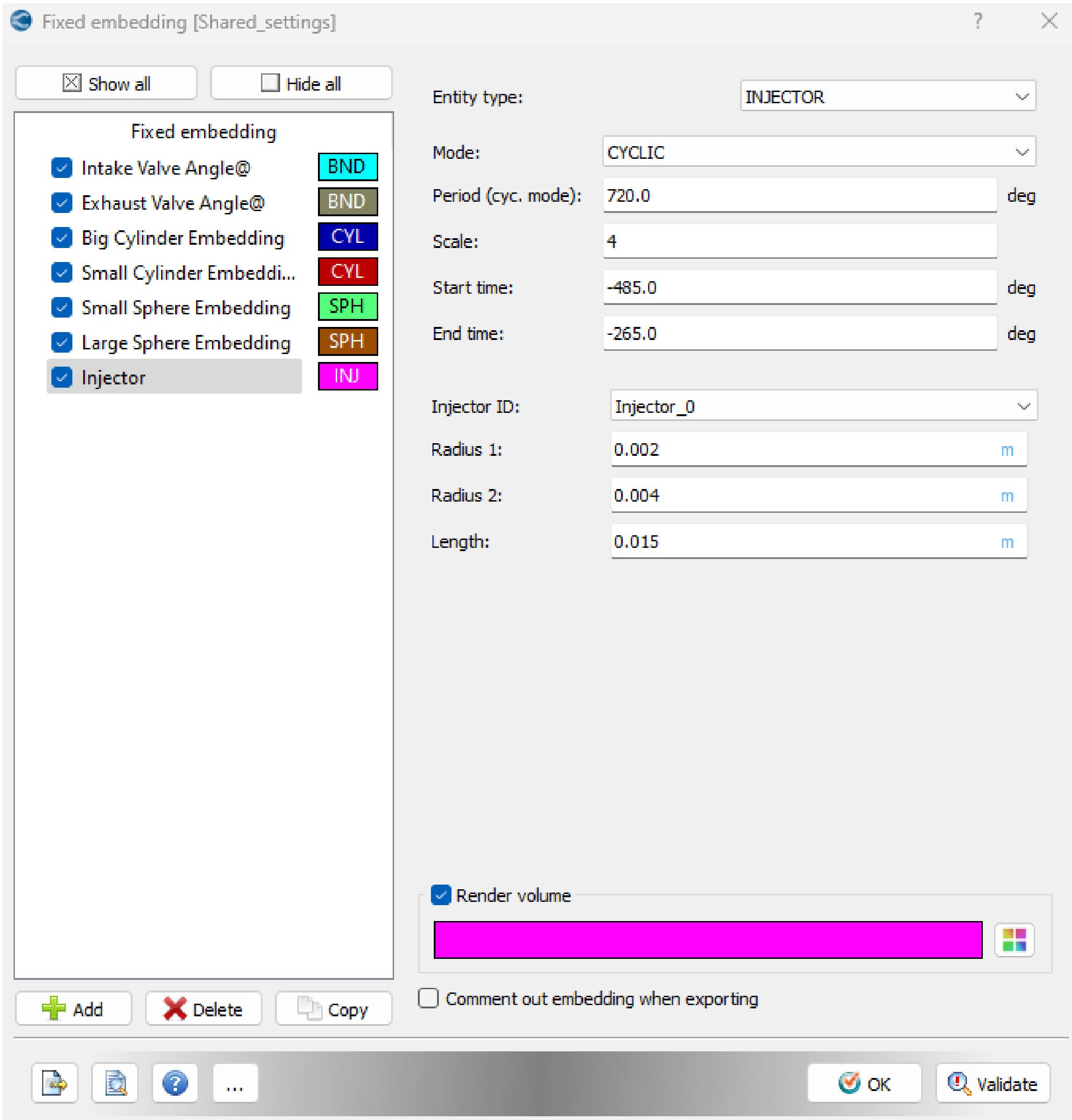

Fixed embedding [Shared_settings]
Show all
Hide all
Fixed embedding
Intake Valve Angle@
BND
Exhaust Valve Angle@
BND
Big Cylinder Embedding
CYL
Small Cylinder Embeddi...
CYL
Small Sphere Embedding
SPH
Large Sphere Embedding
SPH
Injector
INJ
Entity type:
INJECTOR
Mode:
CYCLIC
Period (cyc. mode):
720.0
deg
Scale:
4
Start time:
-485.0
deg
End time:
-265.0
deg
Injector ID:
Injector_0
Radius 1:
0.002
m
Radius 2:
0.004
m
Length:
0.015
m
Render volume
Comment out embedding when exporting
Add
Delete
Copy
...
OK
Validate

Output/Post-Processing

- Post variable Selection

The default selections are maintained in the Typical Variables/Geometry tap.

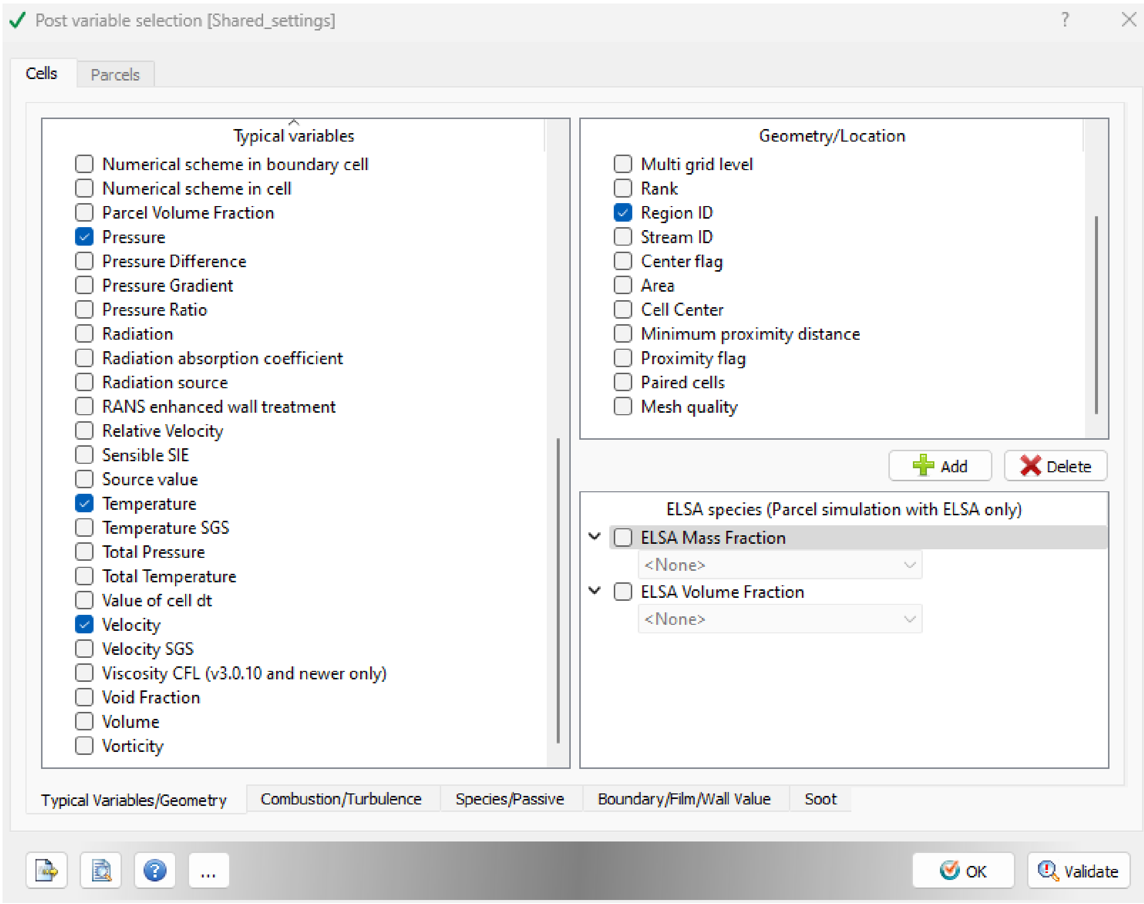

In the Species/Passive tap, select IC_8H_{18} under mass fraction.

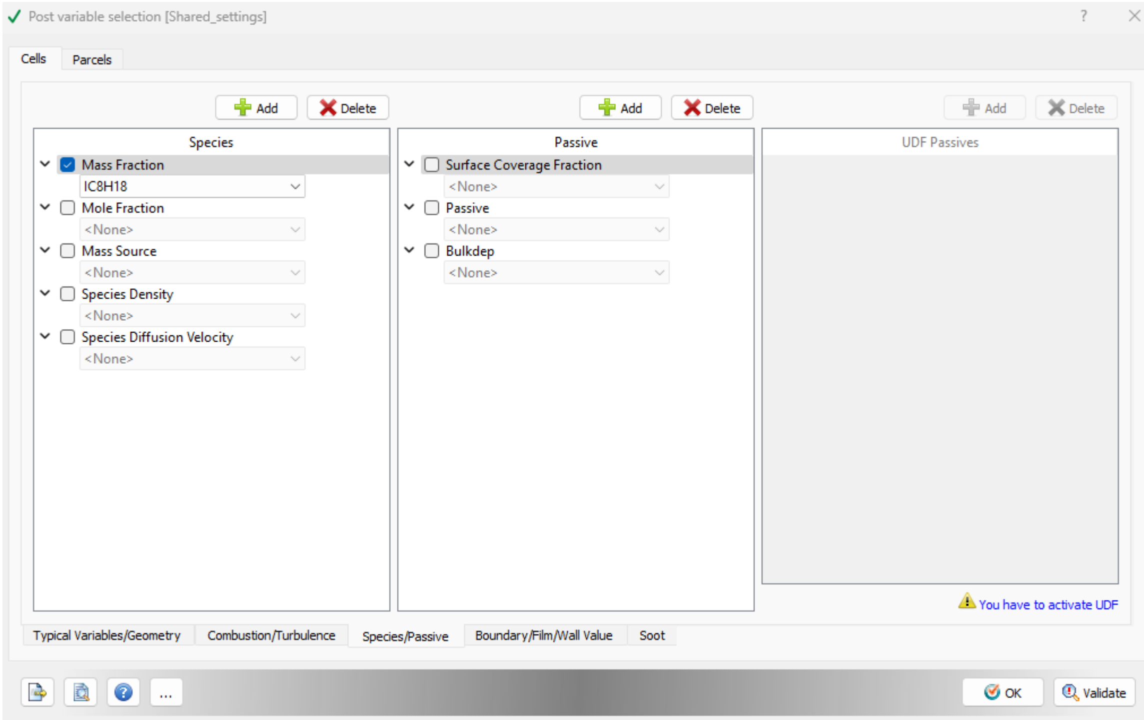

- Output files

The time interval for writing 3D output files and restart output files is set to 2 and 10 deg, respectively. The time interval for writing text output is set to 0.1 deg.

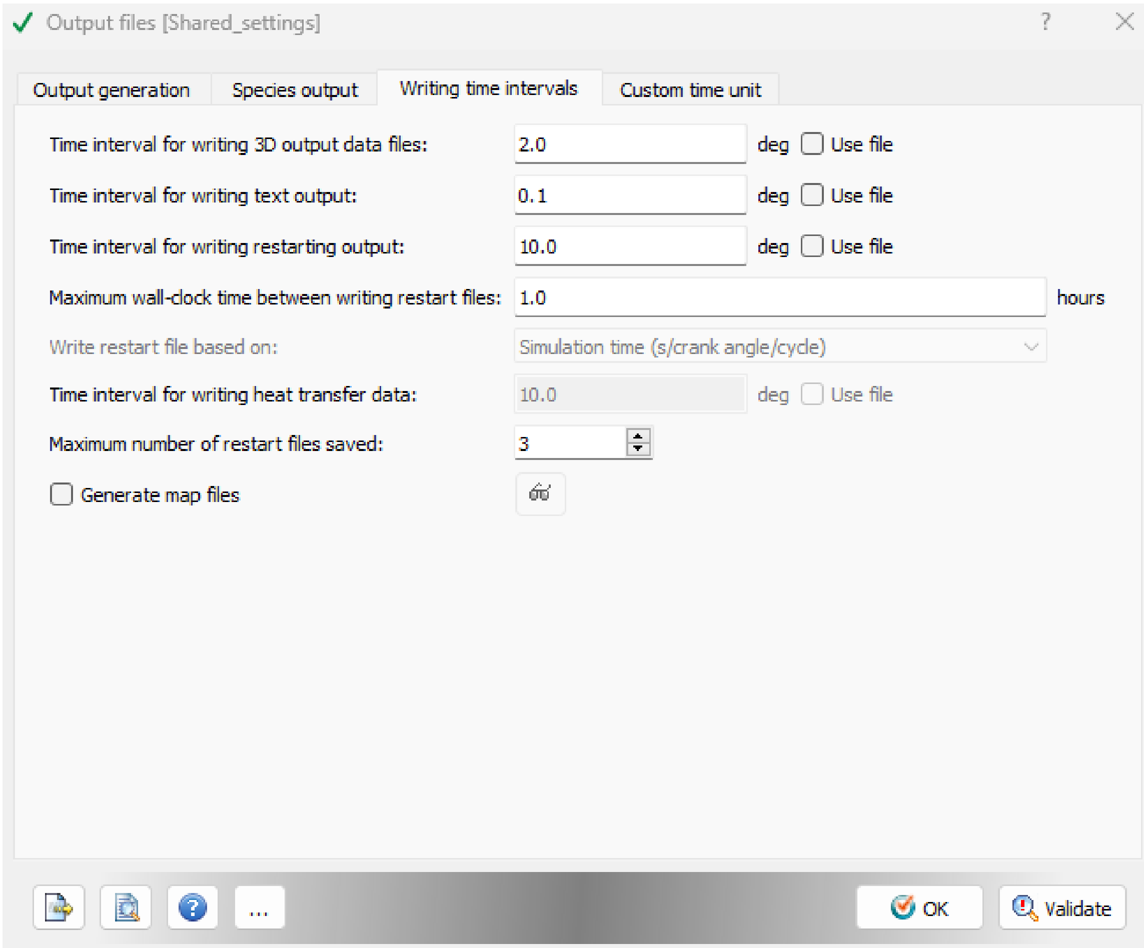

Exporting Input Files

File > Export > Export Input Files

These files will be used in Cygwin to perform the simulation, as CONVERGE CFD does not have a built-in solver.

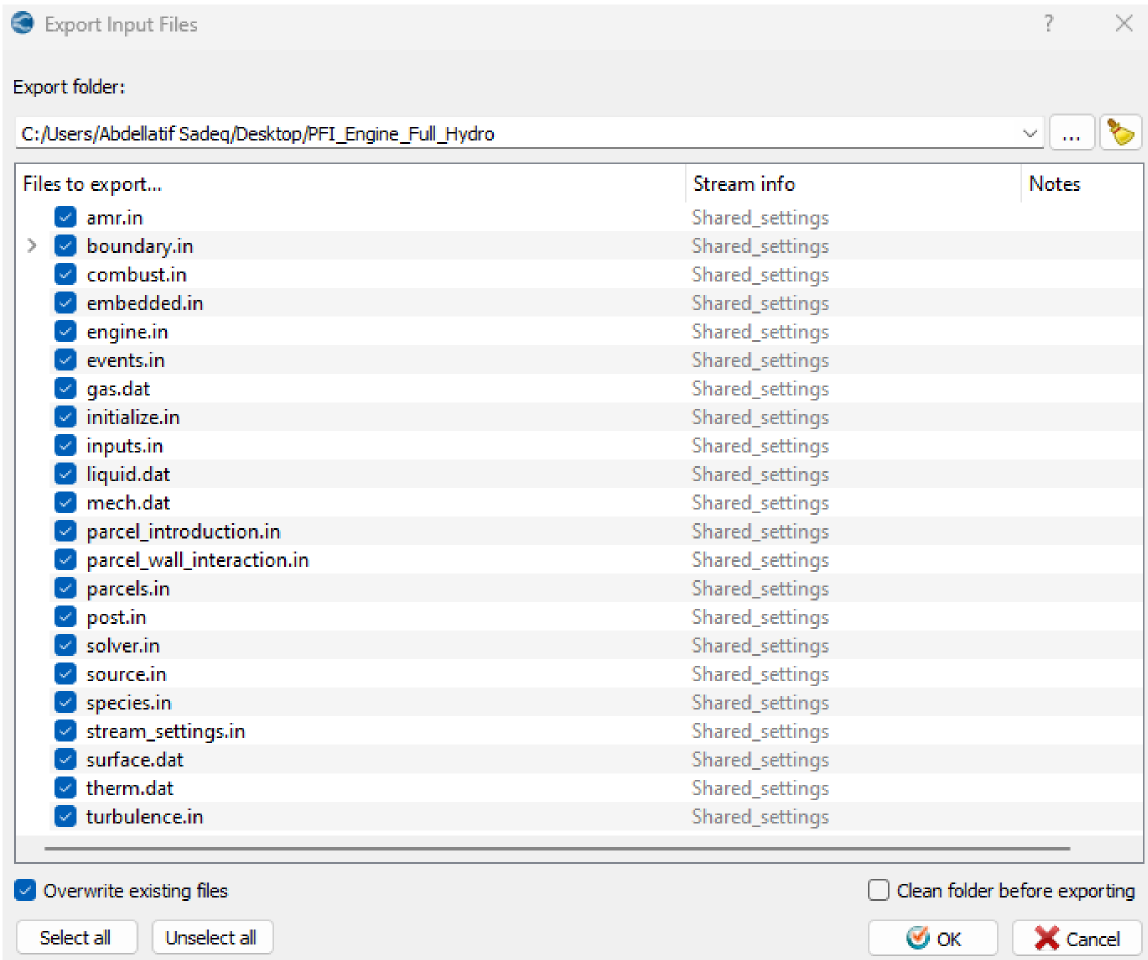

3. Solution Execution

After navigating Cygwin to the directory containing the simulation input files, the following command is used to perform the simulation:

```
mpiexec -n 4 converge --license explore
```

Files are converted for post-processing using CONVERGE CFD software. To start, navigate to the 'Post-Processing 3D' tab. Specify the directory containing the case files and select the desired post-processing software format for the file conversion.

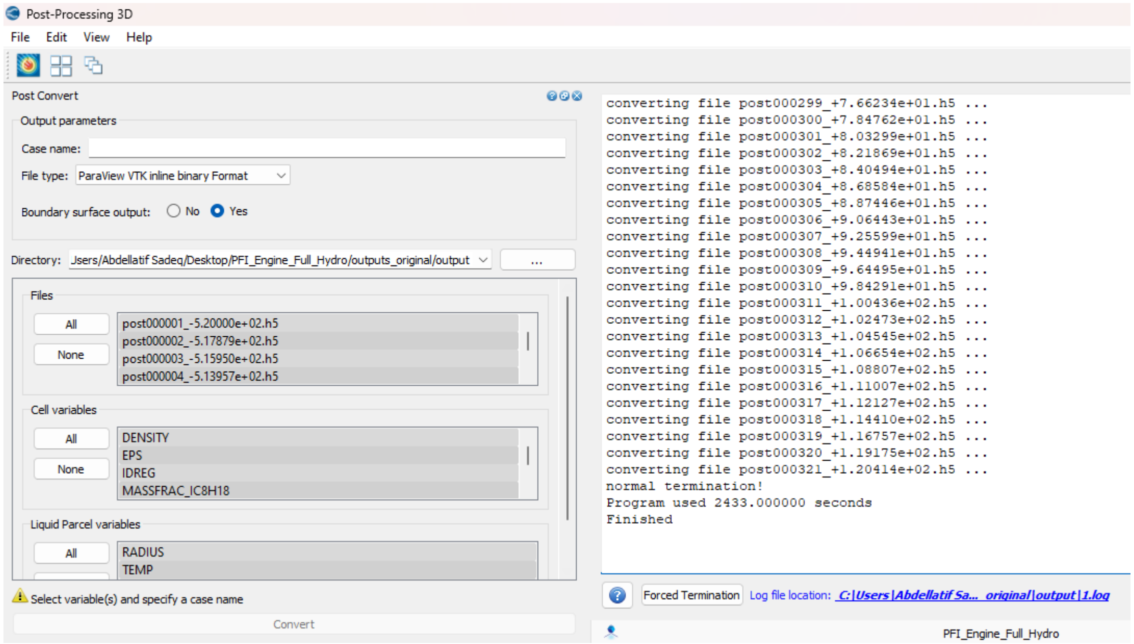

4. Post-Processing

The case is now prepared for post-processing. To begin post-processing in ParaView, select the .vtm Group file.

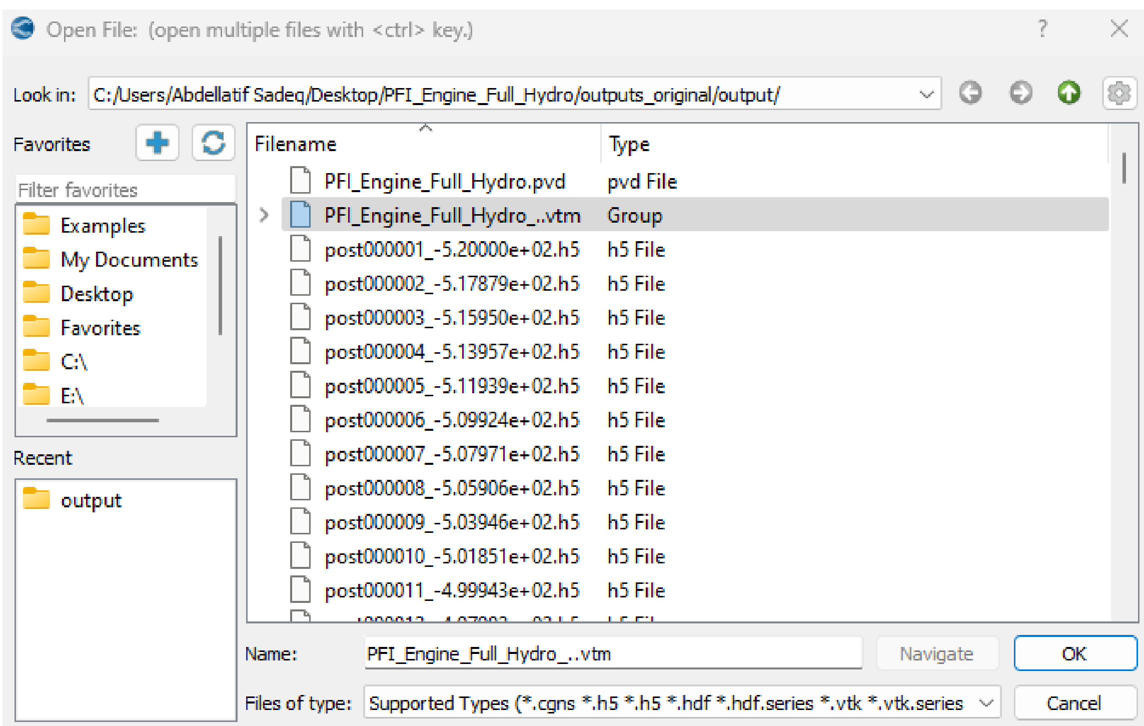

- Import geometry in ParaView

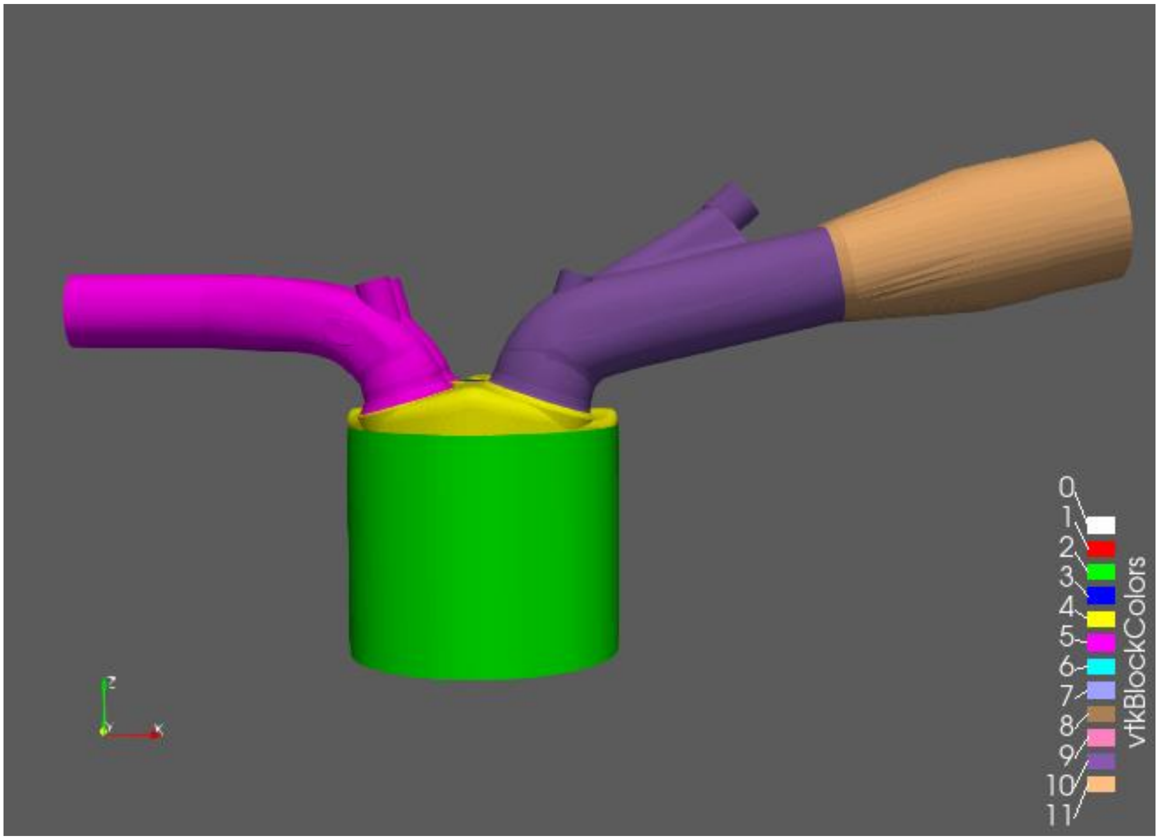

- Mesh Generation

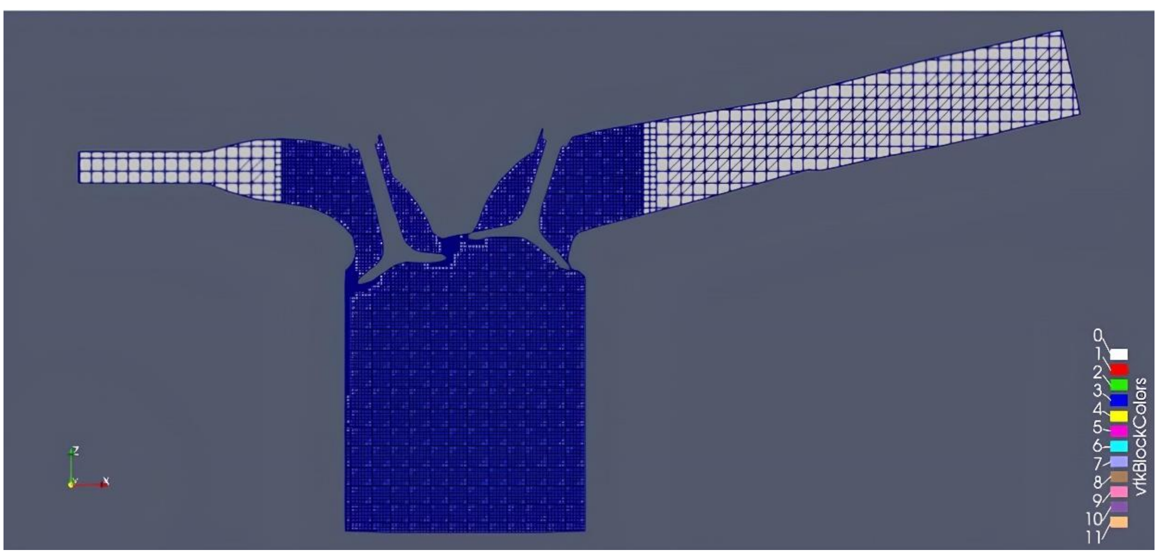

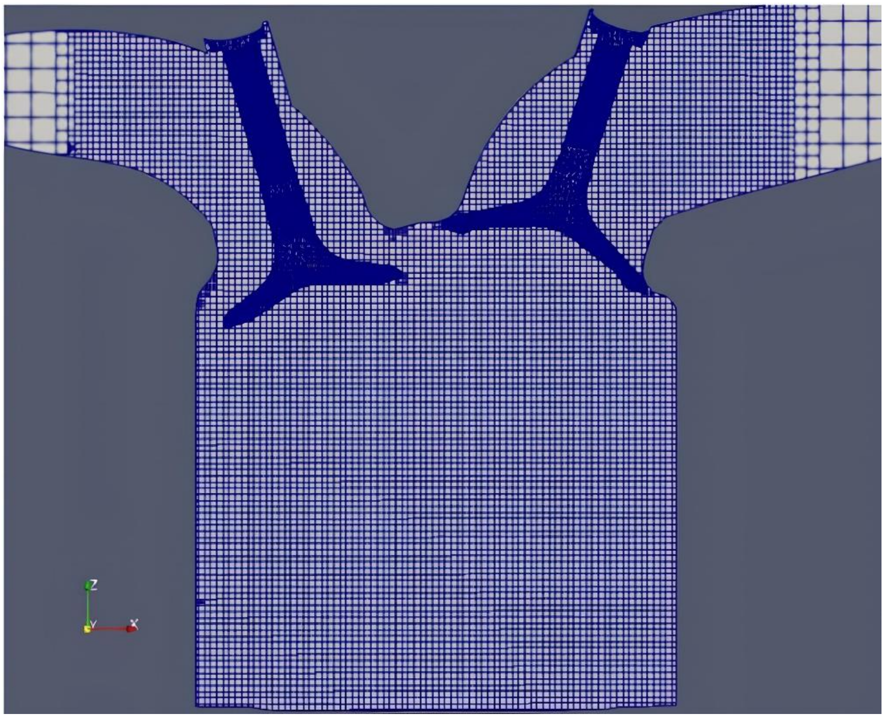

Results and Discussions

1. What is the compression ratio of this engine?

The compression ratio (CR) in an internal combustion engine refers to the extent to which the air-fuel mixture is compressed before ignition [14]. It is mathematically defined as the ratio of the maximum volume of the combustion chamber, when the piston is at its farthest position from the cylinder head (bottom dead center) to the minimum volume, when the piston is at its closest position to the cylinder head (top dead center).

$$Compression\ Ratio\ (CR) = \frac{Maximum\ Volume\ (V_{max})}{Minimum\ Volume\ (V_{min})}$$

For example, a CR of 10 indicates that the air-fuel mixture is compressed to one-tenth of its original volume by the piston's movement within the cylinder. However, the theoretical maximum CR determined by the cylinder geometry may not always be achieved, particularly if the intake valve closes after the piston begins its compression stroke. In such cases, backflow of the mixture can occur, reducing the effective CR. While a higher CR generally enhances thermal efficiency, it also increases the risk of engine knocking [1].

By analyzing the volume vs. crank angle plot of the cylinder region, V_{max} and V_{min} can be determined, enabling the calculation of the engine's CR as follows:

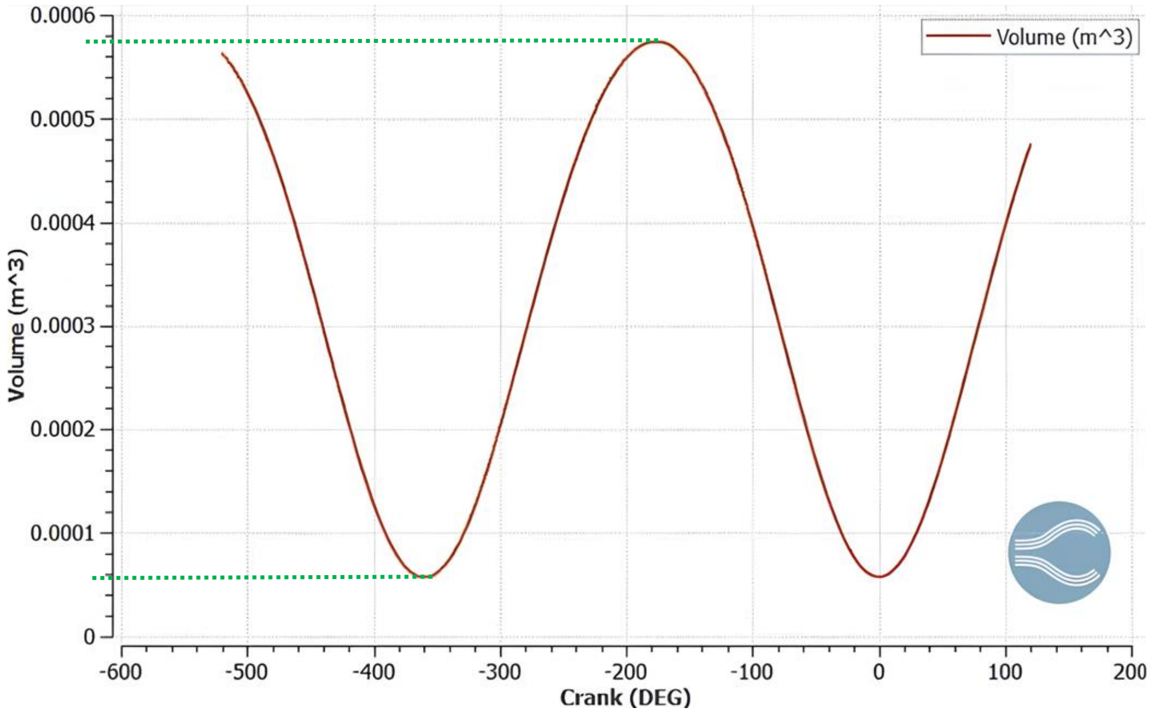

From the provided volume vs. crank angle plot, CR can be calculated as:

$$CR = \frac{V_{max}}{V_{min}} = \frac{0.000574}{5.75 * 10^{-5}} = 9.98$$

2. Why do we need a wall heat transfer model? Why cannot we predict the wall temperature from the CFD simulation?

A wall heat transfer model is essential for accurately simulating and predicting the heat transfer and wall temperature in internal combustion engines [15]. Modern engines are highly optimized systems where improving performance requires precise understanding of thermal behavior. Engine thermodynamic models, supported by wall heat transfer models, significantly enhance the accuracy of predictions related to engine performance, reducing experimental costs and overall development time.

Heat transfer modeling involves capturing three distinct processes: the transfer of heat from the hot gases to engine components, the conduction of heat within the engine parts, and the dissipation of heat to the coolant and lubricating oil [16]. These complex interactions cannot be adequately captured without a dedicated wall heat transfer model, as it ensures a more realistic representation of the thermal behavior and its influence on engine efficiency and reliability.

CFD simulations alone cannot predict the actual wall temperature because they primarily calculate the temperature of the fluid layer near the wall (not the material surface itself) [17]. The near-wall temperature obtained through CFD is influenced by the choice of turbulence models, wall functions, and grid quality (e.g., Y+ values). While CFD provides a detailed understanding of fluid dynamics and heat transfer phenomena, predicting the wall temperature directly would require highly refined grids and computational resources, often leading to impractical simulations.

Furthermore, CFD-based predictions are susceptible to errors when simulating thermal phenomena such as critical heat flux (CHF) or dry-out positions, as turbulence models and wall functions may not fully capture these effects [18]. Therefore, wall heat transfer models are employed to bridge this gap, accurately predicting the temperature at the material surface and enabling better thermal management of the engine.

3. Calculate the combustion efficiency of this engine

In real engine applications, the combustion process is often incomplete, meaning that not all the energy content of the fuel supplied to the engine is released during combustion [19]. Several factors influence the efficiency of the combustion process, with key aspects being the air-fuel intake ratio and the atomization quality of the fuel (droplet size). For combustion to occur, the fuel inside the cylinder requires sufficient oxygen. If there is insufficient oxygen, incomplete combustion occurs, leading to reduced energy release and lower overall efficiency.

Analyzing the exhaust gases of an internal combustion engine reveals both incomplete combustion products (e.g., carbon monoxide (CO), nitrogen oxides (NO_x), unburned hydrocarbons (HC), and soot particles (PM)) and complete combustion products (e.g., carbon dioxide (CO_2) and water vapor (H_2O)) [20].

The combustion efficiency (η_c) is defined as the ratio of the energy released by the burned fuel to the theoretical energy content of the total fuel mass supplied during one complete engine cycle [19]:

$$\eta_c = \frac{Total\ Heat\ Released\ (Q)}{Mass\ of\ Fuel\ (m_f) * Lower\ Heating\ Value\ (LHV)}$$

In this analysis, Q is derived by integrating the Heat Release Rate (HRR) over the entire combustion duration, as represented by the area under the integrated HRR vs. crank angle curve within the cylinder region, as follows:

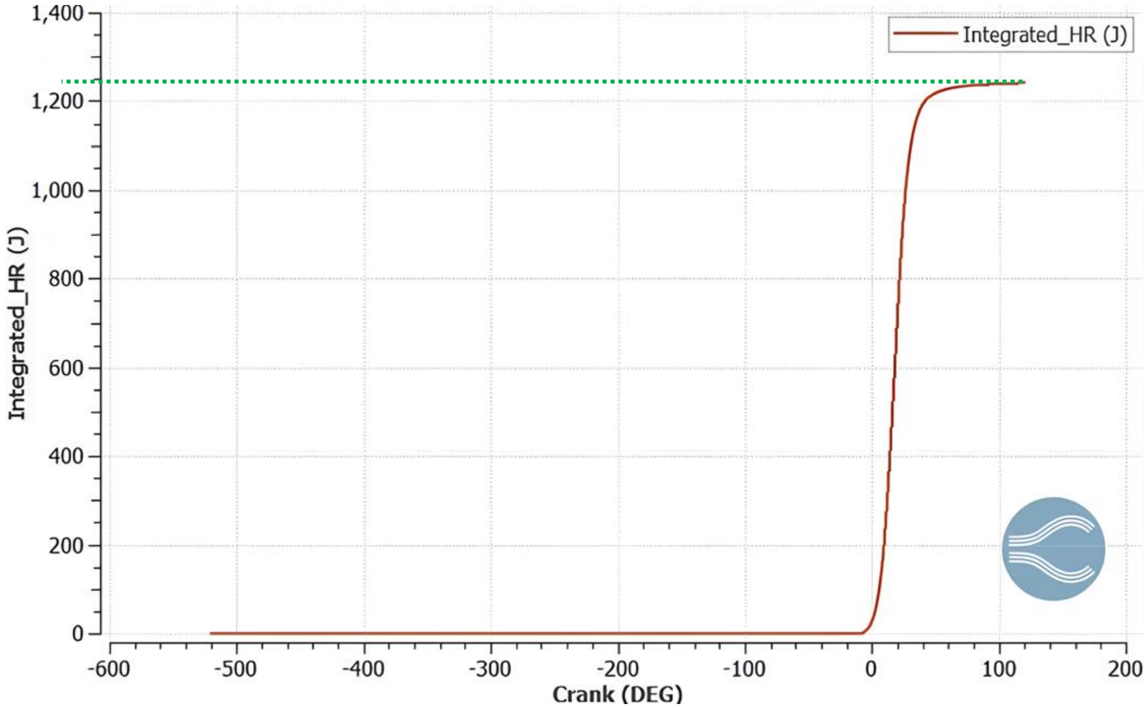

Based on the plot:

$$\eta_c = \frac{Q}{m_f * \text{LHV}} = \frac{1.241}{(3 * 10^{-5}) * 44000} = 0.94\ (or\ 94\%)$$

4. Use the engine performance calculator to determine the power and torque for this engine.

To calculate the power, the following formula is used [19]:

$$Power\ (P) = \frac{Work\ (W)}{Time\ (t)}$$

Based on the engine performance calculator,

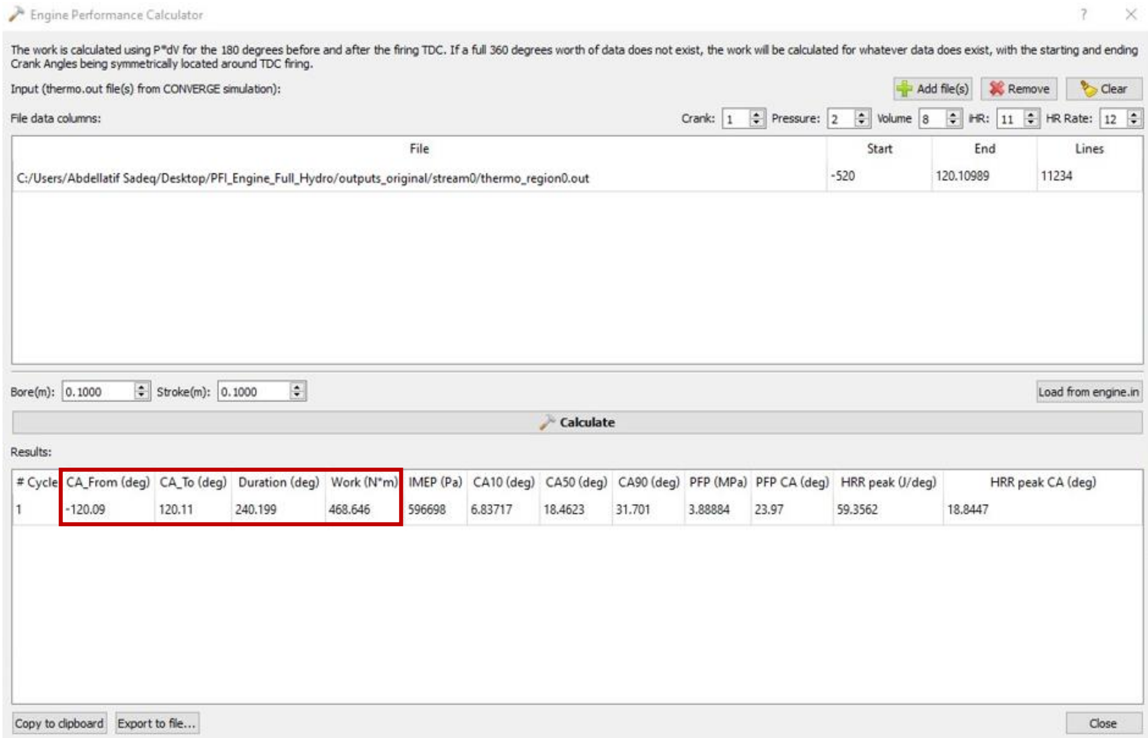

1. **Work Output (*W*):**

   W = 468.646 N·m (calculated from engine performance metrics).

2. **Duration of Work (*θ*):**

   The work duration spans *θ* = 240.199 degrees of crankshaft rotation.

3. **Engine Speed (*N*):**

   Engine speed is specified as *N* = 3000 RPM (Revolutions Per Minute).

4. **Rotational Speed (*f*):**

   To convert to revolutions per second (RPS):

$$f = \frac{N}{60} = \frac{3000}{60} = 50 \text{ RPS}$$

5. **Angular Velocity (*ω*):**

   Total angular displacement per second is:

$$\omega = f * 360 = 50 * 360 = 18000 \text{ degrees per second}$$

6. **Time Duration (*t*):**

   To calculate the time for the given crank angle duration:

$$t = \frac{\theta}{\omega} = \frac{240.199}{18000} = 0.01334 \text{ seconds}$$

7. **Power (*P*):**

To calculate the power, divide the work per time:

$$P = \frac{W}{t} = \frac{468.646}{0.01334} = 35.13 \text{ KW}$$

Torque (T) Calculation:

$$P = \frac{(2\pi NT)}{60},$$

$$T = \frac{(P * 60)}{(2\pi N)} = \frac{(35.13 * 1000 * 60)}{(2 * 3.14 * 3000)} = 111.88 \text{ N} \cdot \text{m}$$

5. What is the significance of CA10, CA50 and CA90?

CA10, CA50, and CA90 are critical parameters that describe the combustion phasing in internal combustion engines, providing detailed insights into the timing and progression of the combustion process [21]. These values represent the crank angles at which 10%, 50%, and 90% of the total heat release occurs, respectively, and are determined through the integration of the Apparent Heat Release Rate (AHRR). CA10 marks the early stage of combustion, indicating the point where ignition begins and the first 10% of the fuel's energy is released. This parameter is essential for assessing ignition timing and understanding the early flame development within the cylinder. CA50, which signifies the point at which 50% of the cumulative heat release is achieved, represents the transition from the premixed combustion phase to the diffusion phase. It is widely regarded as a key indicator of optimal combustion phasing, with its position relative to top dead center (TDC) influencing engine efficiency, performance, and emissions. Lastly, CA90 denotes the point where 90% of the total heat release is complete, indicating the conclusion of the combustion process and providing insights into the overall combustion duration.

The duration between CA10 and CA90, referred to as CA10–90, measures the total combustion time and is a crucial metric for analyzing the efficiency of energy conversion from the fuel [22]. A shorter combustion duration typically reflects higher combustion efficiency and reduced emissions, while prolonged durations may indicate incomplete or inefficient combustion. The positions of CA10, CA50, and CA90 are influenced by factors such as spark timing, fuel-air mixture preparation, and combustion chamber conditions. Early spark timing accelerates heat release and reduces combustion duration but may increase the risk of knock or excessive pressure rise rates. Conversely, retarded spark timing shifts these phases later, potentially reducing efficiency and increasing emissions [23].

Additional Insightful Plots

Pressure

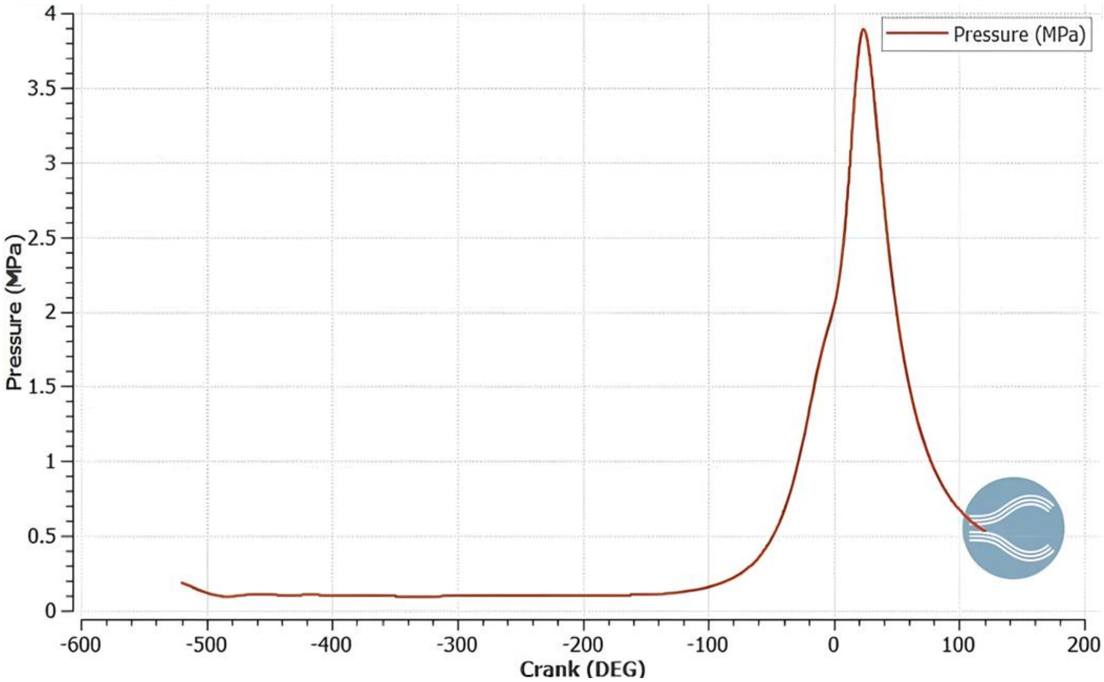

The pressure plot illustrates the in-cylinder pressure variation across the engine cycle, highlighting a sharp peak of approximately 3.9 MPa near TDC, corresponding to the combustion phase. This peak reflects the rapid energy release from the air-fuel mixture and is crucial for engine efficiency and performance. The gradual pressure rise during the compression stroke demonstrates the effect of the compression ratio, while the sharp decline after the peak represents energy transfer during the expansion stroke. The smooth curve suggests optimized combustion phasing and ignition timing, ensuring efficient energy utilization and minimal mechanical stress.

Mean Temperature

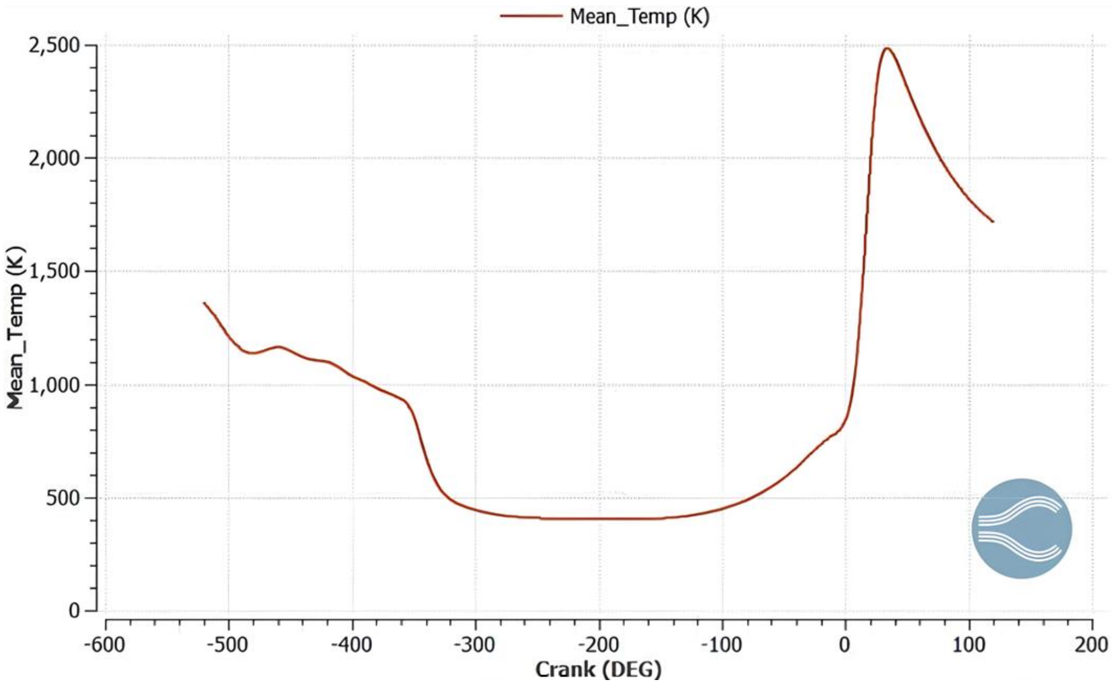

The temperature plot depicts the mean in-cylinder temperature variation throughout the engine cycle, showcasing a significant peak around TDC due to the rapid combustion of the air-fuel mixture. The temperature rises sharply to approximately 2500 K, indicating efficient energy release during combustion. The decrease in temperature during the expansion stroke reflects the conversion of thermal energy into mechanical work. The relatively lower temperature during the intake and compression strokes highlights the influence of pre-combustion cooling and compression heating. This profile underscores optimized combustion timing and efficient energy transfer within the cylinder.

Heat Release Rate

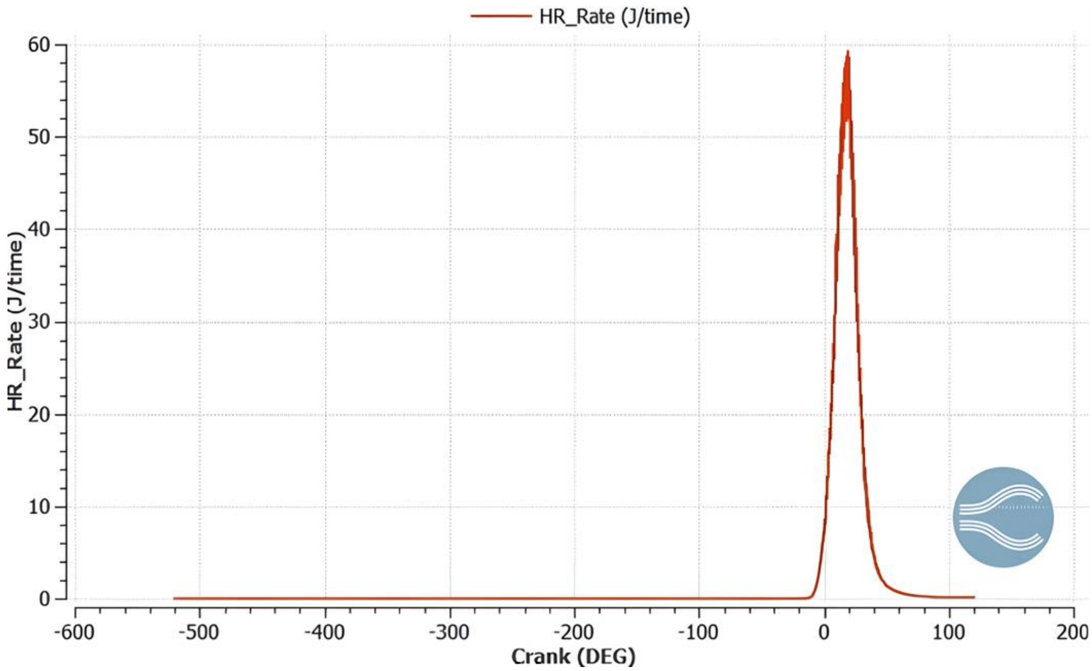

The HRR plot illustrates the energy liberation during the combustion process as a function of crank angle. A sharp peak around TDC signifies the rapid release of chemical energy from the fuel due to ignition and subsequent flame propagation. This steep rise highlights efficient combustion, while the narrow width of the peak indicates a fast and well-controlled combustion process. Prior to the peak, the HRR remains minimal, corresponding to the compression stroke where negligible energy release occurs. After the peak, the HRR quickly diminishes, reflecting the completion of combustion and the transition to the expansion stroke. This plot underscores the importance of precise ignition timing and optimized air-fuel mixing for achieving high combustion efficiency and power output.

Total Parcels

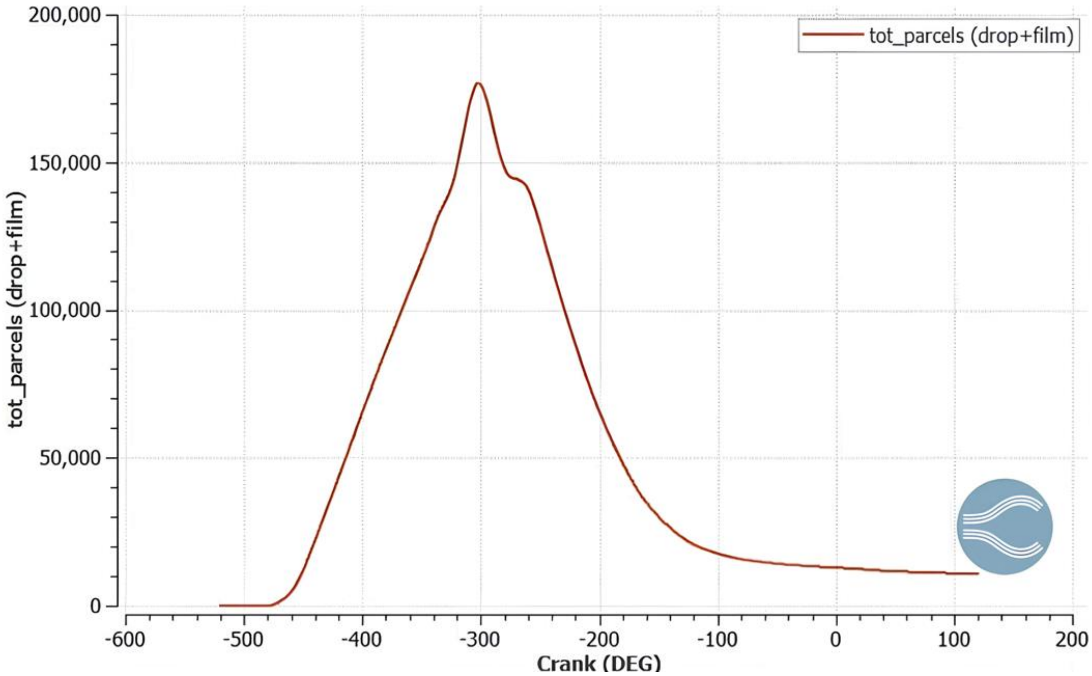

The total parcels plot (representing both droplets and film) provides valuable insight into the fuel spray and evaporation dynamics during the engine cycle. The initial rise in parcel count corresponds to the start of injection, as fuel droplets are introduced into the cylinder. The peak, observed around -300 crank degrees, signifies the point where the maximum number of parcels, both in droplet form and as wall film, is present due to active injection and spray atomization.

As the crank angle progresses toward combustion, the number of parcels declines sharply, reflecting the evaporation of droplets and the subsequent mixing of vaporized fuel with air. By the time combustion occurs near TDC, most of the fuel has transitioned into vapor, leaving minimal parcels. The gradual decline post-combustion highlights the continued evaporation of any residual droplets or wall film. This plot is crucial for assessing injection timing, spray dynamics, and the efficiency of fuel vaporization, all of which directly influence combustion quality and emissions.

Spray Penetration

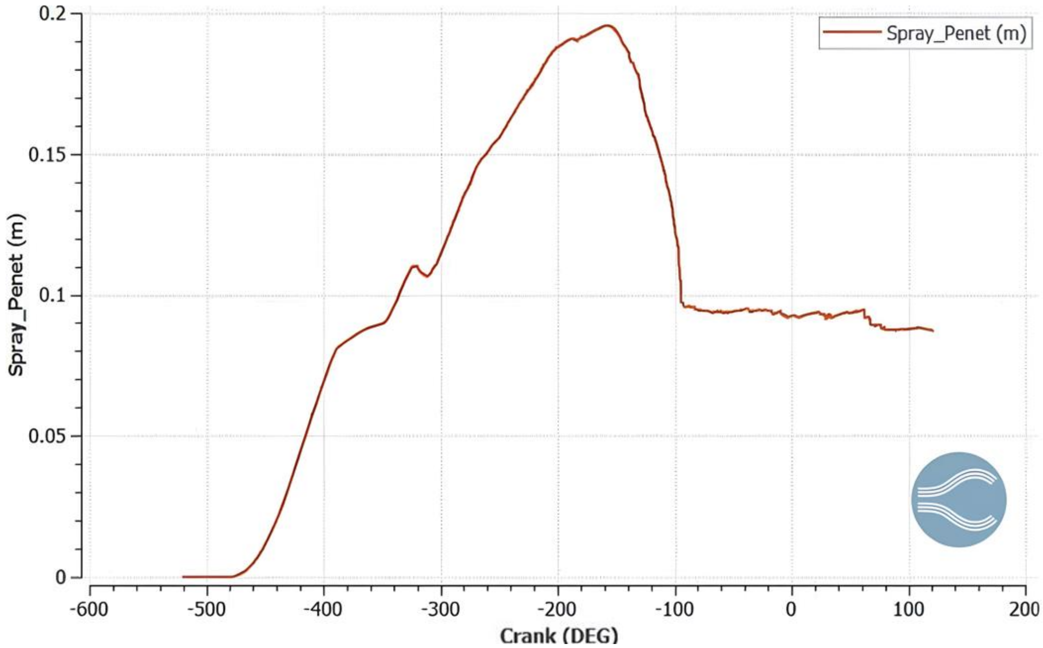

The spray penetration plot aligns well with the specified injection timing. Injection begins at -480.0 degrees, marking the introduction of fuel droplets into the cylinder. From this point, the penetration distance starts to increase as the injection progresses, driven by the high momentum of fuel entering the chamber. The steady rise in penetration continues beyond the start of injection, reflecting the combined effects of injection velocity and atomization.

The injection duration is 191.2 degrees, which means the injection process concludes around -288.8 degrees. By this point, the penetration reaches a significant level, but the momentum of the spray carries it further, peaking at approximately -150 degrees. This peak penetration reflects the culmination of spray dynamics before dissipation and evaporation dominate.

Following the end of injection, the penetration length begins to decline as the fuel droplets interact with the cylinder walls and surrounding air, transitioning into vapor. The leveling off for penetration closer to TDC indicates the stabilization of the fuel-air mixture, preparing for combustion. This behavior highlights the interplay between injection timing, spray dynamics, and air-fuel mixing, critical for achieving efficient combustion and minimizing emissions.

Videos

The following videos were uploaded to YouTube:

1. Mesh Animation for Computational Domain Visualization

This animation showcases the computational mesh used in the numerical simulation, emphasizing the grid's structure and levels of refinement.

Available at: https://youtu.be/kGKeqt4l8Bc

2. Fuel Spray Dynamics Visualization in Combustion Modeling

This animation illustrates the dynamics of fuel spray within the combustion chamber, showcasing its formation, dispersion, and interaction with the surrounding air and chamber walls.

Available at: https://youtu.be/_pyHtHOt8oo

3. Temperature Contours Visualization in Combustion Analysis

This animation displays temperature contours across the entire PFI engine, including the intake port, exhaust port, and cylinder region, highlighting the thermal distribution and gradients throughout the combustion process.

Available at: https://youtu.be/_btnv0VThFs

References

1. B. Yang, Z. Zheng, P. Chen, H. Zha, N. Ma, and M. Yao, "An Investigation into the Effect of Early Injection and Port-Fuel Injection on Combustion and Emissions of a Heavy-Duty Gasoline Engine," *Neiranji Gongcheng/Chinese Internal Combustion Engine Engineering*, vol. 39, pp. 34–41, Feb. 2018. DOI: 10.13949/j.cnki.nrjgc.2018.01.006.

2. R. Golzari, Y. Li, and H. Zhao, *Impact of Port Fuel Injection and In-Cylinder Fuel Injection Strategies on Gasoline Engine Emissions and Fuel Economy*, Oct. 2016. DOI: 10.4271/2016-01-2174.

3. H. Zhao, "Overview of Gasoline Direct Injection Engines," in *Book Chapter*, pp. 1–19, Dec. 2010. DOI: 10.1533/9781845697327.1.

4. M. H. H. Ishak, F. Ismail, S. Che Mat, M. S. Abdul Aziz, M. Z. Abdullah, and A. Aizat, "Numerical Study on the Influence of Nozzle Spray Shape on Spray Characteristics Using Diesel and Biofuel Blends," *Biofuels*, vol. 12, pp. 1–13, Apr. 2019. DOI: 10.1080/17597269.2019.1583717.

5. J. Zhang, J. Mi, and H. Wang, "A New Mesh-Independent Model for Droplet/Particle Collision," *Journal of Heat and Mass Transfer*, pp. 622–630, Jan. 2012. DOI: 10.1080/02786826.2011.649809.

6. M. S. Dodd, D. Mohaddes, A. Ferrante, and M. Ihme, "Analysis of Droplet Evaporation in Isotropic Turbulence Through Droplet-Resolved DNS," *International Journal of Heat and Mass Transfer,* vol. 172, Jun. 2021. DOI: 10.1016/j.ijheatmasstransfer.2021.121157.

7. A. Omidvar and H. Khaleghi, "An Analytical Approach for Calculation of Critical Weber Number of Droplet Breakup in Turbulent Gaseous Flows," *Arabian Journal for Science and Engineering*, vol. 37, Dec. 2012. DOI: 10.1007/s13369-012-0319-x.

8. A. Risi, T. Donateo, A. Sciolti, M. Calò, and M. Gaballo, "A New Energy-Based Model for the Prediction of Primary Atomization of Urea-Water Sprays," *SAE Technical Papers*, Apr. 2009. DOI: 10.4271/2009-01-0902.

9. M. J. Brandt et al., "Chapter 14 - Hydraulics," in *Twort's Water Supply*, 7th ed., Butterworth-Heinemann, pp. 581–619, 2017. DOI: 10.1016/B978-0-08-100025-0.00014-4.

10. A. Kumar, J. A. Boussom, and N. Van Dam, "Large-Eddy Simulation Study of Injector Geometry and Parcel Injection Location on Spray Simulation of the Engine Combustion Network Spray G Injector," *Journal of Engineering for Gas Turbines and Power*, vol. 146, no. 8, pp. 081003 (13 pages), Feb. 2024. DOI: 10.1115/1.4063957.

11. M. Raju, M. Wang, and P. Senecal, *Dynamic Chemical Mechanism Reduction for Internal Combustion Engine Simulations*, vol. 2, SAE Technical Papers, Apr. 2013. DOI: 10.4271/2013-01-1110.

12. A. Azrin, I. Yusri, K. Sudhakar, M. N. Che Wan, A. Zainal, and A. P. P. Abdul Majeed, "An overview of the spark plug engine profile in a spark ignition engine," *IOP Conference Series: Materials Science and Engineering*, vol. 1092, p. 012030, Mar. 2021. DOI: 10.1088/1757-899X/1092/1/012030.

13. J. A. Gutiérrez Suárez, C. H. Galeano Urueña, and A. Gómez Mejía, "Adaptive Mesh Refinement Strategies for Cost-Effective Eddy-Resolving Transient Simulations of Spray Dryers," *ChemEngineering*, vol. 7, no. 5, p. 100, Oct. 2023. DOI: 10.3390/chemengineering7050100.

14. E. Porpatham, A. Ramesh, and B. Nagalingam, "Effect of compression ratio on the performance and combustion of a biogas-fuelled spark ignition engine," *Fuel*, vol. 95, pp. 247–256, May 2012. DOI: 10.1016/j.fuel.2011.10.059.

15. S. Liu, Y. Qi, Z. Lin, W. Liu, G. Lu, B. Wang, Y. Liu, and Z. Wang, "A wall heat transfer model and a skeletal reaction mechanism of iso-octane for CFD simulation of gasoline engines," *Energy Conversion and Management*, vol. 298, Dec. 2023. DOI: 10.1016/j.enconman.2023.117784.

16. A. Broatch, P. Olmeda, X. Margot, and J. Escalona, "New approach to study the heat transfer in internal combustion engines by 3D modelling," *International Journal of Thermal Sciences*, vol. 138, pp. 405–415, Apr. 2019. DOI: 10.1016/j.ijthermalsci.2019.01.006.

17. T. Knopp, L. Eça, S. L. Toxopeus, D. Fritsch, A. Gargiulo, and K. T. Lowe, "Errors and uncertainties in CFD validation for non-equilibrium turbulent boundary layer flows at high Reynolds numbers," *Journal of Turbulence*, pp. 399–422, May 2024. DOI: 10.1080/14685248.2024.2360195.

18. M. A. Habib, M. A. Nemitallah, and M. El-Nakla, "Current status of CHF predictions using CFD modeling technique and review of other techniques especially for non-uniform axial and circumferential heating profiles," *Annals of Nuclear Energy*, vol. 70, pp. 188–207, Aug. 2014. DOI: 10.1016/j.anucene.2014.03.016.

19. R. Mohsin and Z. Majid, "Comparative study on exhaust emission and engine performance of single cylinder spark-ignited engine operated on gasoline and natural gas," *International Journal of Advanced Engineering Applications*, vol. -, pp. 35–43, Jan. 2012.

20. D. E. Winterbone, "10 - Thermodynamics of Combustion," in *Advanced Thermodynamics for Engineers*, Butterworth-Heinemann, 1997, pp. 182–207. DOI: 10.1016/B978-034067699-8/50012-0.

21. V. T. Ngo, "Experimental investigations on combustion and emission characteristic of GCI engine fuelled E20 blend," *Chemical Engineering*, article no. 1826078, published online Sep. 30, 2020. DOI: 10.1080/23311916.2020.1826078.

22. H. Yuan, T. Tsukuda, Y. Yang, G. Shibata, Y. Kobashi, and H. Ogawa, "Effects of Chemical Compositions and Cetane Number of Fischer-Tropsch Fuels on Diesel Engine Performance," *Energies*, vol. 15, article no. 4047, May 2022. DOI: 10.3390/en15114047.

23. S. Binjuwair and A. Alkudsi, "The effects of varying spark timing on the performance and emission characteristics of a gasoline engine: A study on Saudi Arabian RON91 and RON95," *Fuel*, vol. 180, pp. 558–564, Sep. 2016. DOI: 10.1016/j.fuel.2016.04.071.